

# Biological fixation of nitrogen and carbon in the northern Indian Ocean

A thesis submitted in partial fulfilment of the requirements  
for the degree of

**Doctor of Philosophy**

by

**Himanshu Saxena**

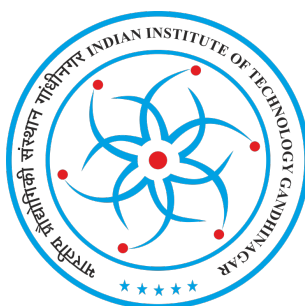
(Roll No. 17330013)

Under the guidance of

**Dr. Arvind Singh**

Geosciences Division

Physical Research Laboratory, Ahmedabad, India



Discipline of Earth Sciences

Indian Institute of Technology Gandhinagar, India

2022





*to*  
*my family and teachers*



## **Declaration**

I, Himanshu Saxena, declare that this written submission represents my ideas in my own words, and where others' ideas or words have been included, I have adequately cited and referenced the original sources. I also declare that I have adhered to all principles of academic honesty and integrity and have not misrepresented or fabricated or falsified any idea/data/fact/source in my submission. I understand that any violation of the above can cause disciplinary action by the Institute and can also evoke penal action from the sources which have thus not been properly cited or from whom proper permission has not been taken when needed.

Himanshu Saxena  
(Roll no. 17330013)



## Certificate

It is certified that the work contained in the thesis entitled “*Biological fixation of nitrogen and carbon in the northern Indian Ocean*” by Mr. Himanshu Saxena (roll no. 17330013), has been carried out under my supervision and this work has not been submitted elsewhere for a degree.

Dr. Arvind Singh

(Thesis Supervisor)

Geosciences Division

Physical Research Laboratory

Unit of Department of Space, Government of India

Ahmedabad, 380009, Gujarat, India.



# Acknowledgements

*This piece of writing is a fruit of several seasons over many years, whose seedling was gardenened by the supervisor's expertise and nurtured under the stimuli of colleagues, friends and dear ones. I would like to thank them all here.*

*I am thankful of my mentor Dr. Arvind Singh for his immense support and relentless patience during the course of this thesis. I express my sincere gratitude to him for his invaluable guidance and encouragement. His wisdom and knowledge were a never-ending source of inspiration that not only have motivated me learn and explore new possibilities but helped me in evolving as a researcher during this journey.*

*I express sincere regards to the members of my doctoral studies committee (DSC), Prof. Neeraj Rastogi, Prof. Sanjeev Kumar and Dr. Narendra Ojha, for their critical evaluation and fruitful suggestions. I am indebted to my collaborators Dr. Praveen Rahi (NCCS, Pune), Dr. Mar Benavides (Aix-Marseille Univ., Marseille) and Dr. Mini Raman (SAC, Ahmedabad) for enriching my knowledge in the field of microbiology. I would like to extend my deepest gratitude to the geosciences faculty members at Physical Research Laboratory (PRL), Prof. M.G. Yadava, Prof. R. D. Deshpande, Prof. J. S. Ray, Prof. Ravi Bhushan, Prof. A. D. Shukla, Dr. A. K. Sudheer, Dr. V. Goswami and Dr. A. H. Laskar for their valuable inputs during seminars and course work. I am thankful to all the staff members of the geosciences division, especially Jaldhi T Mehta for handling expeditions related documents and paper work. I am obliged to the Department of Space, Govt. of India for the research grant offered to me for PhD at PRL. I extend my sincere gratitude to Dr. Anil Bhardwaj, Director, PRL and Prof. Sudhir K. Jain, Director, IIT Gandhinagar for providing me necessary facilities to carry out my research work. I am also thankful to Dean and academic committee of PRL and IIT Gandhinagar academics. This thesis would not have been possible without the support of staff members of PRL library, computer centre, administration, accounts section, purchase, stores and CMG during this period. I express my profound gratitude to all the members of PRL workshop for timely carving and providing excellent experimental apparatus. I am grateful to the staff of canteen, housekeeping, dispensary and security personnel for providing me a healthy and safe stay at PRL. I extend my special regards to all my teachers, specifically Sadhana Ma'am, my school biology teacher and the first one to introduce me the true essence of the subject that still motivates me.*

*I will be forever thankful to my colleagues turned friends for making this journey a joyous experience. I am thankful to all my lab mates for their kind support. I could never thank Dr. Deepika Sahoo for passing her earned knowledge and expertise through discussions and teaching experimental techniques. I am thankful for her guidance during the initial research phase and unending cooperation during my entire PhD tenure. I am very grateful to Dr. Niharika Sharma for being an outstanding mentor and friend, always*

*encouraging and supporting me, and for being the cause (of many) and part of the fun occasions. I am indebted to Sangeeta Verma, Dr. Abdur Rahman and Mahesh Gaddham for their limitless support during experiments and instrumentation. I am very thankful of Nazir for being a caring, supporting and extremely helpful mate during my PhD. I specially thank Ajayeta, Deepak, Atif, Jitender and Siddhartha for being wonderful mates during our cruise expeditions. I acknowledge my earlier and present colleagues of the geosciences division, Dr. Pullabhatla Kiran Kumar, Dr. Iftikhar Ahmed, Dr. Rupa Ganguly, Dr. Bivin George, Dr. K. Satish, Dr. Anil Patel, Amit, Milan, Adil, Rohit, Sanjit, Swagatika, Shreya, Tatsat, Devaprasad and Chandrima for every support they have extended towards me.*

*I am deeply indebted to Shanwlee, Sana, Kamlesh, Partha, Akanksha, Ankit, Atif, Deepak and Vikas with whom I spent the happiest and most blissful moments of my PhD. I had the most joyful, memorable and treasured moments with them. Many thanks to all my batchmates. I am grateful to my family for their unconditional love, concern and sacrifice, without which this work would not have been possible. Despite my best efforts, it is nearly impossible to name everyone who has contributed to this research journey in some way. I am grateful to each and every one of them for their assistance in completing this thesis work.*

***Himanshu Saxena***



# Abstract

The elements carbon (C) and nitrogen (N) form the backbone of life, since all the major cellular components such as genetic materials, proteins and energy carrier molecules are stemmed from these elements. In the marine environment, the scarcity of N often limits the growth and productivity of phytoplankton in most of the surface oceans. Though the most abundant form of N, i.e., dinitrogen gas ( $\text{N}_2$ ), comprises about 78% of the Earth's atmosphere, it is inaccessible to most of the phytoplankton. The majority of phytoplankton are unable to assimilate  $\text{N}_2$  but require the bioaccessible or reactive forms of N, such as ammonium ( $\text{NH}_4^+$ ), nitrate ( $\text{NO}_3^-$ ) and nitrite ( $\text{NO}_2^-$ ). Notably, a specialised group of prokaryotes, termed diazotroph, is capable of  $\text{N}_2$  fixation — a process of breaking the highly stable triple bond in the  $\text{N}_2$  molecule and converting (or fixing) it to  $\text{NH}_4^+$ .

$\text{N}_2$  fixation fuels the cellular N-needs of phytoplankton and thus, constrains the Earth's climate by influencing marine C fluxes through sequestration of atmospheric  $\text{CO}_2$ . Therefore, understanding the process of  $\text{N}_2$  fixation by which newly fixed N is added to the ocean is essential for accurate quantification and ultimately to forecasting oceanic productivity. Additionally, in order to forecast accurate quantification of oceanic productivity, it is also essential to precisely estimate the present marine C budget. The prerequisite estimate of marine C budget is imprecise owing to inaccurate estimations of  $\text{CO}_2$  sources and sinks. One such area for recognition in the C budget is the unaccounted sink of  $\text{CO}_2$  via chemoautotrophic inorganic C assimilation (i.e., chemoautotrophic C fixation) within the aphotic zone.

$\text{N}_2$  fixation rates based on direct field measurements are scarce with extremely high variability both spatially and temporally, lacking large regions of the global ocean especially the Indian Ocean. The northern Indian Ocean is a unique basin which contains different biogeochemical gradients with eutrophic, oligotrophic and  $\text{O}_2$  deficient waters, and experiences a strong seasonal reversal of monsoon circulations. Yet, the studies on

N<sub>2</sub> fixation so far conducted in the Indian Ocean before the commencement of this thesis work have mostly focused on regions with *Trichodesmium* (photoautotrophic diazotroph) blooms in the northwestern part of the Indian Ocean (i.e., the Arabian Sea). Hence, the thesis, primarily focuses on marine N<sub>2</sub> fixation and its contribution in the regulation of marine primary production, with an additional effort to assess the significance of C fixation within the aphotic zone of the water column. The thesis reports the results of N<sub>2</sub> fixation rates from the euphotic and aphotic zone of the Bay of Bengal (i.e., the north-eastern Indian Ocean) and the Arabian Sea for the summer and spring monsoon and the winter monsoon, respectively. The results of C fixation rates from the euphotic zone of the Bay of Bengal and the euphotic and aphotic zone of the Arabian Sea are also discussed in the thesis.

The euphotic zone N<sub>2</sub> fixation rates were mostly low ( $< 1 \text{ nmol N L}^{-1} \text{ d}^{-1}$ ) in the oligotrophic Bay of Bengal contrary to the traditional assumption of oligotrophy favouring the diazotrophy. However, the upper bound of the observed N<sub>2</sub> fixation rates was higher than that reported in other oceanic regimes, such as the Eastern Tropical South Pacific, the Tropical Northwest Atlantic, and the Equatorial and Southern Indian Ocean. N<sub>2</sub> fixation contributed maximum up to 2% of primary production in the Bay of Bengal. The anticipated reason for low N<sub>2</sub> fixation rates in the Bay of Bengal could be cloud cover and turbidity due to copious riverine discharge during the summer monsoon and unexpected instability of the water column owing to the least fresh water induced stratification during the spring inter-monsoon. Volumetric N<sub>2</sub> fixation rates measured in the euphotic and aphotic zone of the Bay of Bengal were equally low, but interestingly, significantly higher N<sub>2</sub> fixation rates occurred below the oxygen minimum zone (OMZ) ( $> 600 \text{ m depth}$ ) with  $0.5 < \text{O}_2 \leq 1.6 \text{ mL L}^{-1}$ , rather than within the OMZ with  $\text{O}_2 \leq 0.5 \text{ mL L}^{-1}$ . This suggests that low concentrations of O<sub>2</sub> and NO<sub>3</sub><sup>-</sup> are not a firm niche requirement for diazotrophs.

N<sub>2</sub> fixation rates in the Arabian Sea were higher in the convection dominated regions than in the convection unaffected regions during the winter monsoon owing to lower N:P ratios and higher iron availability in the convection dominated regions. The aphotic zone N<sub>2</sub> fixation rates were low ( $< 0.1 \text{ nmol N L}^{-1} \text{ d L}^{-1}$ ), but accounted for up to 95% of whole water column rates. N<sub>2</sub> fixation rates in the OMZ of the Arabian Sea were modest and comparable with another OMZs of the Eastern Tropical North and South Pacific.

The average C fixation rates in the suboxic waters of the OMZs of the Arabian Sea were significantly higher than in the hypoxic waters of the OMZ, which was likely related to nutrients availability and to the preferential dominance of nitrite oxidisers and anammox bacteria in the suboxic waters of the OMZ. The extrapolation of measured aphotic zone C fixation to the global ocean amounts to up to 15% of primary production of the global ocean. The results obtained during the course of this thesis work provide quantitative evidences that N and C budget are largely unbalanced owing to overlooked N<sub>2</sub> and C fixation potential in the aphotic zone of the global ocean.

Keywords: Nitrogen fixation, C fixation, photosynthesis, chemosynthesis, nutrients, oxygen minimum zone, Indian Ocean, Bay of Bengal, Arabian Sea



# Contents

<b>Abstract</b>	<b>i</b>
<b>List of Tables</b>	<b>ix</b>
<b>List of Figures</b>	<b>xi</b>
<b>List of Abbreviations</b>	<b>xv</b>
<b>1 Introduction</b>	<b>1</b>
1.1 Background . . . . .	1
1.2 Ecological niches within the water column . . . . .	3
1.2.1 Nitrogenase enzyme: a diazotrophic niche decider . . . . .	3
1.2.2 Environmental controls . . . . .	5
1.2.3 Classical niche: the euphotic zone . . . . .	6
1.2.4 Novel niche: the aphotic zone . . . . .	6
1.3 N <sub>2</sub> fixation in the global ocean . . . . .	7
1.4 C fixation in the global ocean . . . . .	9
1.5 The northern Indian Ocean . . . . .	10
1.5.1 The Bay of Bengal . . . . .	11
1.5.2 The Arabian Sea . . . . .	11
1.5.3 Previous studies in the northern Indian Ocean . . . . .	12
1.6 Scope of the present work . . . . .	13
<b>2 Materials and Methods</b>	<b>15</b>
2.1 Sampling . . . . .	15
2.2 Environmental parameters . . . . .	17
2.2.1 Nutrients concentration measurement . . . . .	18

2.2.2	Dissolved inorganic carbon concentration . . . . .	19
2.3	N <sub>2</sub> and C fixation rates measurement . . . . .	21
2.3.1	Principle . . . . .	21
2.3.2	Tracer preparation . . . . .	22
2.3.3	Sampling and tracer addition . . . . .	23
2.3.4	Incubation . . . . .	23
2.3.5	Filtration and preservation . . . . .	24
2.3.6	Sample preparation . . . . .	24
2.3.7	Mass spectrometric analysis . . . . .	25
2.3.8	Estimation of fixation rates . . . . .	29
2.4	Cyanobacterial community analysis . . . . .	32
2.5	Statistical analyses . . . . .	33
<b>3</b>	<b>N<sub>2</sub> and C fixation in the Bay of Bengal during the summer monsoon</b>	<b>35</b>
3.1	Introduction . . . . .	35
3.2	Materials and Methods . . . . .	36
3.3	Results . . . . .	37
3.3.1	Environmental conditions . . . . .	37
3.3.2	Nutrients . . . . .	38
3.3.3	N <sub>2</sub> and C fixation rates . . . . .	39
3.4	Discussion . . . . .	40
3.5	Conclusions . . . . .	45
<b>4</b>	<b>N<sub>2</sub> and C fixation in the Bay of Bengal during the spring inter-monsoon</b>	<b>47</b>
4.1	Introduction . . . . .	47
4.2	Materials and Methods . . . . .	48
4.3	Results . . . . .	50
4.3.1	Environmental conditions and nutrients . . . . .	50
4.3.2	N <sub>2</sub> and C fixation rates and their environmental controls . . . . .	51
4.3.3	Cyanobacterial abundance . . . . .	54
4.4	Discussion . . . . .	56
4.4.1	N <sub>2</sub> and C fixation in the euphotic zone of the Bay of Bengal . . . . .	56
4.4.2	N <sub>2</sub> fixation in the aphotic zone of the Bay of Bengal . . . . .	57

4.4.3	Environmental controls of diazotrophy and C fixation . . . . .	58
4.4.4	Environmental controls of cyanobacterial communities . . . . .	60
4.5	Conclusions . . . . .	61
<b>5</b>	<b>N<sub>2</sub> fixation in the Arabian Sea during the winter monsoon</b>	<b>63</b>
5.1	Introduction . . . . .	63
5.2	Materials and Methods . . . . .	65
5.3	Results . . . . .	67
5.3.1	Environmental conditions . . . . .	67
5.3.2	Nutrients . . . . .	68
5.3.3	N <sub>2</sub> fixation rates . . . . .	69
5.4	Discussion . . . . .	72
5.4.1	Highest N <sub>2</sub> fixation concurs with <i>Trichodesmium</i> bloom . . . . .	72
5.4.2	N <sub>2</sub> fixation in N <sub>r</sub> -rich and N <sub>r</sub> -deficient waters . . . . .	73
5.4.3	Active non-cyanobacterial diazotrophy in the Arabian Sea . . . . .	74
5.4.4	Is N <sub>2</sub> fixation insufficient to compensate N <sub>r</sub> -loss through denitrifi- cation? . . . . .	75
5.5	Conclusions . . . . .	76
<b>6</b>	<b>Contribution of dark C fixation towards C sink in the ocean aphotic zone</b>	<b>79</b>
6.1	Introduction . . . . .	79
6.2	Materials and Methods . . . . .	81
6.3	Results . . . . .	82
6.3.1	Environmental conditions . . . . .	82
6.3.2	C fixation rates . . . . .	83
6.4	Discussion . . . . .	86
6.4.1	Light C fixation in the Arabian Sea . . . . .	86
6.4.2	Dark C fixation in the Arabian Sea . . . . .	87
6.4.3	Dark C fixation intensifies OMZs . . . . .	88
6.4.4	Chemoautotrophs responsible for dark C fixation . . . . .	88
6.4.5	Role of dark C fixation in the global ocean . . . . .	90
6.4.6	Dark C fixation — a sink or a source of greenhouse gases? . . . . .	91
6.5	Conclusions . . . . .	92

<b>7</b>	<b>Summary and scope for future works</b>	<b>93</b>
7.1	Summary . . . . .	93
7.1.1	N <sub>2</sub> and C fixation in the Bay of Bengal during the summer monsoon	93
7.1.2	N <sub>2</sub> and C fixation in the Bay of Bengal during the spring inter- monsoon . . . . .	94
7.1.3	N <sub>2</sub> fixation in the Arabian Sea during the winter monsoon . . . . .	94
7.1.4	Contribution of dark C fixation towards C sink in the ocean aphotic zone . . . . .	95
7.2	Scope for future works . . . . .	95
	<b>References</b>	<b>97</b>
	<b>List of Publications</b>	<b>131</b>
	<b>Presentations at Conferences and Schools</b>	<b>133</b>
	<b>Publications attached with the thesis</b>	<b>135</b>



# List of Tables

2.1	Sampling locations with date and maximum depth of sampling. . . . .	16
3.1	Details of sea surface temperature (SST), sea surface salinity (SSS), deep chlorophyll maxima (DCM), mixed layer depth (MLD), N:P, depth integrated N <sub>2</sub> and C fixation rates at each station. . . . .	38
4.1	Details of sea surface temperature (SST), sea surface salinity (SSS), mixed layer depth (MLD), deep chlorophyll maxima (DCM) and chlorophyll <i>a</i> at each station. . . . .	50
4.2	N <sub>2</sub> and C fixation rates in different sections of the water column. Note that C fixation rates were measured in the euphotic zone only. . . . .	54
4.3	Depth-integrated C fixation rates, euphotic and aphotic zone N <sub>2</sub> fixation rates, N <sub>2</sub> fixation contribution to C fixation and aphotic zone N <sub>2</sub> fixation contribution to water column N <sub>2</sub> fixation at each station. Depth range for depth-integrated rates is indicated in brackets. . . . .	54
5.1	Details of sea surface temperature (SST), sea surface salinity (SSS), mixed layer depth (MLD) at each station. . . . .	68
5.2	Depth-integrated light, dark and aphotic zone N <sub>2</sub> fixation rates and contribution of aphotic zone to column N <sub>2</sub> fixation rates at each station. BD stands for below detection. Note that ‘contribution of aphotic zone to column N <sub>2</sub> fixation’ due to below detection/unavailable rates in the aphotic zone are indicated as hyphen. . . . .	71
5.3	Average of light, dark and aphotic zone N <sub>2</sub> fixation rates at convective and non-convective stations. Number of data points are indicated in brackets. .	73

5.4	$N_r$ input in the euphotic zone, aphotic zone and water column of the Arabian Sea, estimated using $N_2$ fixation rates from the respective zones. . . .	75
6.1	Dark C fixation associated with the global dark ocean. . . . .	90

# List of Figures

1.1	A brief schematic indicating the role of $N_2$ and C fixation in constraining the Earth's climate. The schematic of diazotrophs is modified from <i>Zehr and Capone (2020)</i> . . . . .	3
1.2	N cycle in the euphotic zone and the aphotic zone containing $O_2$ -depleted waters. The schematic of diazotrophs is inspired and modified from <i>Zehr and Capone (2020)</i> . . . . .	4
2.1	Sampling stations in the Bay of Bengal and the Arabian Sea during three research cruise expeditions: ORV <i>Sagar Nidhi</i> (SN-132), ORV <i>Sindhu Sankalp</i> (SSK-127) and ORV <i>Sagar Kanya</i> (SK-364). The sampling location labels SN, S and SK numbered stations show sampling during SN-132, SSK-127 and SK-364 cruises, respectively. . . . .	15
2.2	Niskin bottles and CTD, $O_2$ concentration, fluorescence and photosynthetically active radiation sensors mounted on the rosette sampler during the <i>Sindhu Sankalp</i> (SSK-127) cruise in the Bay of Bengal. . . . .	17
2.3	SKALAR autoanalyzer at the Physical Research Laboratory, Ahmedabad, India. . . . .	18
2.4	Schematic of UIC $CO_2$ Coulometer modified after "CM140 Total Inorganic Carbon Analysis by Acidification and Coulometric Detection ( <a href="https://www.uicinc.com/cm140-carbon-analysis/">https://www.uicinc.com/cm140-carbon-analysis/</a> )". . . . .	21
2.5	Flow diagram of $N_2$ and C fixation rates measurement. . . . .	22
2.6	FLASH 2000 EA connected to Thermo Delta V Plus-IRMS at the Physical Research Laboratory, Ahmedabad, India. . . . .	26
2.7	A schematic showing elemental analyser connected to isotope ratio mass spectrometer via Conflo. . . . .	28

3.1	Sampling stations (SN1–SN8) superimposed on sea surface salinity (obtained from Multi-Mission OISSS Global Dataset V1.0 for Jul 2018) in the Bay of Bengal during the research cruise expedition ORV <i>Sagar Nidhi</i> (SN–132) . . . . .	37
3.2	Vertical profiles of (a) temperature (T), (b) salinity, (c) $\text{NO}_x$ , (d) $\text{NO}_2^-$ , (e) $\text{PO}_4^{3-}$ and (f) $\text{P}^*$ at each station. . . . .	38
3.3	Vertical profiles of $\delta^{15}\text{N}$ of natural PON at each station. . . . .	39
3.4	Vertical profiles of average volumetric rates of (a) $\text{N}_2$ fixation and (b) C fixation at each station. . . . .	40
3.5	Euphotic zone integrated N demand, $\text{N}_2$ fixation rates and contribution of $\text{N}_2$ fixation to C fixation at each station. . . . .	41
4.1	Sampling stations (S1–S7) superimposed on sea surface chlorophyll <i>a</i> (4 km resolution data obtained from Aqua/MODIS for Apr 2019) in the Bay of Bengal during the research cruise expedition ORV <i>Sindhu Sankalp</i> (SSK–127). $\text{N}_2$ and C fixation experiments were performed at stations S1–S6. . . . .	49
4.2	Vertical profiles of (a) temperature (T), (b) salinity, (c) $\text{NO}_x$ , (d) $\text{PO}_4^{3-}$ and (e) chlorophyll <i>a</i> at each station. Note the difference in depth for the chlorophyll <i>a</i> profile and that the top of the y-axis is extended for all the profiles except for chlorophyll <i>a</i> profile. . . . .	51
4.3	Vertical profiles of (a) average $\text{N}_2$ fixation rates (solid symbols), (b) average C fixation rates (open symbols) and (c) $\text{O}_2$ concentrations in the euphotic (white background) and aphotic zone (shaded background). Circles represent the coastal Bay of Bengal and triangles represent the central Bay of Bengal stations. Note that the y-axis of the euphotic zone is extended. . . . .	52
4.4	Spearman’s correlation coefficient ( $r$ ) of C fixation, $\text{N}_2$ fixation, and cyanobacteria and their communities, with their potential environmental controls. Significant correlations are indicated for $p < 0.05$ . Note that only the parameters which significantly correlated with each other are indicated. . . . .	53
4.5	Vertical profile of relative abundance of cyanobacterial communities with respect to total cyanobacterial sequences. . . . .	55

5.1	Sampling stations (SK1–SK14) superimposed on sea surface temperature (4 km resolution data obtained from Aqua/MODIS for Dec 2019) in the Arabian Sea during the research cruise expedition ORV <i>Sagar Kanya</i> (SK–364) . . . . .	66
5.2	Vertical profiles of (a) temperature (T), (b) salinity, (c) O <sub>2</sub> , (d) NO <sub>x</sub> , (e) PO <sub>4</sub> <sup>3–</sup> and (f) P* at each station. White solid circles in (a) mark the mixed layer depth. Note the top of the y-axes is extended. . . . .	69
5.3	Vertical profiles of average light, dark and aphotic zone N <sub>2</sub> fixation rates. The inset zooms the large variable region of N <sub>2</sub> fixation rates. Open black circles represent the rates below minimum quantifiable rates (MQR). . . .	70
5.4	<i>Trichodesmium</i> bloom observed near coastal station SK1. . . . .	70
6.1	Sampling stations (SK1–SK14) superimposed on sea surface temperature (4 km resolution data obtained from Aqua/MODIS for Dec 2019) in the Arabian Sea during the research cruise expedition ORV <i>Sagar Kanya</i> (SK–364) . . . . .	81
6.2	Vertical profiles of (a) temperature (T), (b) salinity, (c) chlorophyll <i>a</i> (Chl <i>a</i> ), (d) O <sub>2</sub> , (e) NO <sub>x</sub> , (f) PO <sub>4</sub> <sup>3–</sup> and (g) NO <sub>2</sub> <sup>–</sup> at each station. Black open, solid black, white and yellow circles in the O <sub>2</sub> profile mark the seawater sampling depths for incubation experiments corresponding to the euphotic zone, aphotic zone’s oxycline, suboxic and hypoxic waters, respectively. Note the difference in depth for the Chl <i>a</i> profile and that the top of the y-axes is extended for all the profiles except for Chl <i>a</i> profile. . . . .	82
6.3	Vertical profile of C fixation rates in the euphotic and aphotic zone. Shaded background indicates the OMZ within the aphotic zone. Note the break in the y-axis between 200 and 600 m. . . . .	83

6.4	C fixation rates (a) at sea surface ( $\mu\text{mol C L}^{-1} \text{ d}^{-1}$ ), (b) in the euphotic zone ( $\text{mmol C m}^{-2} \text{ d}^{-1}$ ) and (c) in the aphotic zone ( $\text{mmol C m}^{-2} \text{ d}^{-1}$ ) at sampling stations (SK1–SK14) in the Arabian Sea. Background contours: (a) Chl <i>a</i> : sea surface chlorophyll <i>a</i> concentration (4 km resolution data obtained from Aqua/MODIS for Dec 2019), (b) SST: sea surface temperature (4 km resolution data obtained from Aqua/MODIS for Dec 2019) and (c) SSS: sea surface salinity (40 km resolution data obtained from RSS-SMAP-NASA for Dec 2019). Note that sampling in the aphotic zone was not done at SK1. . . . .	84
6.5	Spearman’s correlation matrix with correlation coefficient ( <i>r</i> ). Indicated correlations are significant at $p < 0.05$ . Note that only the parameters which significantly correlated with light and/or dark C fixation are indicated.	85

# List of Abbreviations

<b>Anammox</b>	Anaerobic ammonium oxidation
<b>ATP</b>	Adenosine triphosphate
<b>C</b>	Carbon
<b>CO<sub>2</sub></b>	Carbon dioxide
<b>CTD</b>	Conductivity temperature depth
<b>DCM</b>	Deep chlorophyll maxima
<b>DIC</b>	Dissolved inorganic carbon
<b>DNA</b>	Deoxyribonucleic acid
<b>EA</b>	Elemental analyzer
<b>Fe</b>	Iron
<b>IAEA</b>	International atomic energy agency
<b>IRMS</b>	Isotope ratio mass spectrometer
<b>MLD</b>	Mixed layer depth
<b>N</b>	Nitrogen
<b>NH<sub>4</sub><sup>+</sup></b>	Ammonium
<b>NO<sub>3</sub><sup>-</sup></b>	Nitrate
<b>NO<sub>2</sub><sup>-</sup></b>	Nitrite
<b>NO<sub>2</sub></b>	Nitrogen dioxide
<b>NO<sub>x</sub></b>	Oxides of nitrogen
<b>O<sub>2</sub></b>	Oxygen
<b>ORV</b>	Oceanographic research vessel

<b><math>\text{PO}_4^{3-}</math></b>	Phosphate
<b>POC</b>	Particulate organic carbon
<b>PON</b>	Particulate organic nitrogen
<b>RNA</b>	Ribonucleic acid
<b>V-PDB</b>	Vienna-Pee Dee Belemnite
<b><math>\delta^{13}\text{C}</math></b>	Carbon isotope composition of POC and DIC with V-PDB as standard
<b><math>\delta^{15}\text{N}</math></b>	Nitrogen isotope composition of PON with air as standard
<b>‰</b>	per mil (or parts per thousand)



# Chapter 1

## Introduction

### 1.1 Background

The ocean food web is built on phytoplankton — world’s smallest primary producers. The energy they translate from the Sun into biochemical compounds via the process of photosynthesis gets passed up to the food chain, and thereby sustains the life of all sizes. Phytoplankton fix atmospheric carbon dioxide ( $\text{CO}_2$ ) — a potent greenhouse gas — into their organic matter, a process known as primary production or carbon (C) fixation. Marine phytoplankton account for  $\sim 50\%$  of global primary production ([Field et al., 1998](#); [Whitman et al., 1998](#)).

The element C forms the backbone of life. Next to C, the element nitrogen (N) plays a fundamental role in budding and nourishing life components ([Schindler, 1975](#); [Smith, 1984](#)), since all the major cellular components such as genetic materials (e.g., deoxyribonucleic acid (DNA) and ribonucleic acid (RNA)), proteins and energy carrier molecules (e.g., adenosine triphosphate (ATP)) are stemmed from these elements. The C and N requirement for life is enormous. For every 100 atoms of C assimilated into the cell, around 2 to 20 atoms of N are required depending on the organism ([Stern and Elser, 2002](#)). C in the form of  $\text{CO}_2$  is usually abundant enough to not limit primary production. In fact, the atmospheric concentration of  $\text{CO}_2$  has relentlessly increased from  $\sim 277$  parts per million (ppm) in 1750 to  $\sim 407$  ppm in 2018 ([Joos and Spahni, 2008](#); [Dlugokencky and Tans, 2018](#)). Instead, the scarcity of N often limits the growth and productivity of

phytoplankton in most of the surface oceans ([Moore et al., 2013](#); [Falkowski et al., 1998](#)). Though the most abundant form of N, i.e., dinitrogen gas ( $\text{N}_2$ ), is over  $400 \mu\text{mol L}^{-1}$  in seawater, it is inaccessible to most of the phytoplankton. Analogically, it is the same situation as rhymed by Samuel Taylor Coleridge in his poem *The Rime of the Ancyent Marinere* for a thirsty mariner surrounded by seawater — *water, water everywhere but not a drop to drink*. Likewise the majority of phytoplankton are unable to assimilate  $\text{N}_2$  but require the bioaccessible or reactive forms of N ( $\text{N}_r$ ), such as ammonium ( $\text{NH}_4^+$ ), nitrate ( $\text{NO}_3^-$ ), nitrite ( $\text{NO}_2^-$ ) and dissolved organic N (DON). Notably, a specialised group of free-living and symbiotic prokaryotes, termed diazotroph, is capable of  $\text{N}_2$  fixation — an intracellular process of breaking the highly stable triple bond in the  $\text{N}_2$  molecule and converting (or fixing) it to  $\text{NH}_4^+$ .

$\text{N}_2$  fixation fuels the cellular N-needs of phytoplankton by providing a natural fertiliser ([Tyrrell, 1999](#); [Falkowski et al., 1998](#)) and can sustain up to 50% of primary production in some of the oceanic regions ([Karl et al., 1997](#)). Conclusively,  $\text{N}_2$  fixation constrains the Earth's climate by influencing marine C fluxes through sequestration of atmospheric  $\text{CO}_2$  (Figure 1.1). Therefore, understanding the process by which newly fixed N is added to the ocean is essential for accurate quantification and ultimately to forecasting oceanic productivity and C dynamics. Hence, this thesis primarily focuses on marine  $\text{N}_2$  fixation and its contribution in the regulation of marine primary production.

Additionally, in order to forecast accurate quantification of oceanic productivity, it is also essential to precisely estimate the present marine C budget. While various  $\text{CO}_2$  removal mechanisms are being approached to remove around 1000 billion tons of  $\text{CO}_2$  from the atmosphere by 2100 by increasing oceanic  $\text{CO}_2$  uptake ([Boyd et al., 2019](#)), the prerequisite estimate of C sources and sinks is imprecise ([Burd et al., 2010](#)). One such area for recognition in the C budget is the unaccounted sink of  $\text{CO}_2$  via chemoautotrophic inorganic C assimilation (i.e., chemoautotrophic C fixation) within the aphotic zone (i.e., water column below the euphotic zone — the sunlit layer — of the ocean). Hence, in this thesis, an additional effort has been made to assess the significance of C fixation within the aphotic zone of the water column.

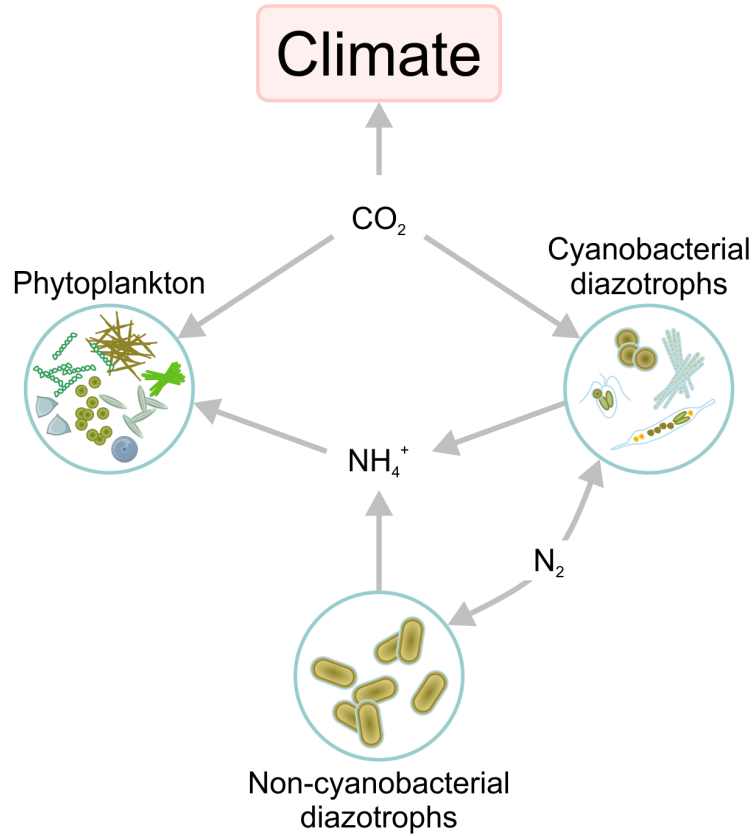
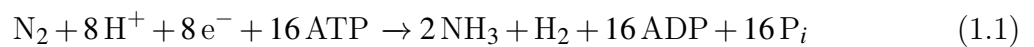


Figure 1.1: A brief schematic indicating the role of  $N_2$  and C fixation in constraining the Earth's climate. The schematic of diazotrophs is modified from [Zehr and Capone \(2020\)](#)

## 1.2 Ecological niches within the water column

### 1.2.1 Nitrogenase enzyme: a diazotrophic niche decider

Diazotrophs are genetically (or say enzymatically) proficient to reduce the most abundant but virtually inert  $N_2$  gas to  $NH_4^+$  (Figure 1.2).  $N_2$  fixation is an energetically expensive process (945 kJ energy per mole of  $N_2$  is required), catalysed by the nitrogenase enzyme complex that hydrolyses 16 molecules of ATP to fix one molecule of  $N_2$  (equation (1.1)).



The nitrogenase enzyme is an ancient enzyme, originated in a completely reduced environment prior to oxygenation of the Earth's atmosphere around 2 billion years ago ([Cheng](#),

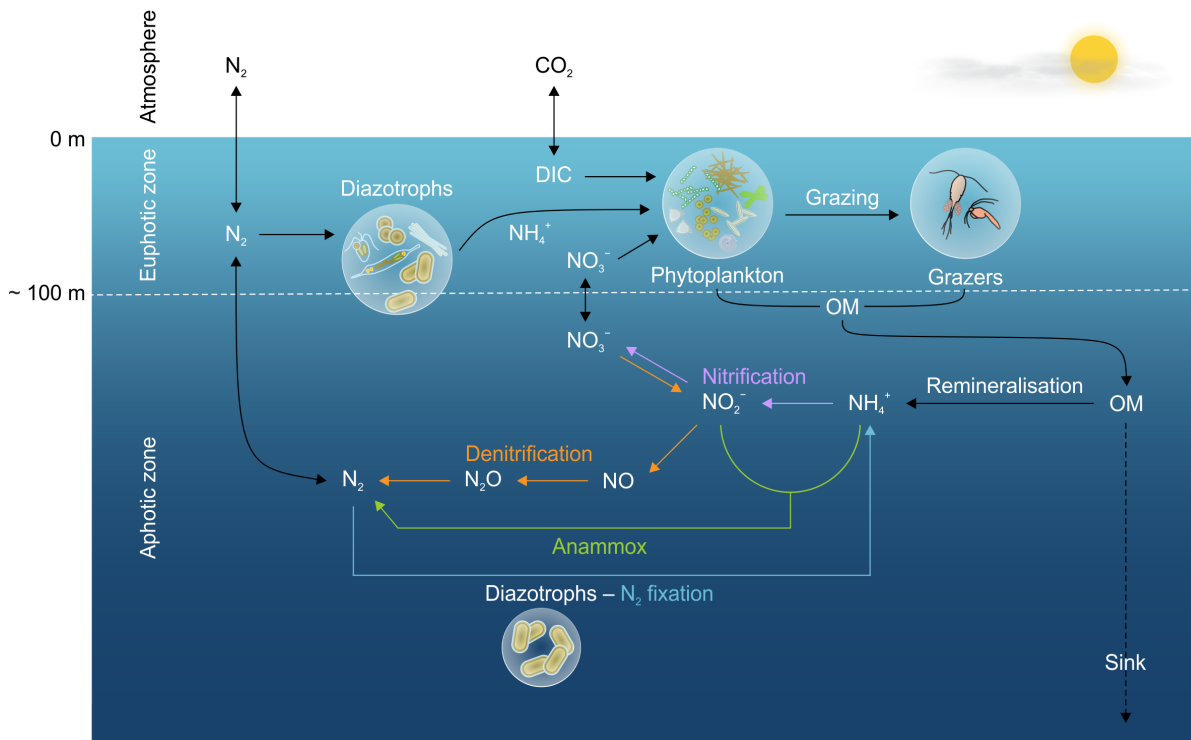


Figure 1.2: N cycle in the euphotic zone and the aphotic zone containing  $O_2$ -depleted waters. The schematic of diazotrophs is inspired and modified from [Zehr and Capone \(2020\)](#)

[2008](#); [Broda and Peschek, 1983](#)). It consists of two structural protein subunits: dinitrogenase (molybdenum-iron (Mo-Fe) protein) and dinitrogenase reductase (Fe protein), their structural polypeptides are encoded by *nifDK* and *nifH* gene, respectively. Diazotrophs with homologous alternative nitrogenases exist with vanadium-iron (V-Fe) or only Fe protein in place of Mo-Fe. The alternative nitrogenases are rare in oceans and less efficient in  $N_2$  binding and reduction ([Eady, 1996](#); [Betancourt et al., 2008](#)). The Mo-Fe nitrogenase is approximately 1.5 times more efficient at  $N_2$  fixation than the V-Fe and approximately 100 times than the Fe-Fe nitrogenase ([Joerger et al., 1988](#); [Miller and Eady, 1988](#)). The nitrogenase is highly sensitive to molecular oxygen ( $O_2$ ), and both of its protein subunits are rapidly and irreversibly inhibited by  $O_2$ , making  $N_2$  fixation an intrinsically anaerobic process ([Eady and Postgate, 1974](#); [Fay, 1992](#)). This sensitivity of nitrogenase towards  $O_2$  has important implications for diazotrophs and the niches they dwell in ([Fay, 1992](#)).

### 1.2.2 Environmental controls

In the ocean, the chemistry and biology are intimately linked, where one shapes the other ([Vernadsky, 1998](#)). Diazotrophs regulate nitrogenase activity in response to various environmental factors, such as the presence of  $N_r$ , availability of nutrients (Fe and  $PO_4^{3-}$ ), and  $O_2$  concentration.

$N_2$  fixation is an energy intensive process and in  $N_r$ -replete environments, diazotrophs obviate the need for  $N_2$  fixation. Generally in  $N_r$ -replete environment, diazotrophs prefer already available  $N_r$  because its assimilation is relatively energetically inexpensive than performing  $N_2$  fixation ([Falkowski, 1983](#); [Zehr, 2011](#)). Thus,  $N_2$  fixation is induced in the  $N_r$ -depleted environments. Additionally, Fe is one of the key controlling factors for  $N_2$  fixation ([Falkowski et al., 1998](#)), as diazotrophs have a relatively high Fe requirement owing to higher Fe content of the nitrogenase enzyme ([Kustka et al., 2003](#)) (38–50 mol Fe per mole of enzyme complex ([Miller and Orme-Johnson, 1992](#))). Amongst the diazotrophs, most prone to Fe limitation are the photosynthetic (or cyanobacterial) diazotrophs, due to the presence of Fe-containing proteins of the photosynthetic units. Cyanobacterial diazotrophs may have Fe requirements 2 to 5 times higher than  $NH_4^+$ -assimilating phytoplankton ([Sañudo-Wilhelmy et al., 2001](#)). [Berman-Frank et al. \(2001\)](#) showed that *Trichodesmium* — one of the major diazotrophs contributing up to 80 Tg of  $N_r$  each year ([Bergman et al., 2013](#)) — require five times as much Fe per C when fixing  $N_2$  than when grown on  $NH_4^+$ . Thus, cyanobacterial diazotrophs require higher Fe than non-cyanobacterial diazotrophs (NCDs) and non-diazotrophic cyanobacteria ([Schoffman et al., 2016](#); [Raven, 1988](#); [Berman-Frank et al., 2007](#)). Other than Fe, diazotrophs need  $PO_4^{3-}$  for cellular growth and various metabolic processes such as respiration and ATP synthesis ([Mills et al., 2004](#); [Sañudo-Wilhelmy et al., 2001](#); [Singh et al., 2019](#)). Further,  $N_2$  fixation is very sensitive to inhibition by  $O_2$  and in its exposure it gets permanently inactivated ([Gallon, 1992](#); [Postgate, 1998](#)). Conclusively, diazotrophs prefer  $N_r$  and  $O_2$ -depleted but Fe and  $PO_4^{3-}$ -replete environments. Other potential environmental controlling factors such as light, temperature and calm sea surface water favour the growth of diazotrophs ([Zehr and Capone, 2021](#)).

### 1.2.3 Classical niche: the euphotic zone

Many of the diazotrophs belong to cyanobacterial lineages dominantly prevailing in the euphotic zone (*Karl et al.*, 2002; *Zehr*, 2011) (Figure 1.2), where photoautotrophy provides the high energetic cost of N<sub>2</sub> fixation (*Fredriksson et al.*, 1998; *Gallon*, 2001; *Karl et al.*, 2008; *Zehr*, 2011) but at the same time it produces O<sub>2</sub>. These cyanobacterial diazotrophs have adapted a number of strategies to separate nitrogenase from photosynthetic O<sub>2</sub> production. Many cyanobacteria fix N<sub>2</sub> at night to avoid O<sub>2</sub> evolved during the photoperiod, or at the center of an aggregate where several layers of cells surrounding the center through respiration or by preventing O<sub>2</sub> diffusion provide a microaerobic environment, or spatially separate N<sub>2</sub> fixation and photosynthesis in heterocyst and vegetative cells, respectively, where specialised heterocyst cells lack the photosystem II responsible for oxygenic photosynthesis (*Gallon*, 1992; *Kumar et al.*, 2010).

### 1.2.4 Novel niche: the aphotic zone

Aside from cyanobacterial diazotrophs, NCDs are also able to fix N<sub>2</sub>, yet their contribution to global marine N<sub>2</sub> fixation is remained to be valued. Majority of them are not constrained by light, with an exception of photoheterotrophic NCDs, and as a result, they are capable of fixing N<sub>2</sub> in the aphotic zone (*Zehr et al.*, 1998; *Riemann et al.*, 2010; *Luo et al.*, 2012; *Zehr and Capone*, 2020) (Figure 1.2). NCDs have broaden the putative biogeography of diazotrophs, indicated by their detection in a wide range of environments such as N<sub>r</sub>-replete, cold and dark deep oceans (*Benavides et al.*, 2018b; *Bombar et al.*, 2016; *Fernandez et al.*, 2011; *Bonnet et al.*, 2013).

Within the aphotic zone, the oxygen minimum zones (OMZs) appear a potential site for N<sub>2</sub> fixation. The OMZs harbour denitrifiers and anammox bacteria that occur only in suboxic (O<sub>2</sub>: 0.02–0.5 mL L<sup>-1</sup> or 1–20 μmol kg<sup>-1</sup>) or anoxic (O<sub>2</sub>: < 0.02 mL L<sup>-1</sup> or < 1 μmol kg<sup>-1</sup>) waters. Denitrifiers are mostly heterotrophs and utilise alternate electron acceptors NO<sub>3</sub><sup>-</sup> and NO<sub>2</sub><sup>-</sup> for respiration and lead to the production of nitrous oxide (N<sub>2</sub>O) and N<sub>2</sub> (Figure 1.2). Anammox bacteria are autotrophs and fix CO<sub>2</sub> while simultaneously respiring NH<sub>4</sub><sup>+</sup> and NO<sub>2</sub><sup>-</sup> to N<sub>2</sub>. As a result, denitrifiers and anammox bacteria deplete

the concentrations of  $\text{NO}_3^-$ ,  $\text{NO}_2^-$  and  $\text{NH}_4^+$  in the dissolved pool through their reduction to  $\text{N}_2$ , that consequently lead to a decrease in  $\text{N}_r:\text{PO}_4^{3-}$  ratios (hereafter N:P ratios) — a believably conducive environment for diazotrophs, and thus, hypothesised to stimulate  $\text{N}_2$  fixation.

The OMZs have ramifications for the euphotic zone primary productivity, but to some extent the OMZs seem to incentivize the  $\text{CO}_2$  sequestration via chemoautotrophy. The OMZs could be favourable for chemoautotrophs since less energy is required to reduce inorganic C to organic C in anaerobic environment compared to aerobic environment (*Hügler and Sievert, 2011; McCollom and Amend, 2005*). Various chemoautotrophs yield energy by oxidising the reduced compounds as electron donors (e.g.,  $\text{NH}_4^+$ ,  $\text{NO}_2^-$ ), which are readily available in the OMZs due to occurrence of remineralisation, denitrification, anammox and ammonium oxidation (Figure 1.2). Though OMZs appear a preferential niche to stimulate C fixation, the oxygenated waters within the aphotic zone are a habitat for chemoautotrophic ammonium oxidisers, nitrite oxidisers and aerobic methane oxidisers (*Middelburg, 2011; Pachiadaki et al., 2017; Valentine et al., 2001*).

### 1.3 N<sub>2</sub> fixation in the global ocean

$\text{N}_2$  fixation rates based on direct field measurements are scarce (*Luo et al., 2012; Landolfi et al., 2018*) and with extremely high variability both spatially and temporally. Moreover,  $\text{N}_2$  fixation rates are largely biased owing to most of the estimations from samples with extensive diazotrophic blooms (e.g., large bloom-forming genus *Trichodesmium*) where  $\text{N}_2$  fixation is likely to be high. All these factors exacerbate the challenge of estimating the contribution of  $\text{N}_2$  fixation to the global marine  $\text{N}_r$  budget,  $\text{CO}_2$  sequestration and future oceanic primary productivity. In addition, the present estimates of the marine  $\text{N}_r$  budget are largely unbalanced with  $\text{N}_r$ -loss exceeding  $\text{N}_r$ -gain rates (*Benavides et al., 2018a*), though the stable isotopes records of ocean sediments suggested a balanced  $\text{N}_r$  inventory for the past 3,000 years (*Altabet, 2007*). The unbalanced  $\text{N}_r$  budget has led to the debate whether the ocean is rapidly losing total  $\text{N}_r$  inventory with years or the  $\text{N}_r$ -source or  $\text{N}_r$ -sink terms are underestimated or overestimated. One probable reason

for the present unbalanced  $N_r$  budget could be inaccurate estimates of  $N_r$  sources (e.g., unrecognised  $N_2$  fixation in its potential niches).

Total marine  $N_2$  fixation rates are often estimated based on N:P ratios of the dissolved pool ( $N^*$  and  $P^*$  method, where  $N^* = [NO_3^-] - 16 \times [PO_4^{3-}]$  and  $P^* = [PO_4^{3-}] - [NO_3^-]/16$  when based on the Redfield ratio ([Redfield, 1934](#))), where N:P ratios lower than the Redfield N:P ratio of 16 is supposed to support  $N_2$  fixation. Large-scale  $N^*$  distributions were used to estimate  $N_2$  fixation rate of 28 Tg N  $y^{-1}$  in the North Atlantic Ocean, which was extrapolated globally to  $\sim 110$  Tg N  $y^{-1}$  ([Gruber and Sarmiento, 1997](#)) and of 59 Tg N  $y^{-1}$  in the Pacific ([Deutsch et al., 2001](#)). [Deutsch et al. \(2007\)](#) reported a global  $N_2$  fixation rate of  $\sim 140$  Tg N  $y^{-1}$  using  $P^*$  distributions coupled with an ocean circulation model. Direct measurements of  $N_2$  fixation rates in the Atlantic Ocean suggested rates of 24 Tg N  $y^{-1}$ , and when extrapolated to the global ocean the rates reached to 177 Tg N  $y^{-1}$  ([Großkopf et al., 2012](#)). [Großkopf et al. \(2012\)](#) further suggested that the contribution of diazotrophs other than *Trichodesmium* is also significant than previously recognised. These indirect approaches of biogeochemical modelling, geochemical-tracer and extrapolation techniques that rely on assumptions lead to differences in diagnosed  $N_2$  fixation rates; thus, require verification by direct field measurements of  $N_2$  fixation rates.

Global database of direct field measurements of  $N_2$  fixation rates with the help of  $^{15}N$  tracer incubation technique has been concluded at 62 Tg N  $y^{-1}$  (geometric mean) and 140 Tg N  $y^{-1}$  (arithmetic mean) for the global ocean ([Luo et al., 2012](#)). Several studies have evidenced active diazotrophy in two of the three major OMZs of the global ocean: the Eastern Tropical North Pacific ([Jayakumar et al., 2017](#); [Selden et al., 2019](#)) and the Eastern Tropical South Pacific ([Bonnet et al., 2013](#); [Chang et al., 2019](#); [Fernandez et al., 2011](#); [Löschner et al., 2014](#)). Moreover, previous studies in other oceanic regions reported depth-integrated aphotic zone  $N_2$  fixation rates between 40 and 95% of the water column (up to 2000 m) activity ([Benavides et al., 2015](#); [Bonnet et al., 2013](#); [Rahav et al., 2013](#)). Yet, the  $N_r$  budget generated so far does not recognise  $N_2$  fixation rates from the aphotic zone of the global ocean.



## 1.4 C fixation in the global ocean

The ocean plays a fundamental role towards CO<sub>2</sub> sequestration through solubility and biological pump. The solubility pump is a physical process in which CO<sub>2</sub> dissolved in surface waters sinks to the ocean's interior. The solubility of gasses is more in colder waters than in warmer waters. Through thermohaline circulation, which is driven by the formation of deep water at high latitudes where seawater is usually colder and denser, CO<sub>2</sub> is transported from the ocean's surface to its interior. The global oceanic CO<sub>2</sub> sink is about 2 Pg C y<sup>-1</sup> from 1994 to 2007 ([DeVries, 2022](#)).

In the biological pump, phytoplankton perform C fixation, convert dissolved inorganic forms of C (i.e., CO<sub>2</sub>, HCO<sub>3</sub><sup>-</sup> and CO<sub>3</sub><sup>2-</sup>) to organic carbon using light as an energy source. Model estimates of the global ocean C fixation results in the net assimilation of 45–57 Pg C y<sup>-1</sup>, which is almost half of the net assimilation by photosynthetic organisms that occurs on the Earth's surface ([Field et al., 1998](#)). Most of the inorganic C that is fixed is respired back to CO<sub>2</sub> in the surface ocean through microbial degradation/remineralisation processes ([Turner, 2015](#)). This respired CO<sub>2</sub> is again reused or released to the atmosphere. But a fraction (5–25%) of the product of C fixation from the euphotic zone sinks as dead organisms and particles ([Rocha and Passow, 2007](#)), where some of it is respired in the intermediate layers and can remain sequestered for years to centuries ([DeVries et al., 2012](#)) and some of it is exported to the deep ocean ([Rocha and Passow, 2007](#)). Through this process, called the biological C pump, CO<sub>2</sub> is sequestered in the interior of the ocean for long periods of time, during which it cannot influence the climate ([Siegenthaler and Sarmiento, 1993](#)). It has been long believed that the biological pump is driven by photosynthetic organisms only, that prevail within the euphotic zone. However, in reality, C fixation may occur in the entire aphotic zone of the global ocean, predominantly by chemoautotrophs. Within the aphotic zone, while OMZs greatly increase the amount of C exported to the deep ocean sediments ([Devol and Hartnett, 2001](#)), they also appear suitable niches for chemoautotrophs.

C fixation in the suboxic and/or sulfidic oceanic basins like Baltic Sea, Cariaco Basin and in the coastal regions of the Eastern Tropical North and South Pacific have

been explored several times (*Günter et al.*, 2008; *Podlaska et al.*, 2012; *Taylor et al.*, 2001; *Vargas et al.*, 2021), but the open oceanic OMZs largely remain unassessed. The contribution of the aphotic zone C fixation in the global ocean towards C sink is widely different. Studies have reported that aphotic zone C fixation between 0.11 and 1.2 Pg C  $y^{-1}$  are associated with chemoautotrophic nitrification of the ammonium released through remineralisation of organic matter in the aphotic zone of the global ocean (*Meador et al.*, 2020; *Middelburg*, 2011; *Wuchter et al.*, 2006). *Reinthal et al.* (2010) extrapolated the measured aphotic zone C fixation rates to the aphotic zone of the global ocean between 0.8 and 1.1 Pg C  $y^{-1}$ . These estimates of the aphotic zone C fixation in the global ocean contribute significantly towards CO<sub>2</sub> drawdown and thus, should not be overlooked in the global C budget estimates. Since most of the studies are based on conversion factors, direct measurements are required for accurate estimates of aphotic zone C fixation and its contribution towards CO<sub>2</sub> sequestration.

## 1.5 The northern Indian Ocean

The database of N<sub>2</sub> fixation rates is limited spatially, lacking large regions of the global ocean especially the Indian Ocean (*Luo et al.*, 2012), despite the fact that the northern Indian Ocean is a unique basin which contains different biogeochemical gradients with eutrophic, oligotrophic and O<sub>2</sub> deficient waters. Additionally, it experiences a strong seasonal reversal of monsoon circulations (i.e., wind directions). Yet, the studies on N<sub>2</sub> fixation so far conducted in the Indian Ocean before the commencement of this thesis work have mostly focused on regions with *Trichodesmium* blooms in the northwestern part of the Indian Ocean (*Ahmed et al.*, 2017; *Capone et al.*, 1998; *Gandhi et al.*, 2011; *Kumar et al.*, 2017).

The northern Indian Ocean possesses twin non-identical basins — the Bay of Bengal and the Arabian Sea positioned at the eastern and the western side of the Indian peninsula, respectively. Both the basins are biogeochemically distinct owing to the influence of several physical processes. During the monsoon season, the winds over the northern Indian Ocean blow from the northeast during December to February (known as northeast or

winter monsoon) and reverse from the southwest direction (known as southwest or summer monsoon) during June to September. The transition periods between these monsoons, which occur from October to November and March to May are known as the fall and spring inter-monsoon, respectively. The seasonal variability in biological activity alternates from being highly productive during monsoons to oligotrophic during inter-monsoon periods in the Bay of Bengal and the Arabian Sea. Yet, both possess perennial OMZs with weaker seasonal variability in subsurface O<sub>2</sub> concentration (*DeSousa et al.*, 1996).

### 1.5.1 The Bay of Bengal

The Bay of Bengal is traditionally considered to have about eight times lower primary productivity in contrast of the Arabian Sea (*Prasanna Kumar et al.*, 2002). The Bay of Bengal receives copious riverine discharge ( $1.6 \times 10^{12} \text{ m}^3 \text{ y}^{-1}$ ) (*Subramanian*, 1993) through Ganges and Brahmaputra River system. But most of the nutrients coming through rivers are used within estuarine and coastal regions (*Prasanna Kumar et al.*, 2002; *Kumar et al.*, 2004; *Singh and Ramesh*, 2011) and does not reach the open Bay of Bengal. Further, the riverine freshwater efflux and heavy rainfall (2 m annually (*Prasad*, 1997)) stratifies the surface water of the Bay of Bengal that prevents the vertical influx of nutrients, and thereby limits primary productivity (*Prasanna Kumar et al.*, 2002). On the contrary, the N<sub>r</sub>-depleted waters create a conducive site for N<sub>2</sub> fixation. The Bay of Bengal receives substantial Fe through dry-deposition (*Srinivas and Sarin*, 2013), with surface dissolved Fe in the range of 0.2 to 0.5 nmol L<sup>-1</sup> in the north (5 °N to 18 °N) (*Grand et al.*, 2015; *Chinni et al.*, 2019). Hence, N<sub>r</sub>-depleted but Fe-replete surface water in the Bay of Bengal might facilitate the sustenance of diazotrophs and their N<sub>2</sub> fixation activity. The OMZs in the Bay of Bengal might also favour N<sub>2</sub> fixation.

### 1.5.2 The Arabian Sea

During the summer monsoon, the wind forcing is the strongest in the Arabian Sea that leads to intense upwelling along Somalia and Oman coast and open ocean, injecting nutrients to the surface and supporting one of the largest marine phytoplankton blooms and primary productivity ( $123 \text{ mmol C m}^{-2} \text{ d}^{-1}$ ) (*Barber et al.*, 2001)) (*Prasanna Kumar*

*et al.*, 2001; *McCreary et al.*, 2009; *Resplandy et al.*, 2011; *Prasanna Kumar and Prasad*, 1996). During the winter monsoon, cool and dry north-easterly winds pass over the Arabian Sea, which lead to surface water cooling and densification due to excess evaporation over precipitation and a net heat loss (*Prasanna Kumar and Prasad*, 1996). This results into convection and consequently, subsurface nutrient-replete and colder water mixes with the surface water due to convective mixing (*Madhupratap et al.*, 1996), as a result, fairly high primary production occurs in the Arabian Sea during the winter monsoon ( $112 \text{ mmol C m}^{-2} \text{ d}^{-1}$  (*Barber et al.*, 2001)).

The isotopic evidence of lower  $\delta^{15}\text{N}$  ( $\sim 6\text{‰}$ ) of  $\text{NO}_3^-$  above the OMZs of the Arabian Sea, in comparison to the highly enriched  $\delta^{15}\text{N}$  ( $\sim 15\text{‰}$ ) of  $\text{NO}_3^-$  within the OMZs (*Brandes et al.*, 1998), and excess  $\text{PO}_4^{3-}$  relative to  $\text{NO}_3^-$  suggest substantial  $\text{N}_2$  fixation in surface waters of the Arabian Sea (*Deutsch et al.*, 2007; *Mulholland and Capone*, 2009). The Arabian Sea also receives almost similar amount of Fe through dry-deposition (*Srinivas and Sarin*, 2013) alike the Bay of Bengal. Therefore, the Arabian Sea appears a perfect test site to examine the role of  $\text{PO}_4^{3-}$  and Fe availability in the vicinity of  $\text{NO}_3^-$  on  $\text{N}_2$  fixation. Moreover, the OMZs in the Arabian Sea might also favour  $\text{N}_2$  fixation.

### 1.5.3 Previous studies in the northern Indian Ocean

Up until the commencement of this work, no  $\text{N}_2$  fixation measurements in the oligotrophic Bay of Bengal were conducted. However in the Arabian Sea,  $\text{N}_2$  fixation rates measurements have been conducted several times but have mostly focused on regions with *Trichodesmium* blooms (*Ahmed et al.*, 2017; *Capone et al.*, 1998; *Gandhi et al.*, 2011; *Kumar et al.*, 2017). It has been reported that heterotrophic diazotrophic proteobacteria are also widely distributed and active in the nutrient-rich as well as oligotrophic waters of the Arabian Sea (*Bird et al.*, 2005; *Bird and Wyman*, 2013; *Jayakumar et al.*, 2012; *Shiozaki et al.*, 2014). Evidently, contrary to the historical observations of the leading role played by cyanobacterial diazotrophs in fixing  $\text{N}_2$  in the global ocean (*Capone et al.*, 1997; *Carpenter et al.*, 2004; *Karl et al.*, 2002), *Shiozaki et al.* (2014) and *Kumar et al.* (2017) discovered that NCDs dominate  $\text{N}_2$  fixation activity in the Arabian Sea.

The OMZs of the Bay of Bengal and the Arabian Sea are likely to be ecologically

advantageous for  $O_2$  and  $N_2$ -sensitive process of  $N_2$  fixation (*Burgess and Lowe, 1996; Deutsch et al., 2007*). Yet in the OMZ of the Arabian Sea only, the diazotrophic composition has been examined and a potential for active  $N_2$  fixation was suggested based on clone library analysis (*Bird and Wyman, 2013; Jayakumar et al., 2012*).

The Bay of Bengal and the Arabian Sea both possesses two of the most intense OMZs of the global ocean. They are well known for the abundance of anammox and nitrifying organisms (*Jayakumar et al., 2009; Lüke et al., 2016; Villanueva et al., 2014*). Yet no measurements have been conducted so far to assess aphotic zone C fixation in the Bay of Bengal and the Arabian Sea.

## 1.6 Scope of the present work

The aim of the present thesis work is to investigate the  $N_2$  and C fixation activity in the euphotic and aphotic zone of the northern Indian Ocean and to assess their potential environmental controls, particularly the influence of  $O_2$  concentration on the rates of  $N_2$  and C fixation. To fulfil this objective the following work is done:

- i.  $N_2$  and C fixation rates were measured in the Bay of Bengal and the Arabian Sea during monsoon and inter-monsoon season. This may help in revealing a quantitative importance of  $N_2$  fixation towards C fixation in the northern Indian Ocean.
- ii. Environmental parameters, such as temperature, salinity, nutrients and  $O_2$  concentrations, were measured in the water column to assess their control on  $N_2$  and C fixation rates variation.
- iii. Cyanobacterial community composition was identified to assess primary producers and cyanobacterial diazotrophs responsible for the observed rates of fixation in the Bay of Bengal.
- iv. Spatially different physicochemical sites in the coastal and open ocean of the Bay of Bengal and the Arabian Sea were sampled to assess the effect of contrasting physicochemical conditions on the rates of fixation and to further generate a spatial

understanding of the processes of  $N_2$  and C fixation. This may help in validating the biogeochemical models.

- v.  $N_2$  fixation by NCDs, dominating in the euphotic zone of the Arabian Sea, was measured to assess if their dominance really played an essential role than the long believed dominance of cyanobacterial diazotrophy in the global ocean.
- vi. The well reported traditional hypothesis of coupling between  $N_r$ -loss and -gain processes in the ocean was tested by assessing  $N_2$  fixation in the surface waters lying above the intense OMZs of the Arabian Sea.
- vii. The hypothesis that chemoautotrophic C fixation contributes significantly to sinking C fluxes in the OMZs of the Arabian Sea was examined. This may further help in resolving another hypothesis, i.e., some of the organic C demand of heterotrophs within the aphotic zone are fulfilled by autochthonously produced organic C.

# Chapter 2

## Materials and Methods

### 2.1 Sampling

To attain the objective of this thesis work, sampling was done during three research cruise expeditions: two in the Bay of Bengal and one in the Arabian Sea. Seawater was sampled from the Bay of Bengal during the summer monsoon (12 Jul – 2 Aug 2018) and the spring inter-monsoon (5–15 Apr 2019) on-board oceanographic research vessel (ORV)

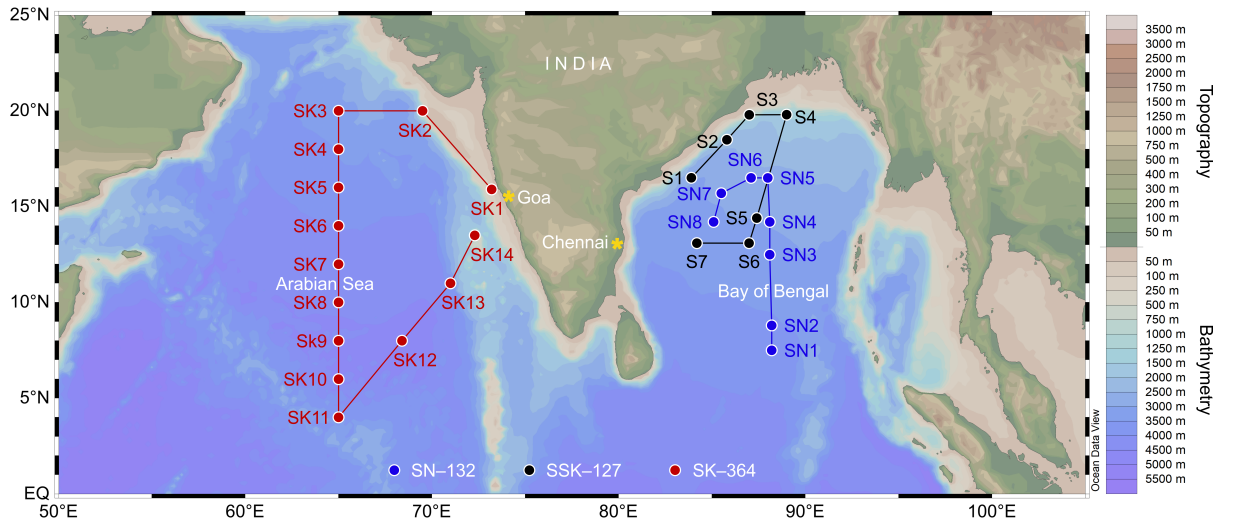


Figure 2.1: Sampling stations in the Bay of Bengal and the Arabian Sea during three research cruise expeditions: ORV *Sagar Nidhi* (SN-132), ORV *Sindhu Sankalp* (SSK-127) and ORV *Sagar Kanya* (SK-364). The sampling location labels SN, S and SK numbered stations show sampling during SN-132, SSK-127 and SK-364 cruises, respectively.

*Sagar Nidhi* (SN-132) and ORV *Sindhu Sankalp* (SSK-127), respectively (Figure 2.1). The Arabian Sea was sampled during the winter monsoon (17 Dec 2019 – 5 Jan 2020) onboard ORV *Sagar Kanya* (SK-364). The details of sampling locations with date and maximum depth of sampling are listed in (Table 2.1). The general sampling and measurement procedures of nutrients, physical parameters and incubation experiments for N<sub>2</sub> and C fixation rates are presented in the succeeding sections. It is recommended to consider methodology of individual chapters for related discrete and detailed specifications.

Table 2.1: Sampling locations with date and maximum depth of sampling.

Station no.	Date of sampling (dd.mm.yyyy)	Latitude (°N)	Longitude (°E)	Maximum sampling depth (m)
<b>SN-132</b>				
SN1	12.07.2018	07.5	88.2	75
SN2	16.07.2018	08.8	88.2	75
SN3	18.07.2018	12.5	88.1	75
SN4	19.07.2018	14.2	88.1	75
SN5	24.07.2018	16.5	88.0	75
SN6	29.07.2018	16.5	87.1	75
SN7	31.07.2018	15.7	85.5	75
SN8	02.08.2018	14.2	85.1	78
<b>SSK-127</b>				
S1	07.04.2019	16.5	83.9	1500
S2	08.04.2019	18.5	85.8	530
S3	09.04.2019	19.8	87.0	1000
S4	10.04.2019	19.8	89.0	1000
S5	12.04.2019	14.4	87.4	1500
S6	13.04.2019	13.1	87.0	1500
S7	14.04.2019	13.1	84.2	1000
<b>SK-364</b>				
SK1	17.12.2019	15.9	73.2	50
SK2	19.12.2019	20.0	69.5	140
SK3	21.12.2019	20.0	65.0	1000
SK4	22.12.2019	18.0	65.0	1000
SK5	23.12.2019	16.0	65.0	1000
SK6	24.12.2019	14.0	65.0	1000
SK7	26.12.2019	12.0	65.0	1000
SK8	27.12.2019	10.0	65.0	1000
SK9	29.12.2019	08.0	65.0	1000
SK10	30.12.2019	06.0	65.0	1000
SK11	31.12.2019	04.0	65.0	1000
SK12	02.01.2020	08.0	68.4	1000
SK13	04.01.2020	11.0	71.0	1000
SK14	05.01.2020	13.5	72.3	1000





Figure 2.2: Niskin bottles and CTD, O<sub>2</sub> concentration, fluorescence and photosynthetically active radiation sensors mounted on the rosette sampler during the *Sindhu Sankalp* (SSK-127) cruise in the Bay of Bengal.

## 2.2 Environmental parameters

The seawater temperature, salinity and density data were obtained using a Sea-Bird “conductivity, temperature and depth” (CTD) rosette sampler, along with O<sub>2</sub> concentration, fluorescence (indicative of chlorophyll *a*) and photosynthetically active radiation data us-

ing probes mounted on the rosette sampler. Seawater samples were collected using Niskin bottles assembled on the rosette sampler (Figure 2.2).

### 2.2.1 Nutrients concentration measurement

Samples for  $\text{NO}_3^-$ ,  $\text{NO}_2^-$  and  $\text{PO}_4^{3-}$  concentration measurements were collected in 60 mL high density polyethylene bottles in duplicates and frozen at  $-20^\circ\text{C}$  until analysis at the onshore Physical Research Laboratory, Ahmedabad, India. Nutrients were measured in an autoanalyzer (SKALAR, The Netherlands). Samples were thawed and gently shaken at room temperature before analysis.

Autoanalyzer works on the principle of “segmented flow analysis”, i.e., segmenting a continuously flowing stream with air bubbles. It is a continuous flow method of wet chemistry where samples and reagents are streamed, segmented with bubbles, pumped through a manifold for reactions and subsequently detected under a flow cell. The autoanalyzer consists of an autosampler, chemistry unit with detectors and data handling unit (Figure 2.3), where the chemistry unit consists of individual channels for automated and simultaneous measurement of  $\text{NO}_x$  (i.e.,  $\text{NO}_3^- + \text{NO}_2^-$ ),  $\text{NO}_2^-$  and  $\text{PO}_4^{3-}$  concentration.



Figure 2.3: SKALAR autoanalyzer at the Physical Research Laboratory, Ahmedabad, India.

$\text{NO}_x$  concentration measurement is based on the method of cadmium reduction. In this method, the sample buffered at  $\text{pH} \sim 8.2$  is reacted with granulated copper-cadmium which reduces  $\text{NO}_3^-$  to  $\text{NO}_2^-$ . The  $\text{NO}_2^-$  produced is measured at 540 nm with already

present  $\text{NO}_2^-$  in the sample, producing a result as a summation of  $\text{NO}_3^- + \text{NO}_2^-$  i.e.,  $\text{NO}_x$  concentration.

$\text{NO}_2^-$  concentration is measured as a reddish-purple colour complex at 540 nm formed as a product of reaction between diazonium compound (formed by diazotizing of sulphanilamide by  $\text{NO}_2^-$  in water sample under acidic conditions) and N-(1-naphthyl) ethylene diamine dihydrochloride.

$\text{PO}_4^{3-}$  concentration measurement is based on the reaction of a mixed reagent of ammonium heptamolybdate and potassium antimony (III) oxide tartrate in an acidic medium with diluted solutions of  $\text{PO}_4^{3-}$  to form an antimony-phospho-molybdate complex. This complex is reduced by ascorbic acid to an intensely blue coloured complex which is measured at 880 nm.

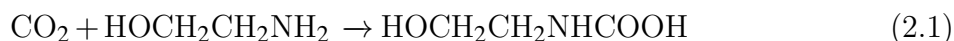
Reliability of produced data was checked every day by running certified reference materials, such as MOOS-3 ( $\text{NO}_x$  (i.e.,  $\text{NO}_3^- + \text{NO}_2^-$ ):  $26.6 \pm 0.3 \mu\text{mol L}^{-1}$ ,  $\text{NO}_2^-$ :  $3.54 \pm 0.05 \mu\text{mol L}^{-1}$ , and  $\text{PO}_4^{3-}$ :  $1.60 \pm 0.15 \mu\text{mol L}^{-1}$ ) from National Research Council, Canada ([Clancy et al., 2014](#)). The detection limit for  $\text{NO}_x$ ,  $\text{NO}_2^-$  and  $\text{PO}_4^{3-}$  was 0.16, 0.06 and  $0.02 \mu\text{mol L}^{-1}$ , respectively.

### 2.2.2 Dissolved inorganic carbon concentration

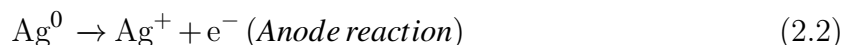
Samples for dissolved inorganic carbon (DIC) concentration measurements were collected in 12 mL exetainers vials (Labco, UK) in duplicates without leaving the headspace and preserved with mercuric chloride (100%  $\text{HgCl}_2$ ) solution to cease the microbial activity. DIC concentration with an analytical precision of  $\pm 2\%$  was measured using a Coulometer (UIC's Model 5012, USA) at the Physical Research Laboratory, Ahmedabad, India. Sodium carbonate ( $\text{Na}_2\text{CO}_3$ ) solution was used as a standard to verify the absolute values of DIC.

Coulometer measures the absolute mass of  $\text{CO}_2$  evolved after sample acidification, following the Faraday's law of electrolysis. Coulometer consists of an acidification unit and a coulometric cell. In the acidification unit, DIC dissolved in the liquid sample ( $\sim 20 \text{ mL}$ ) is converted to  $\text{CO}_2$  gas by acidifying the sample with 5 mL of 40% phosphoric acid and

heating at 80 °C (Figure 2.4). The emitted CO<sub>2</sub> gas is carried by CO<sub>2</sub> free atmospheric air (made by passing air through pre-air scrubber consisting of 45 g potassium hydroxide dissolved in 100 mL of deionised water) via silica gel scrubber (that removes the moisture from CO<sub>2</sub> sample) to the coulometric cathode cell. In the coulometric cell, the titration cell consists of a cathodic and an anodic solution and a platinum cathode and a silver anode dipped in the solutions, respectively. The cell assembly is placed between a light source and a photodetector in the coulometer cell compartment. The cathodic solution consists of a proprietary solution of ethanolamine and a colour (colorimetric) indicator. CO<sub>2</sub> gas passes through the cathodic solution, reacts with ethanolamine and forms a strong titratable acid (hydroxyethylcarbamic acid) that subsequently fades the colour of indicator:



As the hydroxyethylcarbamic acid changes the colour of indicator, the photodetector senses the change in the colour of solution as a percent transmittance (%T). As the %T increases, the titration current gets automatically activated at the rate proportional to the %T increase. The silver anode electrolyses to produce electrons (2.2), which move to the cathode and electrolyses water to H<sub>2</sub> and OH<sup>-</sup> ions (2.4). These OH<sup>-</sup> ions neutralise the hydroxyethylcarbamic acid (2.4) and as a result, the original colour of the indicator returns back and the current stops.



Coulometer works on the principle of Faraday's law of electrolysis: 1 faraday of electricity results in alteration of 1-gram equivalent weight of the substance during electrolysis.

Therefore, the amount of electric current generated, to release OH<sup>-</sup> ions neutralising the acid formed by DIC in the sample, is directly proportional to the amount of DIC present in the sample.

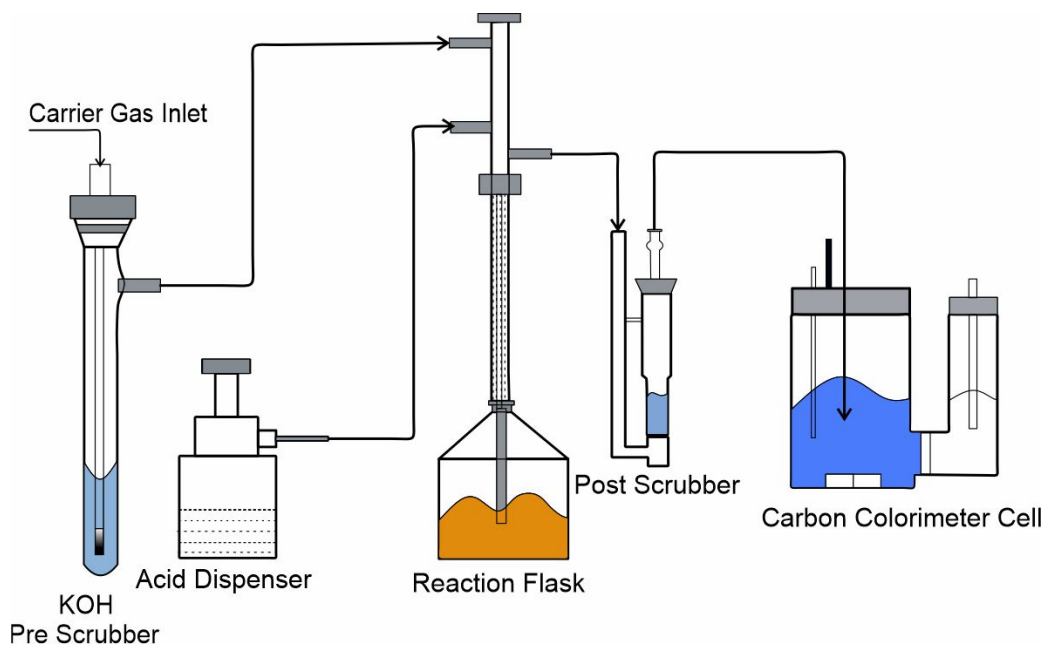


Figure 2.4: Schematic of UIC CO<sub>2</sub> Coulometer modified after “CM140 Total Inorganic Carbon Analysis by Acidification and Coulometric Detection (<https://www.uicinc.com/cm140-carbon-analysis/>)”.

## 2.3 N<sub>2</sub> and C fixation rates measurement

### 2.3.1 Principle

The measurement of N<sub>2</sub> fixation rates is based on the microbial rate of incorporation of added tracer, <sup>15</sup>N-labelled N<sub>2</sub> gas (98 atom% enriched), during incubation experiments (*Montoya et al.*, 1996). Similarly, C fixation rates are estimated based on the <sup>13</sup>C-labelled NaH<sup>13</sup>CO<sub>3</sub> (99 atom% enriched) tracer incorporation during incubation experiments (*Slawyk et al.*, 1977). The mass of particulate organic nitrogen (PON) and particulate organic carbon (POC), as well as their isotopic content, are required from natural (unspiked with tracer) and incubated (spiked with tracer) seawater samples to

calculate the rate of  $N_2$  and C fixation.

Isotopic compositions are denoted by  $\delta$  notation and expressed in ‰ unit:

$$\delta(\text{‰}) = \left( \frac{R_{\text{sample}}}{R_{\text{standard}}} - 1 \right) \times 1000 \quad (2.5)$$

where, R denotes the heavier to lighter isotope ratio.

The steps involved in the estimation of  $N_2$  and C fixation rates are shown in Figure 2.5.

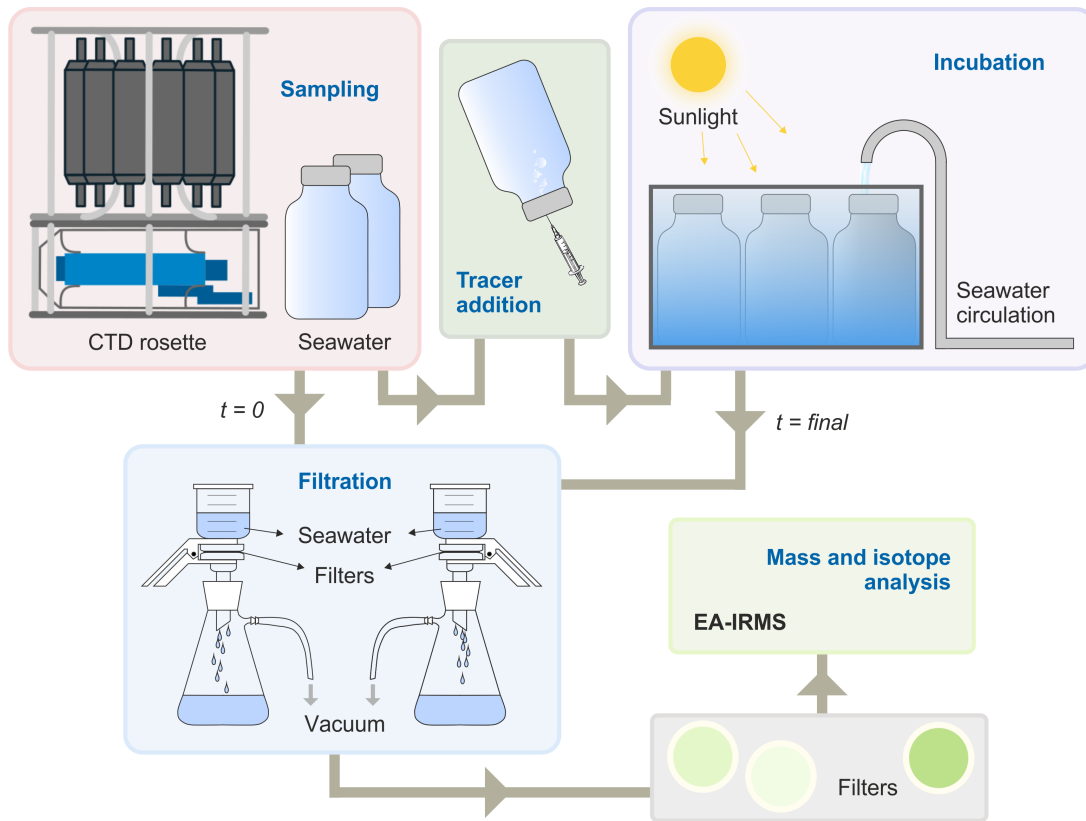


Figure 2.5: Flow diagram of  $N_2$  and C fixation rates measurement.

### 2.3.2 Tracer preparation

$^{15}N$ -labelled tracer: The  $^{15}N_2$  gas (98 atom% enriched) pressurised cylinder was procured from the Cambridge Isotope Laboratories, USA.

$^{13}C$ -labelled tracer: 5 g of  $NaH^{13}CO_3$  (99 atom% enriched; Cambridge Isotope Laboratories, USA; molecular weight: 85 g) was added in a 300 mL of deionized Milli-Q water,



mixed thoroughly to make  $\sim 0.2 \text{ mol L}^{-1}$  homogeneous working solution and stored in a polycarbonate bottle.

### 2.3.3 Sampling and tracer addition

Seawater samples were collected from the euphotic zone at cruise SN-132 and from the euphotic and aphotic zone at cruise SSK-127 and SK-364. Samples for natural seawater signatures were collected in singlicate and their volumes ranged between  $\sim 3.7$  to  $4.7 \text{ L}$  at cruise SN-132,  $2$  to  $4.7 \text{ L}$  at cruise SSK-127 and up to  $2.35 \text{ L}$  at cruise SK-364. Samples for tracer addition experiment were taken in duplicates in transparent polycarbonate bottles (Nalgene, USA) without leaving a headspace; the samples were collected in  $\sim 2.35 \text{ L}$  bottles at cruise SN-132, in  $\sim 2.35$  and  $\sim 4.7 \text{ L}$  for the euphotic and aphotic zone sample at cruise SSK-127, respectively, and in  $\sim 2.35$  and  $\sim 4.5 \text{ L}$  for the euphotic and aphotic zone sample at cruise SK-364, respectively. Tracers were added using a gas-tight syringe (Hamilton, UK) just before the beginning of incubation and at less than 10% of its ambient concentration.  $2 \text{ mL}$  of  $^{15}\text{N}_2$  gas was injected through the septum caps into  $2.35 \text{ L}$  sample bottle, while  $4 \text{ mL}$  of  $^{15}\text{N}_2$  gas was injected into  $4.5$  and  $4.7 \text{ L}$  bottle. Similarly,  $2 \text{ mL}$  of  $\text{NaH}^{13}\text{CO}_3$  working solution was pipetted to  $2.35 \text{ L}$  bottle and  $4 \text{ mL}$  to  $4.5$  and  $4.7 \text{ L}$  sample bottle.

### 2.3.4 Incubation

After addition of tracers, the bottles were gently shaken for  $\sim 5 \text{ min}$  to mix the tracers. The sample bottles from the euphotic zone were covered immediately with calibrated light filters to simulate the light conditions from where the samples were taken. Samples collected from the near surface ( $0$ – $10 \text{ m}$ ) were incubated without screening with light filters. The euphotic zone sample containing bottles were placed in an on-board incubator in which sea surface water was circulated to maintain the temperature. While the sample bottles from the aphotic zone were kept in the walk-in cold and dark room ( $\sim 10^\circ\text{C}$ ), which closely simulates the in situ temperature at which samples were collected. All the samples were incubated for  $24 \text{ h}$ , to cover one full day and night period, with an exception at cruise SN-132, where incubation was performed for  $4 \text{ h}$  (from  $10:00$  to  $14:00 \text{ h}$ ) at stations SN1

to SN7 but for 24 h at station SN8 (due to unavailability of CTD during the light period).

### 2.3.5 Filtration and preservation

The natural samples collected were immediately filtered after their collection and incubated samples were filtered after the completion of incubation period. The filters containing particulate matter were stored for the analysis of their PON and POC mass, and  $^{15}\text{N}$  and  $^{13}\text{C}$  isotopic composition in the mass spectrometer.

Filtration: The samples were vacuum filtered ( $< 200$  mm Hg; Millipore, USA) using a filtration unit under dim-light conditions, through pre-combusted (at  $400^\circ\text{C}$  for 4 h)  $0.7\ \mu\text{m}$  pore size Whatman glass microfiber filter (GF/F).

Preservation: The filters were dried overnight in an oven at  $50^\circ\text{C}$  and stored in sterile Petri dish for subsequent analysis in the mass spectrometer at the Physical Research Laboratory, Ahmedabad, India, with an exception at cruise SSK-127. At SSK-127, due to unavailability of oven on the cruise, the sample filters were immediately transferred in Petri dish and stored at  $-20^\circ\text{C}$ . On reaching the laboratory after the completion of cruise expedition, these filters were then dried overnight in an oven at  $50^\circ\text{C}$  and stored in Petri dish.

### 2.3.6 Sample preparation

Prior to mass and isotopic composition analysis in the mass spectrometer, the POC filters were decarbonated to remove inorganic carbon by exposing them to acid fumes with an open beaker of 36% hydrochloric acid (HCl) for 4 h and then dried overnight in an oven at  $50^\circ\text{C}$ , while the PON filters were not treated with the acid fumes following ([Lorrain et al., 2003](#)). Sample filters were packed in tin capsules and then the resultant sample pellets were analysed in the mass spectrometer.



### 2.3.7 Mass spectrometric analysis

The mass and isotopic composition ( $\delta^{15}\text{N}$  and  $\delta^{13}\text{C}$ ) of PON and POC samples were measured using an isotope ratio mass spectrometer (IRMS, Thermo Delta V Plus) coupled with an elemental analyser (FLASH 2000) connected via Conflo IV interface (Figure 2.6).

The analytical precision for both the PON and POC mass was  $< 10\%$ , and for the  $\delta^{15}\text{N}$  and  $\delta^{13}\text{C}$  it was  $< 0.3\text{‰}$  and  $0.1\text{‰}$ , respectively. The standards used for isotopic measurements were IAEA-N-2 ( $(\text{NH}_4)_2\text{SO}_4$ , 21.21%, 20.3‰) for N, and IAEA-CH-3 (Cellulose, 44.40%,  $-24.7\text{‰}$ ) for C, along with the internal laboratory standards. The final values are reported with respect to the international standards: Air-N<sub>2</sub> for  $\delta^{15}\text{N}$  and Vienna-Pee Dee Belemnite (V-PDB) for  $\delta^{13}\text{C}$ . The basic principle of IRMS is to accelerate ionised molecules of gas through a magnetic field in order to separate them by their mass to charge ( $m/q$ ) ratio (Figure 2.7). This basic principle is detailed below.

#### 2.3.7.1 Elemental analyser

Elemental analyser uses a high temperature “flash” combustion method, which ultimately converts all the PON and POC content in a sample to N<sub>2</sub> and CO<sub>2</sub> gas, respectively.

Elemental analyser consists of two reaction chambers (containing a shared combustion and oxidation column and a separate reduction column, both made of quartz tube having melting point of  $\sim 1800^\circ\text{C}$ ), a moisture trap and a gas chromatograph (Figure 2.7). Typically, the reaction columns are of 45 cm in length, with an outer diameter of 1.8 cm and an inner diameter of 1.4 cm; the moisture trap is a tube of length 12 cm, with an outer diameter of 1.5 cm; a gas chromatograph (a molecular sieve of zeolites) is a coiled capillary/column of 100 cm in length, with an outer diameter of 0.4 cm and an inner diameter of 0.16 cm. Additionally, a turret of an autosampler with a carousel, where samples are loaded, is attached to the top of the oxidation chamber, that automates the descent of a sample inside the oxidation column.

The oxidation column is prepared by filling it with silvered cobaltous oxide ( $\sim 3$  cm height) and chromium oxide ( $\sim 12$  cm height), separated ( $\sim 1$  cm height) and bracketed ( $\sim 5$  cm height) by quartz wool. The reduction column is prepared by filling it with



Figure 2.6: FLASH 2000 EA connected to Thermo Delta V Plus-IRMS at the Physical Research Laboratory, Ahmedabad, India.

reduced copper granules ( $\sim 20$  cm) and bracketed by quartz wool ( $\sim 5$  cm). The moisture trap is filled with anhydrous magnesium perchlorate granules and bracketed by quartz wool ( $\sim 1$  cm).

On command, the autosampler drops the capsulated sample inside the column of oxidation chamber. The oxidation chamber, typically set at  $1000^\circ\text{C}$ , thermally combusts the sample with a flash in the presence of purged  $\text{O}_2$  pulse. Upon combustion, the  $\text{O}_2$

and oxidising agents mainly produce the oxides of C, N and hydrogen (H), such as CO<sub>2</sub>, N<sub>x</sub>O<sub>y</sub> and water (H<sub>2</sub>O), respectively. A constant flow of pure helium (He) gas carries these oxidised gases to the reduction column, typically maintained at 600 °C. The copper present inside the reduction column reduces different oxides of N to N<sub>2</sub> gas, but leaves CO<sub>2</sub> and H<sub>2</sub>O in their oxidised yet stable form. The He flow further carries these gases along with a mixture of other gases to the moisture trap, where H<sub>2</sub>O gets absorbed by magnesium perchlorate. The remaining gases with the He flow pass through the gas chromatograph (maintained at around 45 °C), where they are separated based on their retention time inside the zeolite capillary. These separated gases enter into the IRMS via Conflo.

### 2.3.7.2 Isotope ratio mass spectrometer

IRMS (Thermo Delta V Plus) consists of three main components: ion source, analyser and detector (Figure 2.7). Generally, the ion source is made of thorium coated tungsten filament, which emits accelerated electrons upon heating at 1.5 A current and creating a potential difference. These accelerated electrons knock out an electron from the sample gas under vacuum, and as a result, positively ionise them. The accelerated ions exit the ion source through a slit and enters into the analyser.

Gas molecules with charge ( $q$ ) accelerate under voltage ( $V$ ) as:

$$qV = \frac{1}{2}mv^2 \quad (2.6)$$

where  $m$  is the mass of the molecule and  $v$  is the velocity with which it escapes the ion source.

In the analyser, a strong magnetic field and a high voltage ( $\sim 2.5$  kV) potential difference are applied to accelerate the positively charged ions. The direction of the uniform magnetic field is perpendicular to the direction of the moving ions. The geometry of the analyser (i.e., magnetic sector) is such that the ion beam enters and exits the analyser at an angle to facilitate the separation of ions. In the analyser, the ions are separated based on their  $m/q$  ratio. For CO<sub>2</sub> ions, the beams with masses 44, 45, and 46 atomic mass unit (corresponding to <sup>12</sup>C<sup>16</sup>O<sub>2</sub>, <sup>12</sup>C<sup>16</sup>O<sup>17</sup>O, <sup>13</sup>C<sup>16</sup>O<sub>2</sub>, <sup>12</sup>C<sup>17</sup>O<sup>17</sup>O, <sup>13</sup>C<sup>16</sup>O<sup>17</sup>O

and  $^{12}\text{C}^{16}\text{O}^{18}\text{O}$ ) are produced. For  $\text{N}_2$ , beams with 28, 29, and 30 atomic mass units (corresponding to  $^{14}\text{N}_2$ ,  $^{14}\text{N}^{15}\text{N}$ , and  $^{15}\text{N}_2$ , respectively) are produced. These ions follow curvilinear path owing to the Lorentz force, which is balanced by the centripetal force on the ion beam entering perpendicular to the magnetic field ( $B$ ) direction (equation (2.7)):

$$q(\mathbf{v} \times \mathbf{B}) = \frac{mv^2}{r} \quad (2.7)$$

where  $r$  is the radius of curvature. Combining equations (2.6) and (2.7),

$$r^2 = \frac{2mV}{qB^2} \quad (2.8)$$

The beam of isotopically lighter ions ( $^{12}\text{C}^{16}\text{O}^{16}\text{O}$ ;  $m/q = 44$ ) deflects more than the beam of isotopically heavier ions ( $^{13}\text{C}^{16}\text{O}^{16}\text{O}$ ;  $m/q = 45$ ) (equation (2.8)). These deflected ions after acceleration through the analyser, enters into the detector.

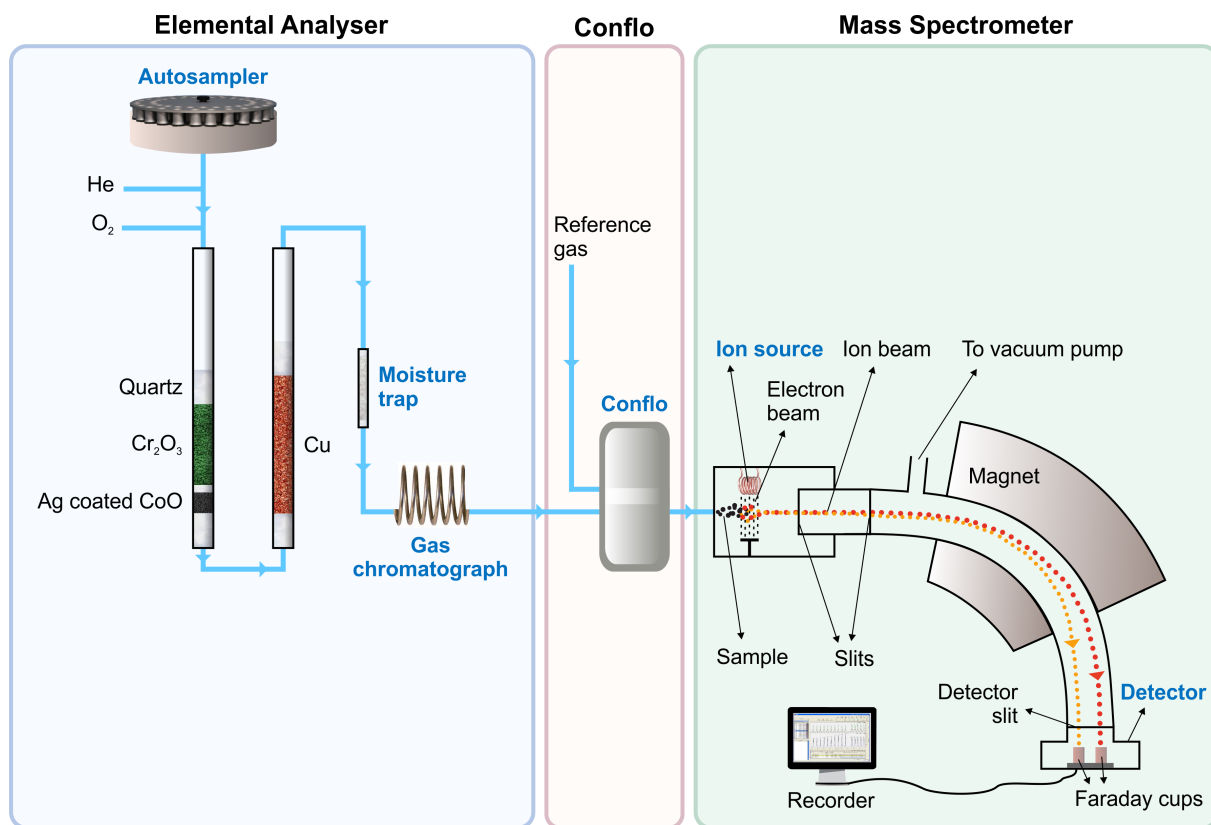


Figure 2.7: A schematic showing elemental analyser connected to isotope ratio mass spectrometer via Conflo.

The detector consists of Faraday cups (i.e., metal cups) connected to resistors ( $\sim 10^9 \Omega$ ), that records the current produced when an ion becomes neutralise after hitting the surface of a metal cup. The movement of an electron from a metal cup to a positively charged ion produces current that is passed through the external high resistance resistors. The voltage across the resistance produced by ions is measured, that is proportional to the number of ions entering into a Faraday cup per unit time.

### 2.3.8 Estimation of fixation rates

Two stable isotopes of N are <sup>14</sup>N and <sup>15</sup>N which contribute 99.636 and 0.364%, respectively, to the total N in the environment. Similarly, C has <sup>12</sup>C and <sup>13</sup>C as two stable isotopes having abundance of 98.887 and 1.113%, respectively. The lower abundance of heavier isotopes is used as a tool for isotope labelling technique ([Dugdale and Wilkerson, 1986](#)), a concept at which tracer incubation experiments are based for the estimation of N<sub>2</sub> and C fixation rates.

The concept of N<sub>2</sub> fixation is based on the isotopic mass balance at the end of the incubation, i.e., the number of <sup>15</sup>N atoms in final PON is equal to the sum of number of <sup>15</sup>N in the initial PON and the number of <sup>15</sup>N atoms from the ambient N<sub>2</sub> gas taken up.

$$A_{PN_f}[PON_f] = A_{PN_0}[PON_0] + A_{N_2}\Delta[PON] \quad (2.9)$$

where,

$A_{PN_f}$  = <sup>15</sup>N atom% in PON at the end of incubation,

$A_{PN_0}$  = <sup>15</sup>N atom% in PON at the start of the incubation,

$A_{N_2}$  = <sup>15</sup>N enrichment in the dissolved phase after tracer addition at the start of the incubation.

$[PON_f]$  = concentration of PON at the end of the incubation,

$[PON_0]$  = concentration of PON at the start of the incubation,

$\Delta[PON]$  = N<sub>2</sub> taken up during incubation.

Since,

$$[PON_f] = [PON_0] + \Delta[PON] \quad (2.10)$$

$$[PON_0] = [PON_f] - \Delta[PON] \quad (2.11)$$

Combining equation (2.9) and equation (2.11),

$$A_{PN_f}[PON_f] = A_{PN_0}([PON_f] - \Delta[PON]) + A_{N_2}\Delta[PON] \quad (2.12)$$

$$[PON_f](A_{PN_f} - A_{PN_0}) = \Delta[PON](A_{N_2} - A_{PN_0}) \quad (2.13)$$

$$\Delta[PON] = [PON_f] \left( \frac{A_{PN_f} - A_{PN_0}}{A_{N_2} - A_{PN_0}} \right) \quad (2.14)$$

In the above equation, all the terms are measured except  $A_{N_2}$ , which is defined as:

$$A_{N_2} = \left( \frac{{}^{15}\text{N}_{\text{tracer}} \times [\text{tracer}] + {}^{15}\text{N}_{\text{natural}} \times [\text{natural}]}{[\text{tracer}] + [\text{natural}]} \right) \quad (2.15)$$

where,

$${}^{15}\text{N}_{\text{tracer}} = {}^{15}\text{N atom\% of tracer},$$

${}^{15}\text{N}_{\text{natural}} = {}^{15}\text{N atom\% of N}_2 \text{ gas already present in the dissolved phase before tracer addition},$

$$[\text{tracer}] = \text{tracer gas concentration at the start of the incubation},$$

$[\text{natural}] = \text{N}_2 \text{ gas concentration already present in the dissolved phase before tracer addition}.$

The natural concentration of dissolved  $\text{N}_2$  was calculated following the formula given

in [Weiss \(1970\)](#), that expresses the solubility of N<sub>2</sub> gas as a function of in situ temperature and salinity.

Volumetric rate of N<sub>2</sub> fixation:

$$N_2 \text{ fixation rate} = \frac{[PON_f]}{t} \left( \frac{A_{PN_f} - A_{PN_0}}{A_{N_2} - A_{PN_0}} \right) \quad (2.16)$$

where  $t$  = incubation time.

The tracer incubation experiments are performed with the following assumptions:

- i. There exist only a single N source for ingestion by phytoplankton.
- ii. Phytoplankton do not discriminate between the heavier and lighter isotopes during fixation.
- iii. There is no excretion of nitrogen by phytoplankton.
- iv. There is no grazing by zooplankton.
- v. <sup>15</sup>N atom% in the dissolved phase remains constant.

Similarly, C fixation rates were calculated likewise to N<sub>2</sub> fixation rates.

$$C \text{ fixation rate} = \frac{[POC_f]}{t} \left( \frac{A_{PC_f} - A_{PC_0}}{A_C - A_{PC_0}} \right) \quad (2.17)$$

where,

$t$  = incubation time,

$A_{PC_f}$  = <sup>13</sup>C atom% in POC at the end of incubation,

$A_{PC_0}$  = <sup>13</sup>C atom% in POC at the start of the incubation,

$A_C$  = <sup>13</sup>C enrichment in the dissolved form after the tracer addition at the start of the incubation.

In the above equation, all the terms are measured except  $A_C$ , which is defined as:

$$A_C = \left( \frac{^{13}\text{C}_{\text{tracer}} \times [\text{tracer}] + ^{13}\text{C}_{\text{natural}} \times [\text{natural}]}{[\text{tracer}] + [\text{natural}]} \right) \quad (2.18)$$

where the measured value of natural concentration of DIC in seawater was used.

Depth-integrated  $\text{N}_2$  and C fixation rates were calculated by the trapezoidal integration of volumetric rates, where mean of volumetric rates was multiplied by the corresponding depth interval and then summed for all the depth intervals. Based on the natural molar POC:PON ratio at each depth, the  $\text{N}_r$  demand to fuel the observed C fixation rates was calculated.  $\text{N}_2$  fixation rates were divided by this demand estimate to calculate the percentage contribution of  $\text{N}_2$  fixation to C fixation rates.

## 2.4 Cyanobacterial community analysis

For the analysis of cyanobacterial community composition, 16S rRNA gene amplicon sequencing was performed. The 16S rRNA gene amplicon sequencing provides the whole prokaryotic community composition. In this thesis, DNA sampling was performed on-board cruise SSK-127 only and cyanobacterial community out of the whole prokaryotic community composition data is discussed in this thesis work. For DNA samples,  $\sim 1$  L seawater was filtered through a 47 mm GTTP filter (0.2  $\mu\text{m}$  pore size) and stored at  $-20^\circ\text{C}$  until analysed. The filters were cut into small parts for DNA extraction using a sterile scalpel blade no. 4 (Himedia laboratories, India) and extracted using the DNA Extraction Kit (QIAGEN DNeasy PowerSoil Pro Kit) according to the manufacturer's protocols. DNA concentration was quantified using a Qubit 2000 UV fluorometer and a dsDNA HS Assay kit (Thermo Fisher Scientific v 3.0).

The 16S rRNA gene amplicon sequencing was performed on the Illumina-MiSeq platform. The hypervariable region V4 of the 16S rRNA gene was targeted for sequencing using the MiSeq 250\*2 paired-end sequencing chemistry. The DNA was quantified using the Qubit dsDNA BR Assay kit (Thermo Fisher Scientific Inc.). 1  $\mu\text{L}$  of each sample was



used for determining concentration using the Qubit 2.0 Fluorometer. PCR amplification of the V4 region of the 16S rRNA gene was carried out using the primer set 515F (5' GTGCCAGCMGCCGCGGTAA) and 806R (5' GACTACHVGGGTATCTAATCC). The thermocycling procedure involved an initial denaturation at 95 °C for 3 min, followed by 20 cycles of 95 °C for 30 seconds, 55 °C for 30 seconds, and 72 °C for 30 seconds, and a final extension at 72 °C for 5 minutes. The PCR steps were performed in triplicates and pooled after amplification. The amplicons with the Illumina adaptors were amplified by using i5 and i7 primers that add multiplexing index sequences and standard adapters required for cluster generation (P5 and P7) as per the standard Illumina protocol. The amplicon libraries were purified by 1X AMPureXP beads, checked on an Agilent DNA 1000 chip on Bioanalyzer 2100, and quantified on a fluorometer by Qubit dsDNA HS Assay kit (Life Technologies). Multiplexing of the equimolar concentration of DNA was carried out in such a way that at least 0.1 million reads were generated for each sample.

All raw sequences were processed using Quantitative Insights into Microbial Ecology (QIIME2 version 2020.8). High-quality sequences were obtained by removing sequences with primer mismatches and average quality scores of  $< 25$  and lengths (excluding the barcode region or primer) of  $< 50$  bp, denoising the reads into amplicon sequence variants (ASVs) with DADA2. Taxonomy was assigned to the ASVs with the SILVA138 database. All possible contaminants were filtered out, including mitochondria, chloroplast, Eukaryota, and unassigned ASVs.

## 2.5 Statistical analyses

Spearman's correlation coefficient at  $\alpha < 0.05$  was used to test the strength of relationships between the rates and environmental parameters. Spearman's correlation analysis was conducted in MATLAB 2021 (noa, 2021), and only the parameters which significantly correlated with the rates are indicated.

A statistically significant difference between the average values of fixation rates was tested following *Chao* (1974). Two mean values ( $\mu_1$  and  $\mu_2$ ) are considered to be significantly different from each other at  $\alpha < 0.05$ , if  $\mu_1 - \mu_2 \geq 1.645 \sqrt{\frac{\sigma_1^2}{n_1} + \frac{\sigma_2^2}{n_2}}$ , where  $\sigma_1$  and

$\sigma_2$  are the standard deviations around the mean values  $\mu_1$  and  $\mu_2$  calculated from data points  $n_1$  and  $n_2$ , respectively.

## Chapter 3

# N<sub>2</sub> and C fixation in the Bay of Bengal during the summer monsoon

### 3.1 Introduction

The Bay of Bengal is surrounded by the Indian subcontinent in the north and north-west and the Andaman and Nicobar Islands in the east. It experiences semi-annual seasonality of the Asian monsoon system ([Gadgil, 2003](#)). Strong southwesterly winds lead to high rainfall over the Indian subcontinent during the summer monsoon whereas northeasterly winds lead to heavy rainfall particularly in the southern states of India. Large freshwater influx ( $1.6 \times 10^{12} \text{ m}^3 \text{ y}^{-1}$ ) ([Subramanian, 1993](#)) from the Ganges and Brahmaputra River system in the Bay of Bengal drives strong water column density gradient leading to stratification and usually high sea surface temperature ([Subramanian, 1993](#); [Shetye et al., 1991](#)). The stratification prevents the upward influx of nutrients in the Bay of Bengal ([Prasanna Kumar et al., 2010b](#)). The input of nutrients through riverine discharge enhances the productivity in the coastal Bay of Bengal ([Choudhury and Pal, 2010](#); [Dutta et al., 2019](#)). Most of the nutrients coming through rivers are used within estuarine and coastal regions ([Prasanna Kumar et al., 2002](#); [Singh and Ramesh, 2011](#)). Thus, riverine nutrients have negligible contribution on biological production of the offshore region of the Bay of Bengal ([Duce et al., 2008](#); [Singh and Ramesh, 2011](#)). In such cases, N<sub>2</sub> fixation in the Bay of Bengal could be of considerable importance for C fixation. The stratified, warm and nutrient-depleted waters of the Bay of Bengal appear to favour diazotrophy.

Yet, the diazotrophy in the euphotic zone of the Bay of Bengal remained unstated with no database for the N<sub>2</sub> fixation rates before the commencement of this thesis work.

The main objectives of the present study were to understand the role of stratification and oligotrophic conditions on N<sub>2</sub> fixation rates in the Bay of Bengal during summer monsoon and to estimate the contribution of N<sub>2</sub> fixation to C fixation in the euphotic zone of the Bay of Bengal.

## 3.2 Materials and Methods

Seawater samples were collected in the Bay of Bengal at eight locations (SN1–SN8) during the summer monsoon (12 Jul – 2 Aug 2018) on-board ORV *Sagar Nidhi* (SN–132) (Figure 3.1). The samples were taken at four depths from the top 75 m of the euphotic zone. The top two sampling depths were fixed at 10 and 25 m. The next two depths were mostly 50 and 75 m but at times one of these depths was changed to match the depth of deep chlorophyll maxima (DCM). Samples were collected from Niskin bottles mounted on a Sea-Bird CTD rosette sampler.

The measurement of nutrients, DIC, mass and  $\delta^{13}\text{C}$  of POC, and mass and  $\delta^{15}\text{N}$  of PON are discussed in Chapter 2.

Indian National Centre for Ocean Information Services Real-Time Automatic Weather Stations provided wind speed data (*Harikumar et al.*, 2013). Mixed layer depth (MLD) was determined based on the variation in temperature (0.2 °C difference from SST) (*de Boyer Montégut et al.*, 2004). The N demand of C fixation rates was calculated using the Redfield ratio (C:N = 106:16, *Redfield* (1934)) by dividing the observed C fixation rates (in molar units) with 6.625. N<sub>2</sub> fixation rates were then divided by the N demand estimate to calculate the percentage contribution of N<sub>2</sub> fixation to C fixation.

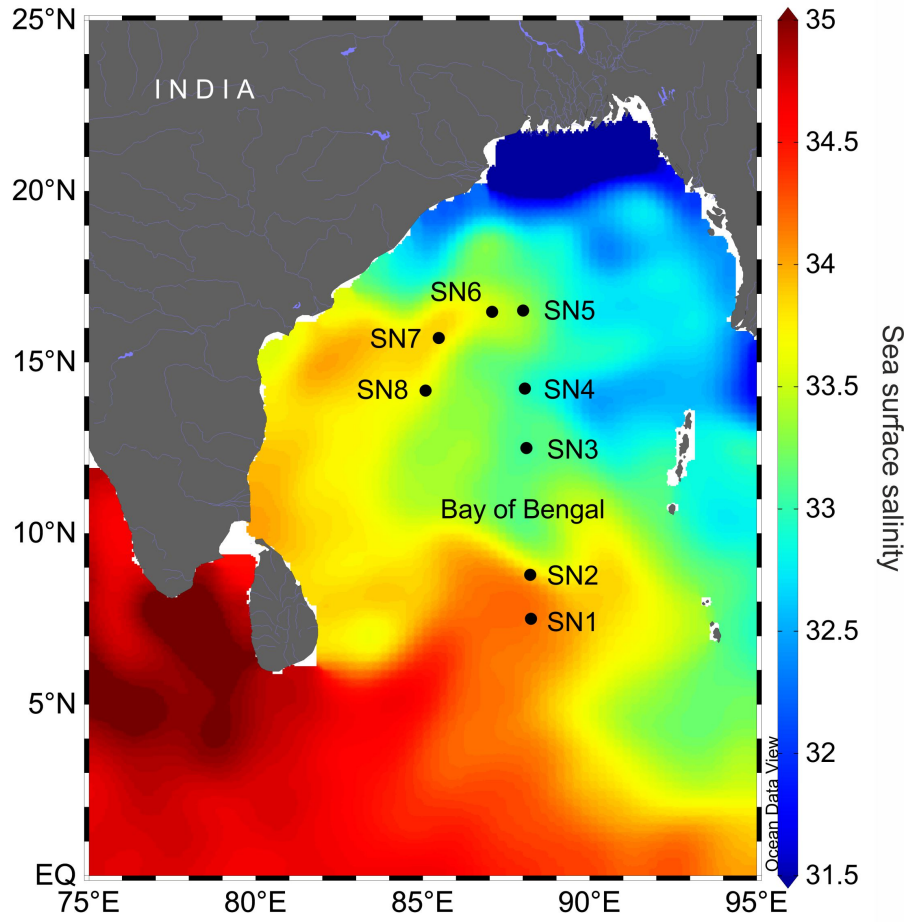


Figure 3.1: Sampling stations (SN1–SN8) superimposed on sea surface salinity (obtained from Multi-Mission OISST Global Dataset V1.0 for Jul 2018) in the Bay of Bengal during the research cruise expedition ORV *Sagar Nidhi* (SN–132)

### 3.3 Results

#### 3.3.1 Environmental conditions

The SST was higher than 28 °C at all the stations (Table 3.1). The lowest SST (28.1 °C) was observed at SN2 and the highest at SN8 (29.1 °C). Salinity varied between 32.8 and 34.4, with the lowest value at SN4 and the highest value at SN2. Surprisingly, no north-south gradient in SST and sea surface salinity was observed in the Bay of Bengal (Figure 3.2). Wind speed ranged between 3.6 to 24.5  $\text{m s}^{-1}$  (average: 11.5  $\text{m s}^{-1}$ ) during the study period and MLD ranged between 41 and 77 m, with the lowest value observed

Table 3.1: Details of sea surface temperature (SST), sea surface salinity (SSS), deep chlorophyll maxima (DCM), mixed layer depth (MLD), N:P, depth integrated N<sub>2</sub> and C fixation rates at each station.

Station	SST (°C)	SSS	DCM (m)	MLD (m)	N:P	N <sub>2</sub> fixation ( $\mu\text{mol N m}^{-2} \text{d}^{-1}$ )	C fixation ( $\text{mmol C m}^{-2} \text{d}^{-1}$ )
SN1	28.8	34.2	75	64	1.2–6.0	$11 \pm 5$	$30 \pm 8$
SN2	28.1	34.4	25	49	4.3–9.4	$6 \pm 6$	$87 \pm 11$
SN3	28.8	33.1	57	52	0.8–12.4	$27 \pm 16$	$39 \pm 4$
SN4	28.5	32.8	55	48	1.5–12.4	$20 \pm 4$	$24 \pm 2$
SN5	28.2	33.5	47	43	1.0–9.2	$4 \pm 4$	$69 \pm 5$
SN6	28.7	33.4	76	77	0.0–6.4	$12 \pm 8$	$58 \pm 13$
SN7	28.7	33.6	55	41	1.7–11.1	$75 \pm 98$	$81 \pm 12$
SN8	29.1	33.0	78	66	1.8–4.6	$41 \pm 6$	$45 \pm 4$

at SN7 and the highest at SN6.

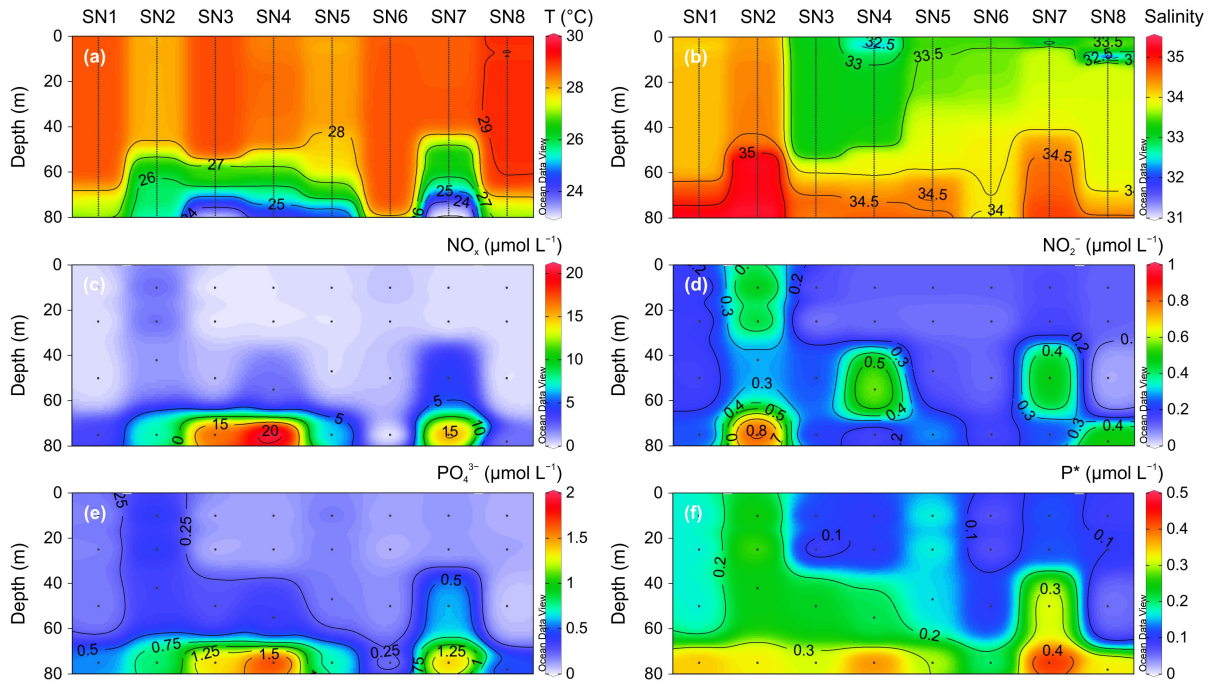


Figure 3.2: Vertical profiles of (a) temperature (T), (b) salinity, (c) NO<sub>x</sub>, (d) NO<sub>2</sub><sup>-</sup>, (e) PO<sub>4</sub><sup>3-</sup> and (f) P\* at each station.

### 3.3.2 Nutrients

The concentration of all the nutrients was above the detection limit, except NO<sub>x</sub> in the upper 25 m of station SN3. In general, NO<sub>x</sub> concentration was lower at the surface

and gradually increased with depth (Figure 3.2c). Similar to  $\text{NO}_x$ ,  $\text{NO}_2^-$  and  $\text{PO}_4^{3-}$  also increased with depth (Figure 3.2d, e). N:P was lower than the Redfield ratio and varied from 0 to 12.4 except at station SN7 (N:P = 16.4; 75 m) (Table 3.1).  $P^*$  was positive throughout the study period (Figure 3.2f), which indicated that  $\text{PO}_4^{3-}$  concentration was in excess of  $\text{NO}_x$ . The  $\delta^{15}\text{N}$  of natural PON increased with depth and varied between 1 to 6‰ at surface with an average of 3.2‰ and 1 to 8‰ at lower depths with an average of 4.5‰ (Figure 3.3).

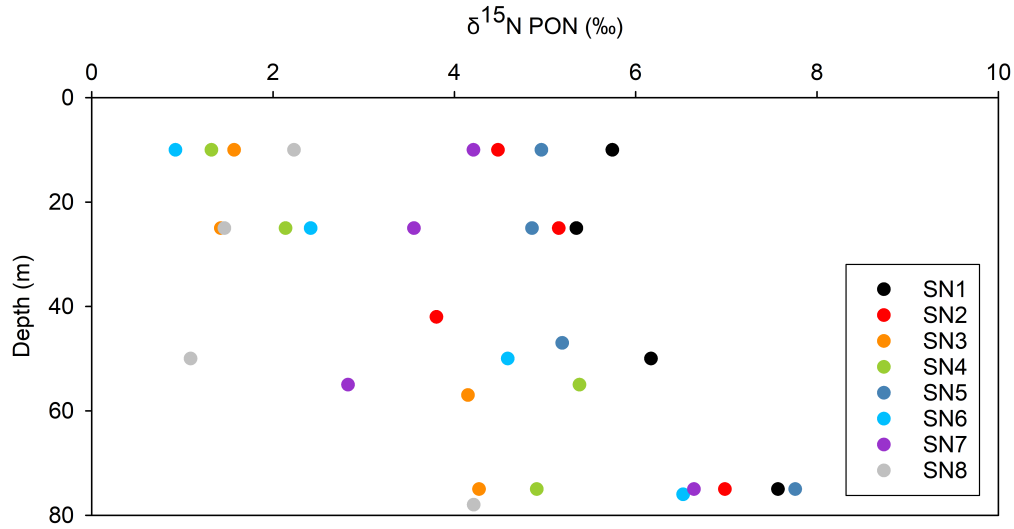


Figure 3.3: Vertical profiles of  $\delta^{15}\text{N}$  of natural PON at each station.

### 3.3.3 $\text{N}_2$ and C fixation rates

Volumetric  $\text{N}_2$  fixation rates varied from 0 (below detection limit) to  $0.56 \text{ nmol N L}^{-1} \text{ h}^{-1}$  with the highest rate at station SN7 (Figure 3.4a). Except at the surface of station SN7, the rates were less than  $0.08 \text{ nmol N L}^{-1} \text{ h}^{-1}$ . The  $\text{N}_2$  fixation rates were higher near the surface and decreased gradually with depth. C fixation rates varied from 1.4 to  $282.2 \text{ nmol N L}^{-1} \text{ h}^{-1}$  (Figure 3.4b) with the highest rate at SN7. The depth integrated  $\text{N}_2$  and C fixation rates ranged between 4 and  $75 \text{ } \mu\text{mol N m}^{-2} \text{ d}^{-1}$  and 24 to  $87 \text{ mmol C m}^{-2} \text{ d}^{-1}$ , respectively, (Table 3.1).  $N_r$  demand estimated based on the Redfield ratio for sustaining the observed C fixation was almost two orders of magnitude greater than the  $N_r$  provided by observed  $\text{N}_2$  fixation (Figure 3.5). Contribution of  $\text{N}_2$  fixation to C fixation was almost negligible ( $< 0.61\%$ ) at all the stations.

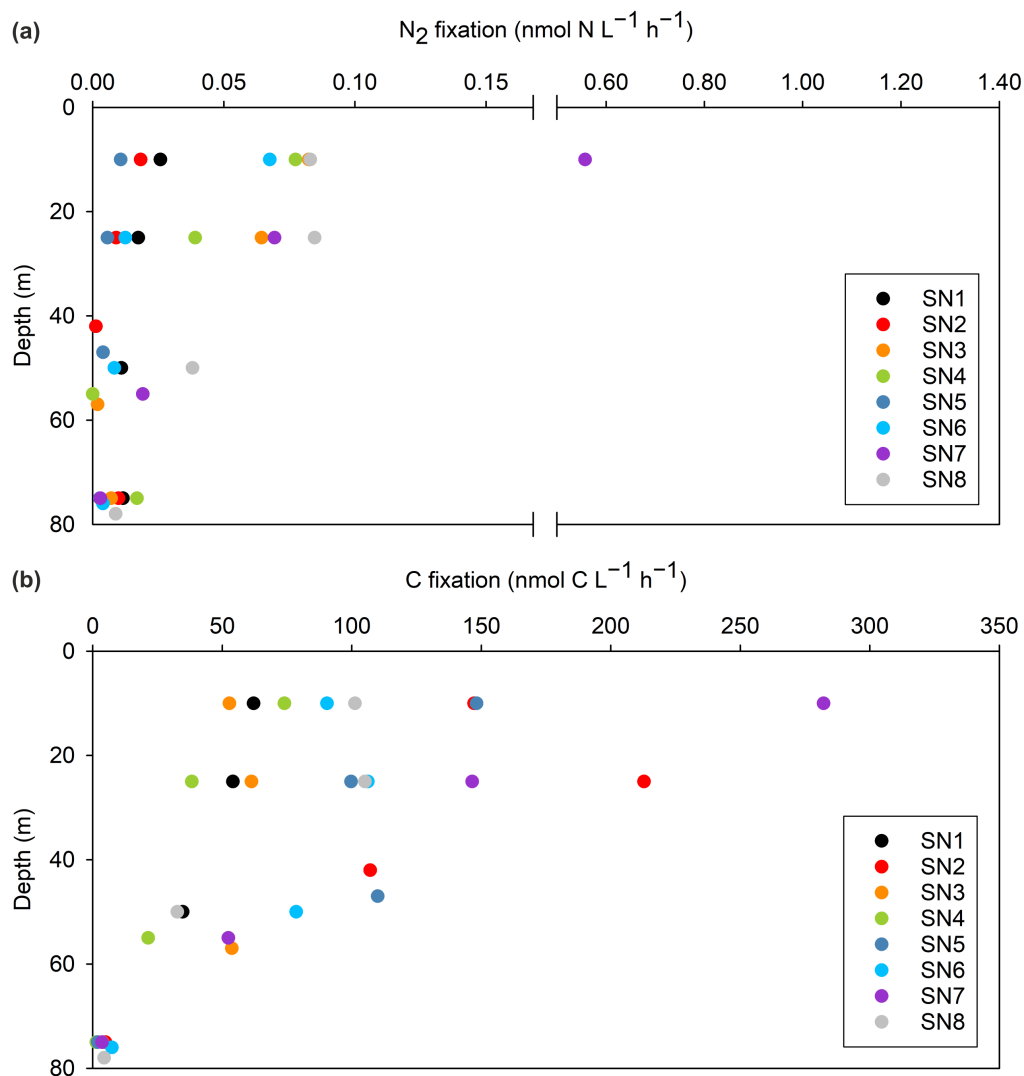


Figure 3.4: Vertical profiles of average volumetric rates of (a)  $N_2$  fixation and (b) C fixation at each station.

### 3.4 Discussion

For C fixation by organisms sunlight, water,  $\text{CO}_2$  and nutrients are needed ([Capone et al., 2008](#)). In the tropical oceans, sunlight is usually not a limiting factor, and water and  $\text{CO}_2$  in the oceans are abundant enough to not limit the C fixation. But the availability of macronutrients (such as  $N_r$  and  $\text{PO}_4^{3-}$ ) and micronutrients (such as Fe) limit C fixation in the sunlit layer of the oceans ([Capone et al., 2008](#)). The ocean receives nutrients through river run off, atmospheric deposition, eddy, upwelling, and cyclones. Primary producers can actively assimilate anthropogenic  $N_r$  also to meet the N demand for their cellular



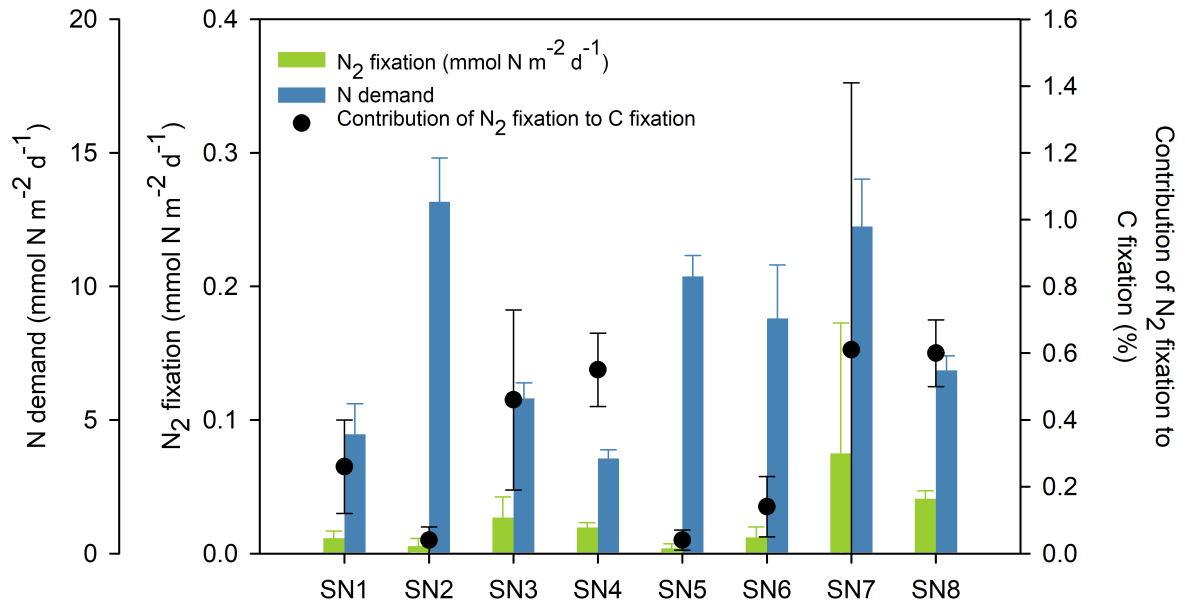


Figure 3.5: Euphotic zone integrated N demand, N<sub>2</sub> fixation rates and contribution of N<sub>2</sub> fixation to C fixation at each station.

activity. Most of the  $N_r$  associated with agricultural and non-agricultural activities in the northern India drains into the Ganges River system, which ultimately meets the Bay of Bengal, potentially bringing large amount of anthropogenic  $N_r$ . However, it is reported that  $\sim 96\%$  of this  $N_r$  does not reach to the open Bay of Bengal and is removed on the land's surface and in the estuarine and the coastal regions (*Krishna et al., 2016; Kumar et al., 2004; Singh and Ramesh, 2011*), leaving  $\sim 0.45 \text{ mmol N m}^{-2} \text{ d}^{-1}$  as the fluvial input to the open Bay of Bengal (*Kumar et al., 2004*). In the Bay of Bengal, it has been reported that the atmospheric  $N_r$  input is  $\sim 0.46 \text{ Tg N year}^{-1}$  (*Singh et al., 2012*). Upwelling in the Bay of Bengal is confined within  $\sim 40 \text{ km}$  of the coastal region along the south-western boundary during summer (*Prasanna Kumar et al., 2002; Shetye et al., 1991*). Copious riverine freshwater discharge ( $1.6 \times 10^{12} \text{ m}^3 \text{ y}^{-1}$ , *Subramanian (1993)*) and heavy rainfall ( $2 \text{ m}$  annually over Bay of Bengal, *Bigg (1995); Prasad (1997)*) during the summer monsoon cause a considerable decrease in sea surface salinity. This leads to intense stratification of the Bay of Bengal. Wind force over the Bay of Bengal is incapable of disrupting surface stratification (*Patra et al., 2007; Prasanna Kumar et al., 2002; Shenoi et al., 2002*). During our observations in the peak summer monsoon time, wind speed went up to  $24.5 \text{ m s}^{-1}$  but MLD was never deeper than  $77 \text{ m}$ . Thus, strongly stratified layers might have inhibited vertical mixing and the supply of nutrients from sub-

surface water to surface (*Prasanna Kumar et al.*, 2002; *Gopalkrishna and Sastry*, 1985). Therefore, based on the above findings, we hypothesised that to sustain the C fixation productivity in the central Bay of Bengal, N<sub>2</sub> fixation might play a crucial role.

Diazotrophs need warm and N<sub>r</sub>-depleted waters to survive (*Capone et al.*, 2008; *Gandhi et al.*, 2011). Surface water in the Bay of Bengal is N<sub>r</sub>-depleted. Along with the need of N<sub>r</sub>-depleted environment, on the contrary, diazotrophs need a PO<sub>4</sub><sup>3-</sup> and Fe-replete environment (*Mills et al.*, 2004; *Singh et al.*, 2017; *Sañudo-Wilhelmy et al.*, 2001). Positive P\* at all the stations indicate the PO<sub>4</sub><sup>3-</sup> concentration in excess of NO<sub>x</sub>. N:P ratio is also less than the Redfield ratio (Table 3.1). Positive P\* (or N:P < 12) indicate that PO<sub>4</sub><sup>3-</sup> is not limiting N<sub>2</sub> fixation rates. Thus, N<sub>2</sub> fixation might be regulated by Fe availability. The dry-deposition fluxes of Fe to the Bay of Bengal are significantly higher compared to those over the Arabian Sea (*Srinivas and Sarin*, 2013) and surface dissolved Fe ranged from 0.2 to 0.5 nmol L<sup>-1</sup> in the northern Bay of Bengal (5 °N to 18 °N) (*Grand et al.*, 2015; *Chinni et al.*, 2019). These reported dissolved Fe concentrations indicate that diazotrophs in the Bay of Bengal are not Fe limited. This in conjunction with warm sea surface water (SST varied between 28 and 29 °C), might create favourable conditions for the growth of diazotrophs. Hence, surface NO<sub>x</sub> depleted and warm water in the Bay of Bengal might facilitate the sustenance of diazotrophs and their N<sub>2</sub> fixation activity.

The δ<sup>15</sup>N of PON depends on the isotopic composition of inorganic nitrogenous nutrient sources (6–8‰ of NH<sub>4</sub><sup>+</sup>, 3–7‰ of NO<sub>3</sub><sup>-</sup>, and 0‰ of atmospheric N<sub>2</sub>) (*Prasanna Kumar et al.*, 2001; *Miyake and Wada*, 1967). Thus, δ<sup>15</sup>N of PON is likely to be close to 0‰ in the presence of diazotrophs (*Altabet and Mccarthy*, 1985). The δ<sup>15</sup>N of natural PON in our study supports the N<sub>2</sub> fixation activity (Figure 3.3). The N<sub>2</sub> fixation rates showed a maximum at surface than subsurface waters. This overall decreasing trend of N<sub>2</sub> fixation rates with depth suggests the role of NO<sub>x</sub> nutrients as deterrable to N<sub>2</sub> fixation activity. Therefore, under oligotrophic conditions, N<sub>2</sub> fixation might play an important role in compensating the N<sub>r</sub> demand of C fixation. But the N<sub>r</sub> demand observed for C fixation rates in the oligotrophic Bay of Bengal during our study was ~300 times higher than the N<sub>r</sub> provided by N<sub>2</sub> fixation and thus, the contribution of N<sub>2</sub> fixation to C fixation was < 1%.

Diazotrophic communities in the euphotic zone of the Bay of Bengal include both

the cyanobacterial and non-cyanobacterial groups. During the pre-summer monsoon, [Wu et al. \(2019\)](#) observed *Trichodesmium* spp. (more abundant) and unicellular diazotrophic cyanobacteria along with proteobacteria (mainly alpha-, beta-, and gamma-proteobacteria) with higher abundance in the equatorial region. During the winter monsoon, [Löscher et al. \(2020\)](#) observed *Synechococcus* and *Trichodesmium* with no evidence of unicellular diazotrophic cyanobacteria. Diatoms-associated diazotrophs have also been reported during the summer monsoon for the same sampling stations as ours ([Bhaskar et al., 2007](#)). Thus, diazotrophic cyanobacteria were observed to be the dominant group in the Bay of Bengal. Diazotrophs require cellular energy to split the  $N_2$  molecule and for this reason, sunlight is an important factor for controlling  $N_2$  fixation by supplying adequate energy to diazotrophs ([Karl et al., 2008](#)). Therefore, performing  $N_2$  fixation during the light period has an advantage that this energy-demanding process can then directly be supported by photosynthesis ([Fredriksson et al., 1998](#)). It has been reported that the activity of nitrogenase enzyme of diazotrophic cyanobacteria is closely related to the photosynthesis ([Gallon, 2001](#); [Karl et al., 2008](#)). The diel cycle of nitrogenase activity in *Trichodesmium thiebautii* results from anew synthesis of nitrogenase each morning and degradation of nitrogenase in the late afternoon and night ([Capone et al., 1990](#)). In addition, there are reports of  $N_2$  fixing endogenous rhythm in some diazotrophic prokaryotes (such as *Synechococcus* RF-1, [Grobbelaar et al. \(1986\)](#) and *Trichodesmium thiebautii*, [Capone et al. \(1990\)](#)). It has also been reported that  $N_2$  fixation is regulated by light energy supplies ([Cai and Gao, 2015](#)). For this reason,  $N_2$  fixation occurs predominantly in surface waters ([Luo et al., 2014](#)). Despite of a favourable niche for  $N_2$  fixation in the Bay of Bengal i.e.,  $NO_3^-$ -poor or  $PO_4^{3-}$ -rich, the rates observed are low in terms of percentage contribution to C fixation ( $< 1\%$ ). This points towards the fact that factors like cloud cover and turbidity might be playing a crucial role in restraining the  $N_2$  fixation in the Bay of Bengal. Being situated in the tropical region, in general, sunlight should not be a limiting factor for the biological production. However, during the summer monsoon, increased cloudiness and sediment load due to enhanced riverine flux decreases the light penetration in the Bay of Bengal. It has been reported that cloud cover and turbidity during the summer monsoon are the reasons for low productivity in the Bay of Bengal than in the Arabian Sea ([Prasanna Kumar et al., 2010a](#); [Gomes et al., 2000](#)). Therefore, it is likely that cloud cover and turbidity might have contributed towards the low rates of

N<sub>2</sub> fixation in the Bay of Bengal.

The N<sub>2</sub> fixation rates observed in our study are higher than the recently reported rates in the Bay of Bengal for Jan 2014 by [Löschner et al. \(2020\)](#) where the rates at DCM were below detection limit though they found the clusters of N<sub>2</sub> fixing microbes. [Löschner et al. \(2020\)](#) targeted OMZ for non-cyanobacterial N<sub>2</sub> fixation rates, while most of the N<sub>2</sub> fixation occurs in the surface waters. C fixation rates in their study ranged from 286 to 1855 nmol C L<sup>-1</sup> d<sup>-1</sup> at the depth of DCM whereas in our study, it varied from 1.4 to 282.2 nmol C L<sup>-1</sup> h<sup>-1</sup> (or 17 to 3386 nmol C L<sup>-1</sup> d<sup>-1</sup>) in the sunlit layer of the Bay of Bengal. This suggests the Bay of Bengal to be more productive during the summer than in the winter monsoon. Another study by [Madhupratap et al. \(2003\)](#) in the summer monsoon of 2001 (Jul–Aug), observed NaH<sup>14</sup>CO<sub>3</sub> based depth-integrated C fixation rates from 7.5 to 18.3 mmol C m<sup>-2</sup> d<sup>-1</sup> along 88 °E and 27.3 to 43.3 mmol C m<sup>-2</sup> d<sup>-1</sup> along the coastal transect. Our rates were between 24 and 87 mmol C m<sup>-2</sup> d<sup>-1</sup> along 88 °E and 45 and 81 mmol C m<sup>-2</sup> d<sup>-1</sup> for station SN6 to SN8. Although there are methodological differences, a ~5 fold increase in C fixation is observed during the summer monsoon in the Bay of Bengal within the period of almost two decades. This is in agreement with the report that states global marine C fixation have increased over the past several decades ([Chavez et al., 2011](#)).

The upper bound of observed depth-integrated N<sub>2</sub> fixation rates in our study is higher than many of the other oceanic regimes of the world ([Benavides, 2015](#); [Singh et al., 2019](#)) such as Eastern Tropical South Pacific ([Knapp et al., 2016](#)), Tropical Northwest Atlantic ([Goering et al., 1966](#)). Depth integrated rates of N<sub>2</sub> fixation in the Arabian Sea and Equatorial Southern Indian Ocean during winter, ranged from about 24.6 to 34.7 and 6.27 to 16.6 μmol N m<sup>-2</sup> d<sup>-1</sup>, respectively ([Shiozaki et al., 2014](#)). This suggests that the Bay of Bengal is more diazotrophically active during summer than the Arabian Sea and Equatorial Southern Indian Ocean during winter. We compared the N<sub>2</sub> fixation rates with C fixation of this study and found the contribution of N<sub>2</sub> fixation to C fixation of about 1.1 to 2.8% for the Arabian Sea and 0.1 to 1.6% for Equatorial Southern Indian Ocean which is not much higher than that observed in the Bay of Bengal. [Chen et al. \(2008\)](#) reported N<sub>2</sub> fixation rates of 1 to 13 μmol N m<sup>-2</sup> d<sup>-1</sup> during different seasons in the South China Sea and the contribution of N<sub>2</sub> fixation to C fixation calculated by us

from their data is about 0.03 to 0.16%. [Church et al. \(2009\)](#) reported  $\text{N}_2$  fixation rates between 20 and  $307 \mu\text{mol N m}^{-2} \text{d}^{-1}$  over a three-year period in the North Pacific Ocean and the contribution of  $\text{N}_2$  fixation to C fixation in this region calculated by us is about 1 to 4%. Thus, in our study the percentage contribution of  $\text{N}_2$  fixation to C fixation in the Bay of Bengal is comparable to other oceanic regimes. We require sustained observations of  $\text{N}_2$  fixation in the Bay of Bengal as our study is limited to one season. There is a chance of high  $\text{N}_2$  fixation during spring and autumn, when high rates of  $\text{N}_2$  fixation were previously observed in the Arabian Sea ([Gandhi et al., 2011](#); [Singh et al., 2019](#)).

At elevated temperature due to recent ocean warming, the higher rates of respiration and the relative low  $\text{O}_2$  concentration in warm seawater are advantageous to keep the  $\text{N}_2$ -fixing cells anoxic for a better nitrogenase activity. *Trichodesmium erythraeum* bloom in high  $p\text{CO}_2$  waters of the Bay of Bengal has been reported ([Shetye et al., 2013](#)). Therefore, in future, as climate becomes warmer due to rise in  $\text{CO}_2$ , increase in  $\text{N}_2$  fixation could be observed due to increase in temperature ([Boyd and Doney, 2002](#)) or high  $\text{CO}_2$  ([Hutchins et al., 2007](#); [Fu et al., 2008](#); [Levitan et al., 2007](#)).  $\text{N}_2$  fixation may stimulate C fixation in the  $\text{N}_r$ -limited oligotrophic Bay of Bengal and thus, provide negative feedback on rising atmospheric  $\text{CO}_2$  levels. Our study may help in understanding the future advancement of  $\text{N}_2$  fixation in the Bay of Bengal as a consequence of global warming.

### 3.5 Conclusions

In this study, we have presented the first  $\text{N}_2$  fixation activity within the sunlit layer of the Bay of Bengal. The oligotrophic Bay of Bengal encounters warm water, excess  $\text{PO}_4^{3-}$  and Fe which are essentials for diazotrophs to flourish and thus, we hypothesised high  $\text{N}_2$  fixation in the Bay of Bengal. But our findings were contrary to our hypothesis. The observed  $\text{N}_2$  fixation rates are low in the Bay of Bengal in terms of percentage contribution ( $< 1\%$ ) to C fixation. Due to summer monsoon, turbidity due to copious riverine discharge and cloud cover over Bay of Bengal might have contributed towards the low rates of  $\text{N}_2$  fixation. Nevertheless, the upper bound of such seemingly low rates is higher than many worlds oceanic regimes. This underscores the global importance of the Bay of Bengal in

the global marine nitrogen cycle. However, our results give an imprint of summer monsoon only. Therefore, a more detailed study is needed to estimate the  $\text{N}_2$  fixation rates in the Bay of Bengal, to understand the effect of different seasons on the rates of  $\text{N}_2$  fixation, and at large to establish the role of  $\text{N}_2$  fixation on C fixation in the Bay of Bengal.

## Chapter 4

# N<sub>2</sub> and C fixation in the Bay of Bengal during the spring inter-monsoon

### 4.1 Introduction

N<sub>2</sub> fixation and the presence of *nifH* genes in the OMZs evidence the efficiency of diazotrophs in the OMZs ([Jayakumar et al., 2017](#); [Jayakumar and Ward, 2020](#); [Löscher et al., 2014](#)), suggesting that diazotrophs play an essential role in controlling N<sub>r</sub> gain in the OMZs. Revealing the phylogenetic identification and potential environmental controls of diazotrophs are critical to understanding the productivity of these ecosystems. While diazotrophy in the OMZs of the Eastern Tropical South Pacific has been explored extensively ([Bonnet et al., 2013](#); [Chang et al., 2019](#); [Fernandez et al., 2011](#); [Knapp et al., 2016](#); [Löscher et al., 2014](#)), the OMZs of the Indian Ocean remained insufficiently understood. The Indian Ocean harbours OMZs in its northern part, separated as the Arabian Sea and the Bay of Bengal. Diazotrophy in the Bay of Bengal is largely under-explored even in its euphotic zone along with the OMZ. It possesses the fourth most intense OMZs of the global ocean with the reported existence of denitrifiers and anammox populations in its OMZ ([Bristow et al., 2017](#); [Johnson et al., 2019](#)).

The seasonal variability of biological activity in the Bay of Bengal oscillates from being productive during monsoons to oligotrophic during inter-monsoon periods, where the latter may provide a supposedly prerequisite for diazotrophy. Traditionally, the Bay

of Bengal is calm during the spring inter-monsoon season. Also, in the Arabian Sea which faces similar environmental conditions as the Bay of Bengal being situated in the similar latitudes, highest N<sub>2</sub> fixation rates in the global ocean were observed during the spring ([Gandhi et al., 2011](#)), and thus, one could expect similar diazotrophic activity in the Bay of Bengal. This motivated us to explore the Bay of Bengal during the spring to assess diazotrophy, its spatial and vertical variability, and potential environmental controls, particularly the influence of O<sub>2</sub> concentrations on N<sub>2</sub> fixation rates. We hypothesised that (a) having observed low N<sub>2</sub> fixation rates during the summer monsoon in the Bay of Bengal (Chapter 3), N<sub>2</sub> fixation should be higher during spring due to favourable stratified and oligotrophic conditions for diazotrophs and (b) N<sub>2</sub> fixation rates in the dark-oxygenated waters below the OMZ should be lower than in the OMZ owing to incompatibility of nitrogenase enzyme with O<sub>2</sub>. To test these hypotheses, we conducted N<sub>2</sub> fixation rates measurements in the euphotic and aphotic zone covering the OMZ and below region of the OMZ of the Bay of Bengal, along with the assessment of cyanobacterial community composition and euphotic zone C fixation rates.

## 4.2 Materials and Methods

Seawater samples were collected in the Bay of Bengal at seven stations (S1–S7) during the spring inter-monsoon (5–15 Apr 2019) on-board ORV *Sindhu Sankalp* (SSK-127) (Figure 4.1). Stations S1 to S4 were near the coast experiencing the most substantial influence of riverine discharge and thus classified as the “coastal Bay of Bengal” stations, whereas S5 to S7 were classified as the “central Bay of Bengal” stations. The seawater samples were collected using Niskin bottles mounted on a Sea-Bird CTD rosette sampler from surface to 1500 m depth covering the euphotic and aphotic zone.

Samples for N<sub>2</sub> and C fixation rates measurement experiments were taken at all stations excluding station S7 (due to technical issues). Samples for N<sub>2</sub> fixation were collected from 3–4 depths in the euphotic zone (3–85 m) targeting oxycline as well and 3–4 depths in the aphotic zone (90–1500 m), while samples for C fixation were taken from the euphotic zone only. Within the aphotic zone, 2–3 depths in the OMZ (90–600



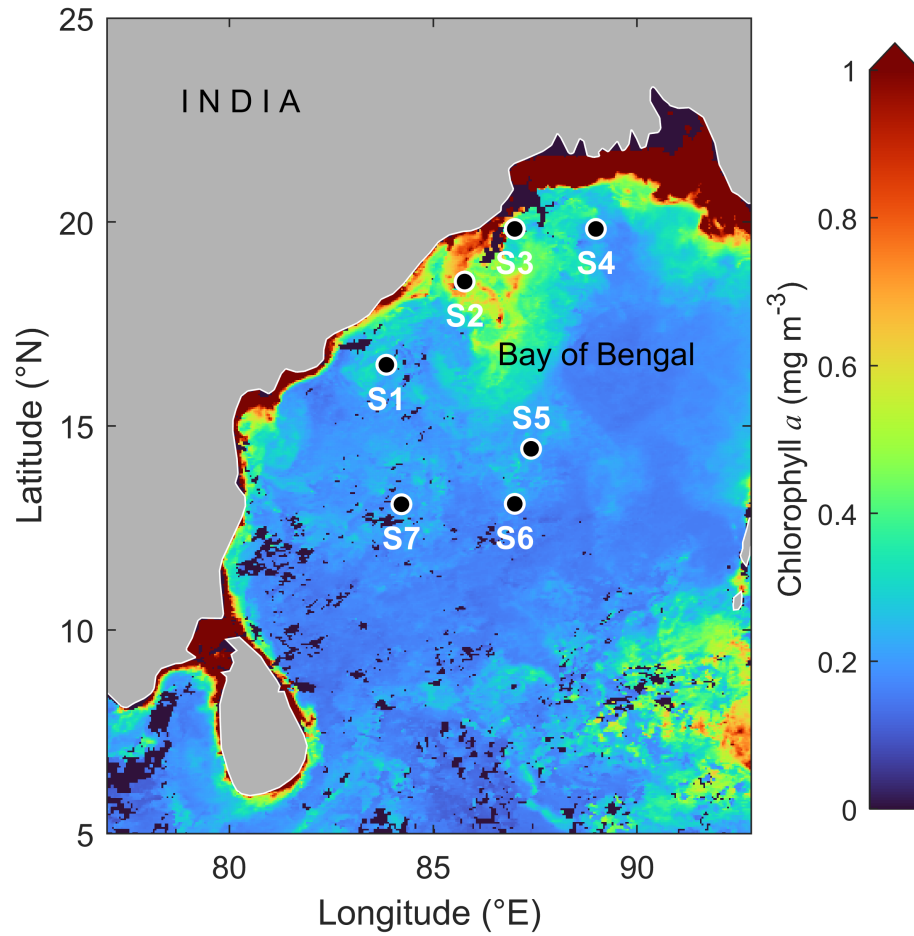


Figure 4.1: Sampling stations (S1–S7) superimposed on sea surface chlorophyll *a* (4 km resolution data obtained from Aqua/MODIS for Apr 2019) in the Bay of Bengal during the research cruise expedition ORV *Sindhu Sankalp* (SSK–127). N<sub>2</sub> and C fixation experiments were performed at stations S1–S6.

m, targeting OMZ start and end) and one depth below the OMZ (600–1500 m) were sampled.

The measurement of nutrients, DIC, mass and  $\delta^{13}\text{C}$  of POC, mass and  $\delta^{15}\text{N}$  of PON and cyanobacterial community composition are discussed in Chapter 2. For chlorophyll *a* concentrations, samples were collected by filtering 1 L seawater onto Whatman glass microfiber filters (GF/F, 25 mm diameter, 0.7  $\mu\text{m}$  pore size) followed by extraction in 90% acetone for 24 h refrigeration. The chlorophyll *a* concentrations were measured in HPLC (Agilent, USA) at the Space Applications Centre, Ahmedabad, India.

Mixed layer depth (MLD) was determined based on the variation in temperature (0.2  $^{\circ}\text{C}$  difference from SST) (*de Boyer Montégut et al., 2004*). The minimum quantifiable

rate for N<sub>2</sub> fixation rate was calculated using standard propagation of errors via observed variability between duplicate samples (*Gradoville et al., 2017*). N<sub>2</sub> fixation rates above minimum quantifiable rates are reported and discussed. Depth-integrated N<sub>2</sub> fixation rates were calculated by the trapezoidal integration of volumetric rates with depth, where N<sub>2</sub> fixation rates below minimum quantifiable rates were assigned with zero value to prevent the overestimation of depth-integrated rates. If N<sub>2</sub> fixation rates were below minimum quantifiable rates at all the depths within a zone, the depth-integrated rates were considered as below detection. Based on the natural molar C:N ratio at each depth, the nitrogen demand to fuel the observed C fixation rates was calculated. N<sub>2</sub> fixation rates were divided by this demand estimate to calculate the percentage contribution of N<sub>2</sub> fixation to C fixation rates.

Table 4.1: Details of sea surface temperature (SST), sea surface salinity (SSS), mixed layer depth (MLD), deep chlorophyll maxima (DCM) and chlorophyll *a* at each station.

Station	SST (°C)	SSS	MLD (m)	DCM (m)	Chlorophyll <i>a</i> (mg m <sup>-2</sup> )
S1	29.0	33.2	30	83	16.4
S2	27.6	33.1	20	55	14.5
S3	28.4	33.0	24	69	21.3
S4	28.0	32.8	34	71	22.5
S5	30.0	32.1	12	61	42.4
S6	30.3	32.3	20	87	16.4
S7	30.2	33.3	27	86	20.5

## 4.3 Results

### 4.3.1 Environmental conditions and nutrients

Sea surface temperature ranged from 27.6 to 30.3 °C and was minimum at station S2 in the coastal Bay of Bengal, whereas maximum at station S6 in the central Bay of Bengal (Table 4.1). Sea surface salinity ranged from 32.1 to 33.2, with the least and the highest sea surface salinity observed at stations S5 and S1, respectively, (Table 4.1). The coastal Bay of Bengal had a much deeper mixed layer depth than the central Bay of Bengal (Table 4.1).

The water column chlorophyll *a* ranged from 14.5 to 42.4 mg m<sup>-2</sup> with the lowest and highest at stations S2 and S5, respectively, (Table 4.1). NO<sub>x</sub> and PO<sub>4</sub><sup>3-</sup> concentrations increased with depth (Figure 4.2c, d). The surface seawater concentration of NO<sub>x</sub> was below detection except for station S4. The dissolved nutrient N:P ratio in the water column was on average 11.2, which was considerably lower than the Redfield Ratio of 16 *Redfield* (1934).

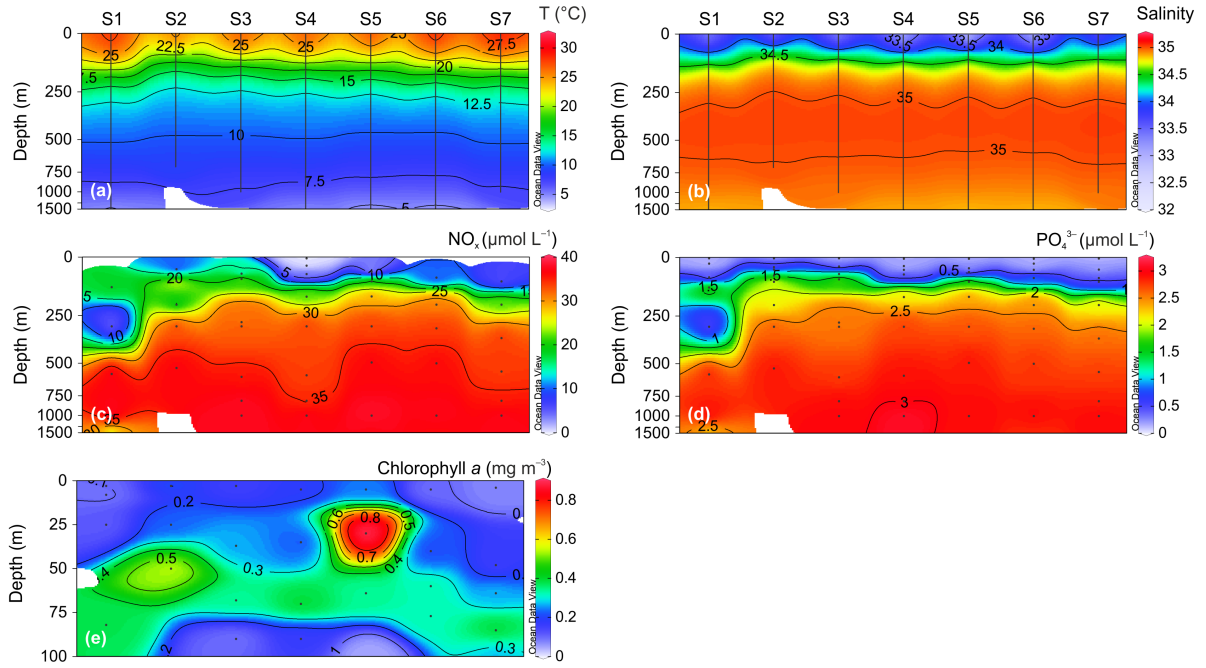


Figure 4.2: Vertical profiles of (a) temperature (T), (b) salinity, (c) NO<sub>x</sub>, (d) PO<sub>4</sub><sup>3-</sup> and (e) chlorophyll *a* at each station. Note the difference in depth for the chlorophyll *a* profile and that the top of the y-axis is extended for all the profiles except for chlorophyll *a* profile.

#### 4.3.2 N<sub>2</sub> and C fixation rates and their environmental controls

The minimum quantifiable rate for N<sub>2</sub> fixation rates ranged between 0.001 and 0.33 nmol N L<sup>-1</sup> d<sup>-1</sup>. N<sub>2</sub> fixation rates were above the minimum quantifiable rate in 10 of the 20 euphotic zone samples and 13 of the 21 aphotic zone samples. The surface N<sub>2</sub> fixation rates ranged from 0.06 to 0.38 nmol N L<sup>-1</sup> d<sup>-1</sup> with the highest rate at station S1 (Figure 4.3a). The N<sub>2</sub> fixation rates in the euphotic zone ranged from 0.02 to 0.38 nmol N L<sup>-1</sup> d<sup>-1</sup> (0.12 ± 0.01 nmol N L<sup>-1</sup> d<sup>-1</sup>, *n* = 10) and in the aphotic zone ranged from 0.02

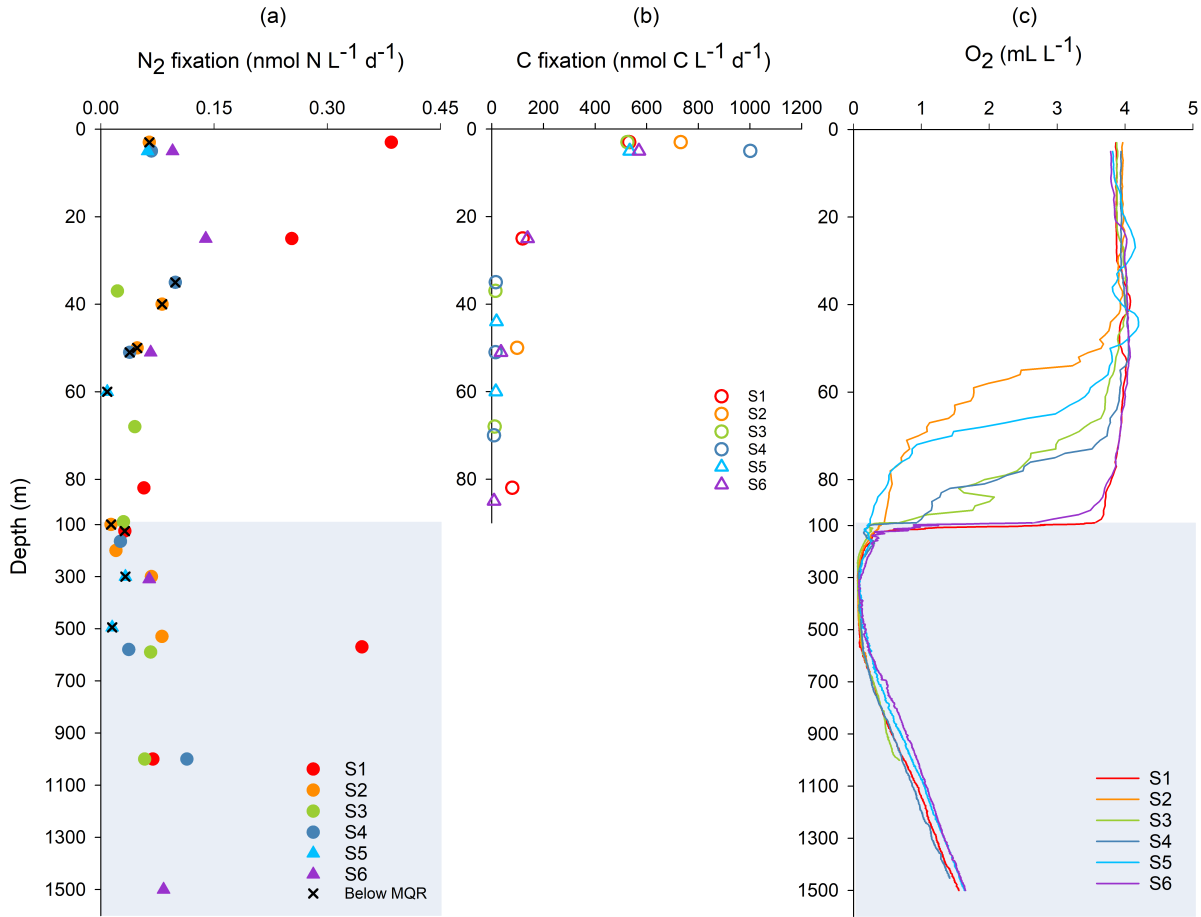


Figure 4.3: Vertical profiles of (a) average N<sub>2</sub> fixation rates (solid symbols), (b) average C fixation rates (open symbols) and (c) O<sub>2</sub> concentrations in the euphotic (white background) and aphotic zone (shaded background). Circles represent the coastal Bay of Bengal and triangles represent the central Bay of Bengal stations. Note that the y-axis of the euphotic zone is extended.

to 0.35 nmol N L<sup>-1</sup> d<sup>-1</sup> ( $0.08 \pm 0.03$  nmol N L<sup>-1</sup> d<sup>-1</sup>,  $n = 13$ ) (Table 4.2), with the highest rate for both zones at station S1 (Figure 4.3a). Within the OMZ where O<sub>2</sub> ≤ 0.5 mL L<sup>-1</sup>, N<sub>2</sub> fixation rates ranged from 0.02 to 0.35 nmol N L<sup>-1</sup> d<sup>-1</sup> ( $0.09 \pm 0.05$  nmol N L<sup>-1</sup> d<sup>-1</sup>,  $n = 8$ ) and after excluding the highest rate, the rates ranged from 0.02 to 0.08 nmol N L<sup>-1</sup> d<sup>-1</sup> ( $0.05 \pm 0.01$  nmol N L<sup>-1</sup> d<sup>-1</sup>,  $n = 7$ ) (Table 4.2). N<sub>2</sub> fixation rates below the OMZ ranged from 0.06 to 0.11 nmol N L<sup>-1</sup> d<sup>-1</sup> ( $0.08 \pm 0.01$  nmol N L<sup>-1</sup> d<sup>-1</sup>,  $n = 4$ ) where  $0.5 < \text{O}_2 \leq 1.6$  mL L<sup>-1</sup>. Excluding the highest N<sub>2</sub> fixation rate from the OMZ, the average rate below the OMZ was significantly higher than within the OMZ. When integrated over the euphotic (3–85 m depth) and aphotic zone (90–1500 m depth), the highest N<sub>2</sub> fixation rates for both zones were observed at station S1 (Table 4.3). The

contribution of the aphotic zone to whole water column (i.e., euphotic + aphotic zone)  $\text{N}_2$  fixation reached up to 100%, with the highest contribution at station S2.  $\text{N}_2$  fixation rates in the euphotic zone were negatively correlated with chlorophyll  $a$  and  $\text{PO}_4^{3-}$  (Figure 4.4). The aphotic zone  $\text{N}_2$  fixation rates were negatively correlated with temperature but positively with  $\text{NO}_x$  and  $\text{PO}_4^{3-}$ .

C fixation rates rapidly decreased with depth and ranged between 8.3 and 1001.4  $\text{nmol C L}^{-1} \text{ d}^{-1}$  ( $235.3 \pm 12.3 \text{ nmol C L}^{-1} \text{ d}^{-1}$ ,  $n = 19$ , (Table 4.2)), with the highest value at coastal station S4 (Figure 4.3b). The surface C fixation rates at the coastal Bay of Bengal ( $697.8 \pm 38 \text{ nmol C L}^{-1} \text{ d}^{-1}$ ,  $n = 4$ ) was significantly higher than at the central Bay of Bengal ( $552.1 \pm 41.5 \text{ nmol C L}^{-1} \text{ d}^{-1}$ ,  $n = 2$ ). The depth-integrated C fixation rates ranged from 9.6 to 19.5  $\text{mmol C m}^{-2} \text{ d}^{-1}$ , with maximum value at coastal station S2 (Table 4.3). C fixation was negatively correlated with salinity, chlorophyll  $a$  and  $\text{PO}_4^{3-}$  but positively with temperature (Figure 4.4).

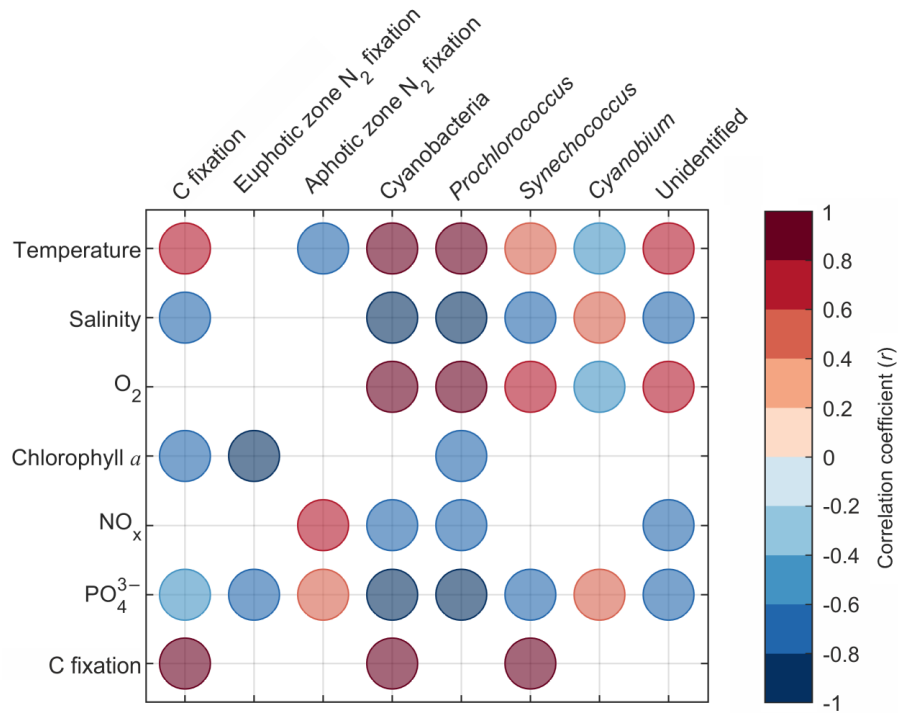


Figure 4.4: Spearman's correlation coefficient ( $r$ ) of C fixation,  $\text{N}_2$  fixation, and cyanobacteria and their communities, with their potential environmental controls. Significant correlations are indicated for  $p < 0.05$ . Note that only the parameters which significantly correlated with each other are indicated.

### 4.3.3 Cyanobacterial abundance

The overall abundance of cyanobacteria ranged from 0.04 to 27.7% (average 8.3%) of the total prokaryotic sequences, where maximum abundance occurred at the surface and then rapidly decreased to the minimum with increasing depth. Among total cyanobacteria, *Prochlorococcus* was the most abundant genus with an average of 54.1% relative abundance, followed by *Cyanobium* and *Synechococcus* (average 17.7 and 15.9% relative abundance, respectively). Unidentified cyanobacteria comprised on average 12.2% rela-

Table 4.2: N<sub>2</sub> and C fixation rates in different sections of the water column. Note that C fixation rates were measured in the euphotic zone only.

	Euphotic zone	Aphotic zone	OMZ	Below OMZ
C fixation rates (nmol C L <sup>-1</sup> d <sup>-1</sup> )	8.3–1001.4 (235.3 ± 12.3)			
N <sub>2</sub> fixation rates (nmol N L <sup>-1</sup> d <sup>-1</sup> )	0.02–0.38 (0.12 ± 0.01)	0.02–0.35 (0.08 ± 0.03)	0.02–0.35 (0.09 ± 0.05) 0.02–0.08* (0.05 ± 0.01)*	0.06–0.11 (0.08 ± 0.01)

\*After excluding the highest N<sub>2</sub> fixation rate within the OMZ.

Table 4.3: Depth-integrated C fixation rates, euphotic and aphotic zone N<sub>2</sub> fixation rates, N<sub>2</sub> fixation contribution to C fixation and aphotic zone N<sub>2</sub> fixation contribution to water column N<sub>2</sub> fixation at each station. Depth range for depth-integrated rates is indicated in brackets.

Station	C fixation (mmol C m <sup>-2</sup> d <sup>-1</sup> )	Euphotic zone N <sub>2</sub> fixation (μmol N m <sup>-2</sup> d <sup>-1</sup> )	N <sub>2</sub> fixation contribution to C fixation (%)	Aphotic zone N <sub>2</sub> fixation (μmol N m <sup>-2</sup> d <sup>-1</sup> )	Aphotic zone N <sub>2</sub> fixation contribution to column N <sub>2</sub> fixation (%)
S1	12.8 ± 3.9 (3–82 m)	15.8 ± 5.9 (3–82 m)	0.3–1.3	166.1 ± 225.6 (125–1000 m)	90.7
S2	19.5 ± 3.7 (3–50 m)	0.0 ± 0.0 (3–50 m)	0.0	22.4 ± 11.2 (100–530 m)	100
S3	9.6 ± 2.8 (3–68 m)	1.4 ± 0.5 (3–68 m)	0.0–1.8	38.0 ± 8.9 (90–1000 m)	94.4
S4	15.7 ± 0.2 (5–70 m)	1.0 ± 0.7 (5–70 m)	0.0–0.1	45.0 ± 14.5 (165–1000 m)	95.2
S5	11.0 ± 0.2 (5–60 m)	1.2 ± 0.8 (5–60 m)	0.0–0.1	0.0 ± 0.0 (100–1500 m)	0.0
S6	10.1 ± 2.4 (5–85 m)	6.1 ± 1.6 (5–85 m)	0.0–1.2	90.7 ± 19.2 (200–1500 m)	93.7

tive abundance. *Trichodesmium* was the least abundant, with an average of 0.1% relative abundance. At the surface water, *Prochlorococcus* dominated, followed by *Synechococcus* (Figure 4.5). *Cyanobium* was dominating at the end of the OMZ. Unidentified cyanobacteria were noticeably abundant at the oxycline and the OMZ start regions. *Trichodesmium* was only observed at the surface of station S7 and the oxycline of stations S2 and S3.

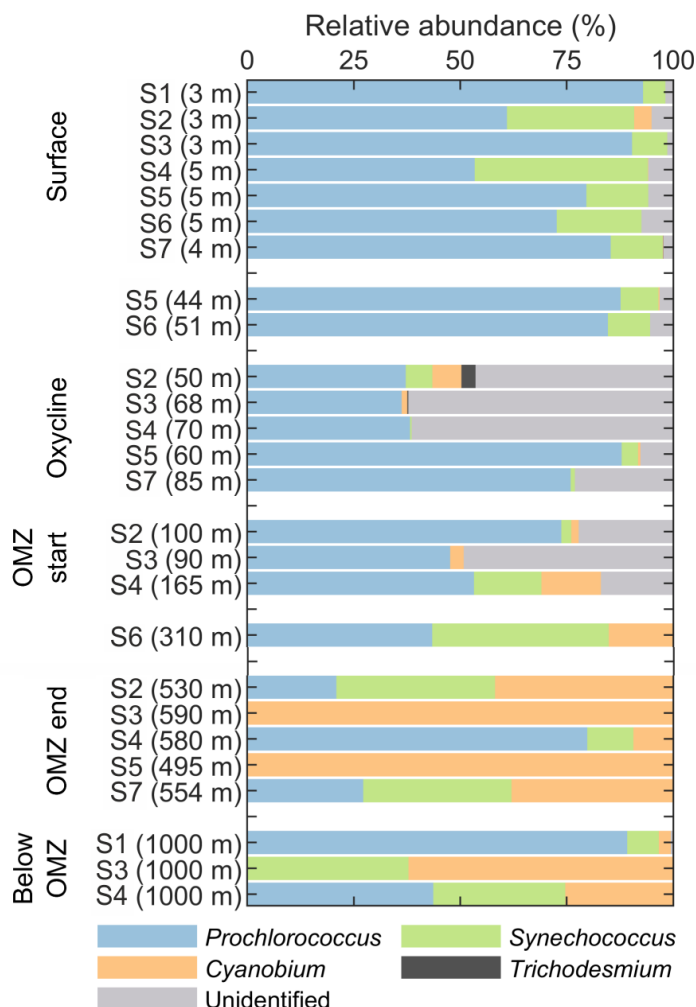


Figure 4.5: Vertical profile of relative abundance of cyanobacterial communities with respect to total cyanobacterial sequences.

Cyanobacteria were positively correlated with temperature,  $O_2$  and C fixation while negatively with salinity and nutrients (Figure 4.4). Similarly, *Prochlorococcus* and *Synechococcus* were positively correlated with temperature,  $O_2$  and negatively with salinity and nutrients. *Synechococcus* was positively correlated with C fixation. Conversely, *Cyanobium* was positively correlated with salinity and  $PO_4^{3-}$  but negatively with temperature and  $O_2$ .

## 4.4 Discussion

### 4.4.1 N<sub>2</sub> and C fixation in the euphotic zone of the Bay of Bengal

In the present study conducted during spring, N<sub>2</sub> fixation rates were detected in both the euphotic and aphotic zone of the Bay of Bengal at all the stations (except at certain depths), with almost equally low average rates in both the zones. The shallow mixed layer depth (up to 34 m) restricted the NO<sub>x</sub> concentration in the euphotic zone. The N:P ratio in the euphotic zone of the Bay of Bengal was below the Redfield Ratio. This indicates towards the potential N limitation for C fixation. Also, the Bay of Bengal is among the high Fe regions (surface dissolved iron, dFe =  $0.44 \pm 0.11$  nmol L<sup>-1</sup>, [Chinni et al. \(2019\)](#)) similar to the Arabian Sea (surface dFe =  $0.68 \pm 0.03$  nmol L<sup>-1</sup>, [Chinni et al. \(2019\)](#)) and the tropical north Atlantic Ocean (surface dFe =  $0.55 \pm 0.29$  nmol kg<sup>-1</sup>, [Fitzsimmons et al. \(2013\)](#)). Despite this, the contribution of N<sub>2</sub> fixation to C fixation was < 2%. One probable reason for such low contribution can be the slower growth of diazotrophs than those of non-diazotrophic microorganisms, owing to respiratory control of intracellular O<sub>2</sub> concentrations ([Landolfi et al., 2015](#); [Zehr and Kudela, 2011](#)). A recent study performed in the euphotic zone of the central Bay of Bengal during the summer monsoon revealed N<sub>2</sub> fixation rates from below detection to 6.7 nmol N L<sup>-1</sup> d<sup>-1</sup> (i.e., up to 0.56 nmol N L<sup>-1</sup> h<sup>-1</sup>) ([Saxena et al., 2020](#)). In that study, the mixed layer depth deepened up to 77 m, N:P ratio in the euphotic zone (average: 4.3, range: 0–12.4) and NO<sub>x</sub> concentrations were considerably higher than in the spring. Despite the conducive conditions for N<sub>2</sub> fixation in the spring, N<sub>2</sub> fixation rates are lower than in the summer monsoon. The N<sub>2</sub> fixation rates in the euphotic zone of the Bay of Bengal are low (1–15.8 μmol N m<sup>-2</sup> d<sup>-1</sup>) compared to other oligotrophic regions, viz. the western Pacific Ocean ( $66 \pm 19$  μmol N m<sup>-2</sup> d<sup>-1</sup>) and the South China Sea ( $51.7 \pm 6.2$  μmol N m<sup>-2</sup> d<sup>-1</sup>) ([Chen et al., 2014](#); [Gimenez et al., 2018](#); [Montoya et al., 2004](#); [Shiozaki et al., 2010](#)). Since diazotrophs prefer calm waters ([Karl et al., 2002](#)), a probable reason for this seasonal trend might be the lesser stable water column during spring owing to least fresh water induced stratification than in the summer monsoon ([Prasanna Kumar et al., 2010b](#)). C fixation ranged from 16.8 to 3386.4 nmol C L<sup>-1</sup> d<sup>-1</sup> (i.e., 1.4 to 282.2 nmol C L<sup>-1</sup> h<sup>-1</sup>)



and the contribution of  $N_2$  fixation to C fixation was  $< 0.6\%$  in the previous study ([Saxena et al., 2020](#)). While comparing these two studies conducted during summer monsoon and spring, the Bay of Bengal seems less photosynthetically and diazotrophically active during spring. The Arabian Sea, located at the same latitude as the Bay of Bengal, witnessed the highest rates of  $N_2$  fixation (up to  $13,500 \text{ nmol N L}^{-1} \text{ d}^{-1}$ , i.e.,  $1125 \text{ nmol N L}^{-1} \text{ h}^{-1}$ ) in the global ocean during spring 2009 and 2010 ([Gandhi et al., 2011](#); [Kumar et al., 2017](#)). In contrast, the Bay of Bengal facing similar warm, stratified and nitrogen-depleted conditions alike the Arabian Sea during spring, witnessed only up to  $0.38 \text{ nmol N L}^{-1} \text{ d}^{-1}$   $N_2$  fixation rate in the euphotic zone.

C fixation is primarily governed by limiting nutrient availability. Station S4 was the only where the  $NO_x$  concentration was above detection limit, resulting in the highest C fixation rate observed at the surface. Surface C fixation rate in the central Bay of Bengal with value  $552.1 \pm 41.5 \text{ nmol C L}^{-1} \text{ d}^{-1}$  was observed; however, [Baer et al. \(2019\)](#) revealed  $68.4 \pm 22.8 \text{ nmol C L}^{-1} \text{ d}^{-1}$  ( $5.7 \pm 1.9 \text{ nmol C L}^{-1} \text{ h}^{-1}$ ) C fixation at 20 m depth in the central Bay of Bengal during Apr 2016. In addition, a previous study conducted by [Sarma et al. \(2019\)](#) during spring (25 Mar to 3 Apr 2018) revealed the same order of magnitude for C fixation (25 to  $1533.3 \text{ nmol C L}^{-1} \text{ d}^{-1}$ ) as in the present study. These observations led us to speculate an increase in C fixation in the Bay of Bengal within this short period. It has been hypothesised that even a slight increase in C fixation may lead to the formation of a dead zone in the Bay of Bengal ([Bristow et al., 2017](#)), demanding further monitoring of C fixation and its consequent effect on  $O_2$  concentrations in the OMZ of the Bay of Bengal.

#### 4.4.2 $N_2$ fixation in the aphotic zone of the Bay of Bengal

$N_2$  fixation rates in the OMZ reached up to  $0.35 \text{ nmol N L}^{-1} \text{ d}^{-1}$ , whereas [Löschner et al. \(2020\)](#) observed below detection rates in the OMZ during the winter monsoon in the Bay of Bengal. But only these two studies conducted so far are inadequate to infer that the OMZ of the Bay of Bengal is more diazotrophically active during spring than in the winter monsoon. In the present study, the OMZ  $N_2$  fixation rates were  $0.05 \pm 0.01 \text{ nmol N L}^{-1} \text{ d}^{-1}$  ( $n = 7$ ) excluding the highest rate, while in the OMZ of the Eastern Tropical

South Pacific rates were  $1.27 \pm 1.2 \text{ nmol N L}^{-1} \text{ d}^{-1}$  ( $n = 13$ ) when O<sub>2</sub> concentrations were completely depleted in the core of the OMZ (*Fernandez et al.*, 2011). Similarly, N<sub>2</sub> fixation rates were higher in the OMZ of the Eastern Tropical North Pacific (O<sub>2</sub> < 100 nmol L<sup>-1</sup>), and reached up to  $1.7 \text{ nmol N L}^{-1} \text{ d}^{-1}$  (*Jayakumar et al.*, 2017). This substantial difference in N<sub>2</sub> fixation rates within the spatially different OMZs can be attributed to different O<sub>2</sub> concentration and its consequence on O<sub>2</sub>-sensitive diazotrophs. Contradictorily in this study, the average N<sub>2</sub> fixation rate below the OMZ were significantly higher ( $0.08 \pm 0.01 \text{ nmol N L}^{-1} \text{ d}^{-1}$ ,  $n = 4$ ) than within the OMZ, which suggests the insensitivity of diazotrophs to O<sub>2</sub>. This is a key outcome of this study, but the sparse measurements in the OMZ of the Bay of Bengal raise the need to further investigate N<sub>2</sub> fixation in the dark-oxygenated waters as well. Conclusively, the aphotic zone appears more diazotrophically active than the euphotic zone of the Bay of Bengal and substantially contributes to reactive nitrogen inputs, with N<sub>2</sub> fixation in the aphotic zone representing 91 to 100% of the water column N<sub>2</sub> fixation, except one station with 0% contribution (Table 4.3). Moreover, previous studies in other regions also reported depth-integrated aphotic zone N<sub>2</sub> fixation rates representing 40 to 95% of the water column (up to 2000 m) activity (*Benavides et al.*, 2015; *Bonnet et al.*, 2013; *Rahav et al.*, 2013). Alongside, this study also corroborates that aphotic zone N<sub>2</sub> fixation accounts for a significant and even predominant fraction of water column N<sub>2</sub> fixation at least in the open ocean. The diazotrophs in the aphotic zone and OMZs are dominated by NCDs (*Chen et al.*, 2019; *Farnelid et al.*, 2013; *Hamersley et al.*, 2011; *Hewson et al.*, 2007; *Jayakumar et al.*, 2012) and thus, the NCD-associated N<sub>2</sub> fixation rates in the present study once again provides quantitative evidence supporting the previous revelations (*Bombar et al.*, 2016). Therefore, given their larger volumes, the N<sub>2</sub> fixation rates in the aphotic zone seem quantitatively important globally. The data set reported here is small, so a more comprehensive analysis of N<sub>2</sub> fixation in the OMZs and other aphotic zones of the ocean is further necessary to estimate its extent in regulating the nitrogen cycle, while considering the fact that global warming is impacting the OMZs.

#### 4.4.3 Environmental controls of diazotrophy and C fixation

Diazotrophs regulate nitrogenase activity in response to various environmental factors including (a) N<sub>r</sub> availability as the preferred source of nitrogenous nutrients, (b) PO<sub>4</sub><sup>3-</sup>

and Fe availability, (c) O<sub>2</sub> concentration, and (d) in the case of cyanobacteria, light intensity. While conventionally, C fixation is solar irradiation dependent and conclusively on light-absorbing pigment chlorophyll *a*, we found a positive correlation of C fixation with temperature but a negative correlation with chlorophyll *a*. However, it is reported that phytoplankton can reduce their chlorophyll *a* concentration when light intensity is high (*Geider et al.*, 1998; *Mignot et al.*, 2014). Euphotic zone N<sub>2</sub> fixation showed a negative but significant correlation with PO<sub>4</sub><sup>3-</sup>, which indicates its consumption during diazotrophs production (*Cloern*, 2021).

Seawater temperature > 25 °C is optimal for nitrogenase activity and the growth of most diazotrophs. Nevertheless, several studies have reported N<sub>2</sub> fixation in the Arctic Ocean and under the Antarctic sea ice (*Blais et al.*, 2012; *Harding et al.*, 2018; *Shiozaki et al.*, 2020). Concurrently, we observed anticorrelation of aphotic zone N<sub>2</sub> fixation with the temperature where it is clearly less than 25 °C (Figure 4.4), which underscores the plasticity of diazotrophs towards temperature and so their spatial distribution. Several studies have suggested that N<sub>2</sub> fixation in the OMZs and suboxic waters is driven by NCDs (*Bird and Wyman*, 2013; *Cheung et al.*, 2016; *Farnelid et al.*, 2013; *Fernandez et al.*, 2011; *Jayakumar et al.*, 2012; *Löscher et al.*, 2014). *Bombar et al.* (2016) investigated that O<sub>2</sub> may control the activity of NCDs because of the sensitivity of nitrogenase enzyme to O<sub>2</sub> and also with the availability of nitrogen because its assimilation is relatively energetically inexpensive than performing N<sub>2</sub> fixation (*Falkowski*, 1983). *Bonnet et al.* (2018) reported a negative correlation of N<sub>2</sub> fixation with NO<sub>3</sub><sup>-</sup> concentrations. Notably, in this study, no such correlation of N<sub>2</sub> fixation with O<sub>2</sub> neither in the euphotic nor in the aphotic zone was observed, but a positive correlation with NO<sub>x</sub> was observed in the aphotic zone. Several studies have shown active N<sub>2</sub> fixation is detected in the presence of high NO<sub>x</sub> concentrations (*Fernandez et al.*, 2011; *Gradoville et al.*, 2017; *Knapp*, 2012; *Tang et al.*, 2020). A recent study has also shown that it is advantageous for NCDs to obtain nitrogen through both NO<sub>x</sub> and N<sub>2</sub> fixation, presumably owing to an increase in their growth efficiency because assimilation of fixed nitrogen is energetically cheaper (*Inomura et al.*, 2018). Consequently, previous studies and our own indicate that NCDs may have a low sensitivity towards NO<sub>x</sub>, as previously suggested by *Bombar et al.* (2016). Conclusively, with this and previous studies highlighting the potential environmental controls on N<sub>2</sub> fixation, we are still unable to gain a firm perspective on NCDs biogeography. This raises

questions of which factors control the distribution and activity of NCDs in the ocean, and thus, extended investigations are needed to understand the biogeography of diazotrophs and their potential habitats.

#### 4.4.4 Environmental controls of cyanobacterial communities

Among cyanobacteria, *Prochlorococcus* dominated the oligotrophic surface water of the Bay of Bengal (Figure 4.5), consistent with previous observation of *Prochlorococcus* preferring waters where nutrients are low (Flombaum *et al.*, 2013). A study by Baer *et al.* (2019) also found *Prochlorococcus* dominating the Bay of Bengal during spring, accounting for ~78% of the autotrophic biomass. *Prochlorococcus* was positively correlated with temperature, suggesting temperature has an apparent effect on their growth (Figure 4.4). *Prochlorococcus* and *Synechococcus* were negatively correlated with nutrients, indicating nutrient consumption during their proliferation. This also suggests that nutrient availability played an essential role in controlling their variable occurrence patterns. Notably, we found a positive correlation of *Synechococcus* with O<sub>2</sub> but no correlation with N<sub>2</sub> fixation (Figure 4.4). Various previous studies have observed *Synechococcus* fixing N<sub>2</sub> aerobically (Goes *et al.*, 2014; Huang and Chow, 1986; Loick-Wilde *et al.*, 2016; Reddy and Mitsui, 1984). However, there are also reports of N<sub>2</sub> fixation by some strains of *Synechococcus* under anaerobic conditions/limited O<sub>2</sub> concentrations (Rippka and Waterbury, 1977; Spiller and Shanmugam, 1987). Since the responses of *Synechococcus* towards O<sub>2</sub> are diverse, which likely affect the N<sub>2</sub> fixation, there is a need to assess *Synechococcus* cell-specific N<sub>2</sub> fixation in the Bay of Bengal to validate its diazotrophic nature in the Bay of Bengal.

The globally predominant diazotroph, which could be responsible for up to half of the assessed marine N<sub>2</sub> fixation (Capone *et al.*, 1997) — *Trichodesmium* — was found at the surface of the Bay of Bengal at station S7 and oxycline of station S2 and S3 only (Figure 4.5). *Trichodesmium* has been seasonally found along the coasts of the Bay of Bengal (Hegde *et al.*, 2008). Shetye *et al.* (2013) reported the blooms of *Trichodesmium* during spring near the Thamnapatnam coast of the Bay of Bengal. However, in the present study conducted in the coastal and the central Bay of Bengal, a very low abundance of *Trichodesmium* was observed. In contrast, high *Trichodesmium* abundance has been

reported several times in the Arabian Sea ([Capone et al., 1998](#); [Gandhi et al., 2011](#); [Jayakumar et al., 2012](#); [Mazard et al., 2004](#)). The reason behind such low *Trichodesmium* abundance in the Bay of Bengal is hard to assess in the present study as they were found at only three depths. Overall, we detected only a few cyanobacterial communities. [Löscher et al. \(2020\)](#) also found a few cyanobacterial clades but a broad diversity of NCDs throughout the water column during the winter monsoon.

## 4.5 Conclusions

Volumetric  $\text{N}_2$  fixation rates estimated in the euphotic and aphotic zone of the Bay of Bengal are equally low. Interestingly, the aphotic zone integrated  $\text{N}_2$  fixation rates contributed up to 100% of water column integrated  $\text{N}_2$  fixation rates, emphasising on  $\text{N}_2$  fixation in the aphotic zone as a significant component of the nitrogen cycle. A positive correlation of  $\text{NO}_x$  nutrient with  $\text{N}_2$  fixation rates in the aphotic zone and significantly higher  $\text{N}_2$  fixation rates below the OMZ than within the OMZ suggest that low concentrations of  $\text{NO}_x$  and  $\text{O}_2$  are not a firm niche requirement for diazotrophs. Thus,  $\text{N}_2$  fixation may not be predominantly limited to the euphotic zone only and may be feasible to other oceanic regions with nitrogen and/or  $\text{O}_2$ -rich conditions. Furthermore, aphotic zones other than OMZs may also contribute significantly to the reactive nitrogen inputs. These findings provide additional insights into diazotrophic activity in environments previously considered uncongenial for diazotrophy. Once assumed unimportant, our study suggests that NCD-driven  $\text{N}_2$  fixation is significant. The data set reported here urges us for comprehensive analyses of  $\text{N}_2$  fixation in the OMZs and other aphotic zones of the ocean, to estimate its extent in regulating the nitrogen cycle.



# Chapter 5

## N<sub>2</sub> fixation in the Arabian Sea during the winter monsoon

### 5.1 Introduction

N<sub>2</sub> fixation fuels the cellular N<sub>r</sub>-needs of primary producers and in turn, influences marine carbon fluxes and the Earth's climate ([Falkowski, 1997](#)). PO<sub>4</sub><sup>3-</sup> and Fe availability exert a strong control on N<sub>2</sub> fixation, but it has long been believed to occur in warm and N<sub>r</sub>-poor marine environments ([Holl and Montoya, 2005](#); [Karl et al., 2002](#); [Singh et al., 2019](#); [Sohm and Webb, 2011](#); [Stal, 2009](#)). Several studies, however, have revealed that N<sub>2</sub> fixation also occurs in N<sub>r</sub>-rich and colder waters of the Arctic Ocean ([Blais et al., 2012](#); [Harding et al., 2018](#); [Sato et al., 2021](#); [Shiozaki et al., 2018](#); [Sipler et al., 2017](#)) and the polar and subtropical front of the Pacific ([Raes et al., 2020](#)). Very recently for the first time, substantial N<sub>2</sub> fixation rates were observed in the Antarctic sea ice waters ([Shiozaki et al., 2020](#)), but it has been challenged owing to very high rates (up to 44 nmol N L<sup>-1</sup> d<sup>-1</sup>) in such a cold (below 0 °C) and NO<sub>3</sub><sup>-</sup>-rich (> 15 µmol L<sup>-1</sup>) environment ([White et al., 2022](#)).

The Arabian Sea is one such oceanic region where upper water column (particularly north of 10 °N) becomes N<sub>r</sub>-rich (~2 µmol L<sup>-1</sup> NO<sub>3</sub><sup>-</sup>) during the winter monsoon ([Madhupratap et al., 1996](#)). During the winter monsoon, cool and dry north-easterly winds pass over the Arabian Sea, which lead to surface water cooling and densification due to

excess evaporation over precipitation and a net heat loss. This results into convection, and consequently, subsurface colder and N<sub>r</sub>-rich waters mix with surface waters due to convective mixing. Conclusively, during the winter monsoon, the upper water column in the northern Arabian Sea becomes relatively colder and N<sub>r</sub>-rich in contrast to the southern Arabian Sea which remains warmer and N<sub>r</sub>-deficient — a believably conducive environment for diazotrophs. Further, isotopic evidence of lower  $\delta^{15}\text{N}$  of  $\text{NO}_3^-$  above the OMZs of the Arabian Sea, in comparison to the highly enriched  $\delta^{15}\text{N}$  of  $\text{NO}_3^-$  within the OMZs, and excess  $\text{PO}_4^{3-}$  relative to  $\text{NO}_3^-$  suggest substantial N<sub>2</sub> fixation in surface waters of the Arabian Sea ([Brandes et al., 1998](#); [Mulholland and Capone, 2009](#)). Thus, the Arabian Sea appears a perfect test site to examine the contrast of nutrients availability on N<sub>2</sub> fixation.

The Arabian Sea harbours a diverse group of diazotrophs, including *Trichodesmium*, unicellular cyanobacteria, and cyanobacterial symbionts ([Mazard et al., 2004](#); [Mulholland and Capone, 2009](#)). It has been reported that heterotrophic diazotrophic proteobacteria are also widely distributed and active in nutrient-rich as well as oligotrophic waters of the Arabian Sea ([Bird et al., 2005](#); [Bird and Wyman, 2013](#); [Jayakumar et al., 2012](#); [Shiozaki et al., 2014](#)). However, until recently, N<sub>2</sub> fixation rates estimation in the Arabian Sea has mostly focused on regions with *Trichodesmium* blooms in the eastern Arabian Sea ([Ahmed et al., 2017](#); [Capone et al., 1998](#); [Gandhi et al., 2011](#); [Kumar et al., 2017](#)). Contrary to the historical observations of the leading role played by cyanobacterial diazotrophs in fixing N<sub>2</sub> in the global ocean ([Capone et al., 1997](#); [Carpenter et al., 2004](#); [Karl et al., 2002](#)), [Shiozaki et al. \(2014\)](#) discovered that NCDs dominate N<sub>2</sub> fixation activity in the Arabian Sea.

The subsurface water of the northern Arabian Sea possesses one of the thickest OMZs of the global ocean (150–1000 m), harbouring denitrifiers and anammox bacteria. These organisms deplete  $\text{NO}_3^-$ ,  $\text{NO}_2^-$  and  $\text{NH}_4^+$  concentrations in the dissolved pool through their conversion to N<sub>2</sub> and consequently lead to a decrease in N:P ratios. The OMZs of the Arabian Sea are likely to be ecologically advantageous for O<sub>2</sub> and N<sub>r</sub>-sensitive process of N<sub>2</sub> fixation ([Burgess and Lowe, 1996](#); [Deutsch et al., 2007](#)), despite the dominance of N<sub>2</sub> fixation in O<sub>2</sub> saturated surface waters. Several studies have evidenced active diazotrophy in two of the three major OMZs of the global ocean: the Eastern Tropical North Pacific ([Jayakumar et al., 2017](#); [Selden et al., 2019](#)) and the Eastern Tropical South



Pacific ([Bonnet et al., 2013](#); [Chang et al., 2019](#); [Fernandez et al., 2011](#); [Löscher et al., 2014](#)). Whereas in the OMZs of the Arabian Sea, only the diazotrophic composition has been examined and a potential for active N<sub>2</sub> fixation was suggested based on clone library analysis ([Bird and Wyman, 2013](#); [Jayakumar et al., 2012](#)). Thus, to evidence the N<sub>2</sub> fixing potential of diazotrophs in the Arabian Sea, we estimated N<sub>2</sub> fixation rates at diverse sites in the Arabian Sea: the coastal area, the nutrient-rich northern Arabian Sea, and the nutrient-deficient southern Arabian Sea. We measured N<sub>2</sub> fixation rates in the euphotic zone under light and dark conditions, which would represent the potential of cyanobacterial and NCDs, respectively, and in the OMZs of the Arabian Sea. We hypothesised that substantial N<sub>2</sub> fixation occurs in the N<sub>r</sub>-rich waters of the northern Arabian Sea owing to lower N:P ratios. But it is unclear if N<sub>2</sub> fixation would preferentially occur in relatively colder and N<sub>r</sub>-rich waters of the northern Arabian Sea or warmer and N<sub>r</sub>-deficient waters of the southern Arabian Sea.

## 5.2 Materials and Methods

Seawater samples were collected in the Arabian Sea at 14 stations (SK1–SK14) from surface to up to 1000 m depth during the winter monsoon (16 Dec 2019 – 6 Jan 2020) on-board ORV *Sagar Kanya* (SK-364) (Figure 5.1). Samples were collected using Niskin bottles mounted on a Sea-Bird CTD rosette sampler.

Samples for N<sub>2</sub> fixation rates measurement experiments were taken from 3–4 depths of the euphotic zone and 3–4 depths of the aphotic zone. In the euphotic zone, samples for light and dark conditions were taken at around surface (5 or 10 m), 25 and 50 m, and/or at 70 or 75 m if present within the euphotic zone. Near coastal station SK1, *Trichodesmium* bloom was observed, but sample was taken from water visibly not affected by the bloom. At shallow station SK1, sampling was not done in the aphotic zone. In the aphotic zone, samples were taken at oxycline, initial and end point of the OMZs. The OMZs were found at all the stations except the coastal station SK1. The waters within the aphotic zone with O<sub>2</sub> ≤ 0.5 mL L<sup>-1</sup> were categorized as “suboxic waters” and with 0.5 < O<sub>2</sub> ≤ 2 mL L<sup>-1</sup> as “dysoxic waters”. The euphotic zone samples for light conditions were incubated

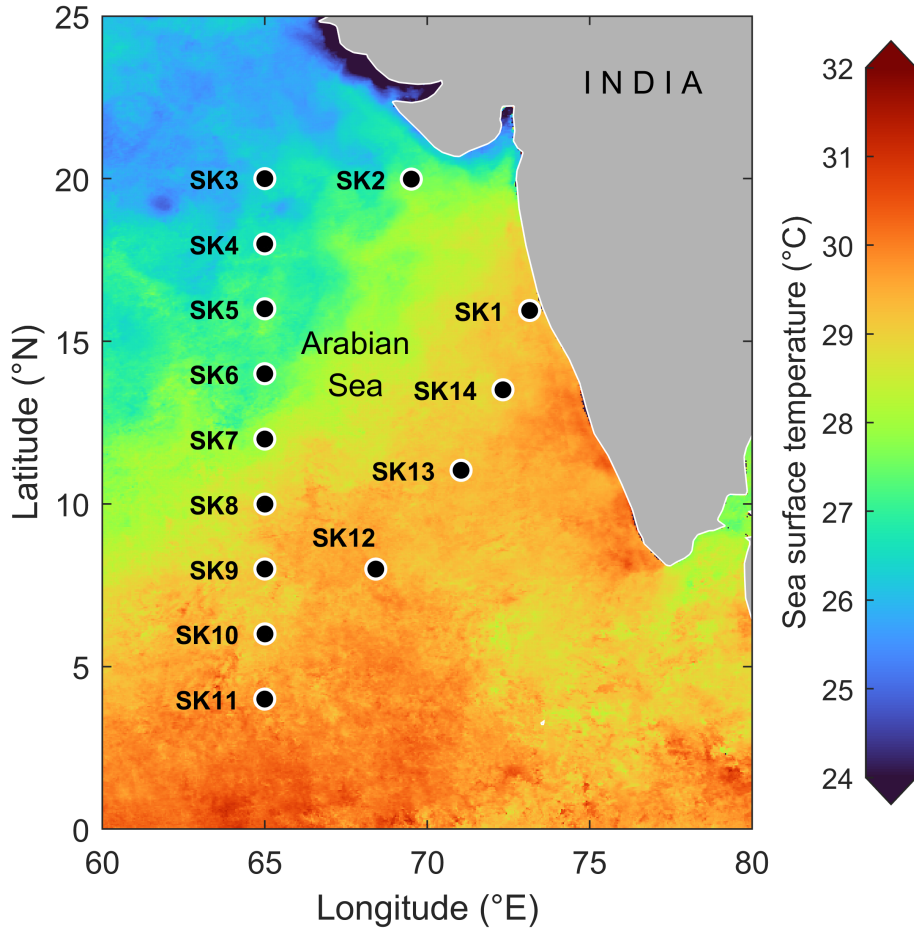


Figure 5.1: Sampling stations (SK1–SK14) superimposed on sea surface temperature (4 km resolution data obtained from Aqua/MODIS for Dec 2019) in the Arabian Sea during the research cruise expedition ORV *Sagar Kanya* (SK–364)

for 24 h as discussed in Chapter 2 and the samples for dark conditions were incubated for 4 h in complete dark conditions. The aphotic zone samples were incubated for 24 h in dark as discussed in Chapter 2.

The measurement of nutrients, DIC, and mass and  $\delta^{15}\text{N}$  of PON are discussed in Chapter 2.

Mixed layer depth (MLD) was determined based on the variation in temperature (0.2 °C difference from SST) (*de Boyer Montégut et al., 2004*).  $P^*$  indicates measure of excess or deficit of  $\text{PO}_4^{3-}$  relative to  $\text{NO}_x$ , was calculated based on the Redfield ratio (N:P=16:1, *Redfield (1934)*) according to *Deutsch et al. (2007)*:  $P^* = [\text{PO}_4^{3-}] - [\text{NO}_x]/16$ . Positive  $P^*$  indicates excess of  $\text{PO}_4^{3-}$  relative to  $\text{NO}_x$ .

Hereafter, N<sub>2</sub> fixation rates for the euphotic zone samples incubated under light

and dark conditions are referred as “light N<sub>2</sub> fixation rates” and “dark N<sub>2</sub> fixation rates”, respectively; whereas N<sub>2</sub> fixation rates for the aphotic zone samples are referred as “aphotic zone N<sub>2</sub> fixation rates”. The minimum quantifiable rates for N<sub>2</sub> fixation rates were also calculated using standard propagation of errors via observed variability between duplicate samples (*Gradoville et al., 2017*). N<sub>2</sub> fixation rates above minimum quantifiable rates are reported and discussed. Depth-integrated N<sub>2</sub> fixation rates were calculated by the trapezoidal integration of volumetric rates with depth, where N<sub>2</sub> fixation rates below minimum quantifiable rates were assigned with zero value to prevent the overestimation of depth-integrated rates. If N<sub>2</sub> fixation rates were below minimum quantifiable rates at all the depths within a zone, the depth-integrated rates were considered as below detection.

## 5.3 Results

### 5.3.1 Environmental conditions

All the measured environmental parameters showed a contrast between the northern and the southern Arabian Sea. SST decreased from 29 °C in the southern to 26 °C in the northern Arabian Sea, where stations SK2 to SK7 showed an explicit contrast in SST with relatively colder waters (< 27 °C) in comparison to the remaining stations (> 28 °C) (Table 5.1). Sea surface salinity increased from 35 in the southern to 36 in the northern Arabian Sea (Table 5.1). Therefore, on the basis of contrasting SST and salinity, we categorised stations SK2 to SK7 as the “convective stations” because they were influenced by winter convection as indicated by colder and denser surface waters (Figure 5.2a, b). The remaining open ocean stations SK8 to SK14, which were relatively warmer and less dense, were categorised as the “non-convective stations”. The station SK1 was excluded from this categorisation because it was the nearest coastal station, influenced by riverine discharge and remained unaffected from convection as indicated by higher SST (28.6 °C) and lower salinity (34.7) (Figure 5.2a, b). The OMZs were found at all the stations except the coastal station SK1. The OMZs with dysoxic waters were present in the southernmost stations (SK9–SK12, where SK9 and SK12 had only a very thin layer of suboxic waters of

around 70 m) and the OMZs with suboxic waters were present in the remaining stations (Figure 5.2c).

Table 5.1: Details of sea surface temperature (SST), sea surface salinity (SSS), mixed layer depth (MLD) at each station.

Station	SST (°C)	SSS	MLD (m)
SK1	28.6	34.7	51
SK2	26.9	36.1	58
SK3	26.3	36.3	57
SK4	25.9	36.1	48
SK5	26.8	36.2	66
SK6	27.2	36.4	42
SK7	27.5	36.2	48
SK8	28.2	36.6	48
SK9	29.1	35.4	44
SK10	29.1	35.2	45
SK11	29.4	35.3	26
SK12	29.1	35.6	71
SK13	29.1	36.1	48
SK14	28.9	36.2	42

### 5.3.2 Nutrients

The influence of convective mixing at stations SK2 to SK7, which brought subsurface nutrients to the upper water column, was visible in their nutrient profiles. The surface water NO<sub>x</sub> concentration ranged between 0.7 and 2.9  $\mu\text{mol L}^{-1}$  at the northern Arabian Sea stations SK3 to SK7, whereas it was below detection at the remaining stations (Figure 5.2d). The surface PO<sub>4</sub><sup>3-</sup> concentration was higher at the convective stations (0.4–0.5  $\mu\text{mol L}^{-1}$ ) in comparison to the non-convective stations (0.2–0.3  $\mu\text{mol L}^{-1}$ ) (Figure 5.2e). The stoichiometric ratios of N:P at surface of convective stations ranged from 1.8 to 5.4, while in the water column of all the stations ranged from 0.8 to 14.1 ( $9.8 \pm 3.8$ ,  $n = 106$ ), suggestive of N limitation. P\* was positive at all the depths and relatively more positive in the water column of the convective stations than that of the non-convective stations (Figure 5.2f).

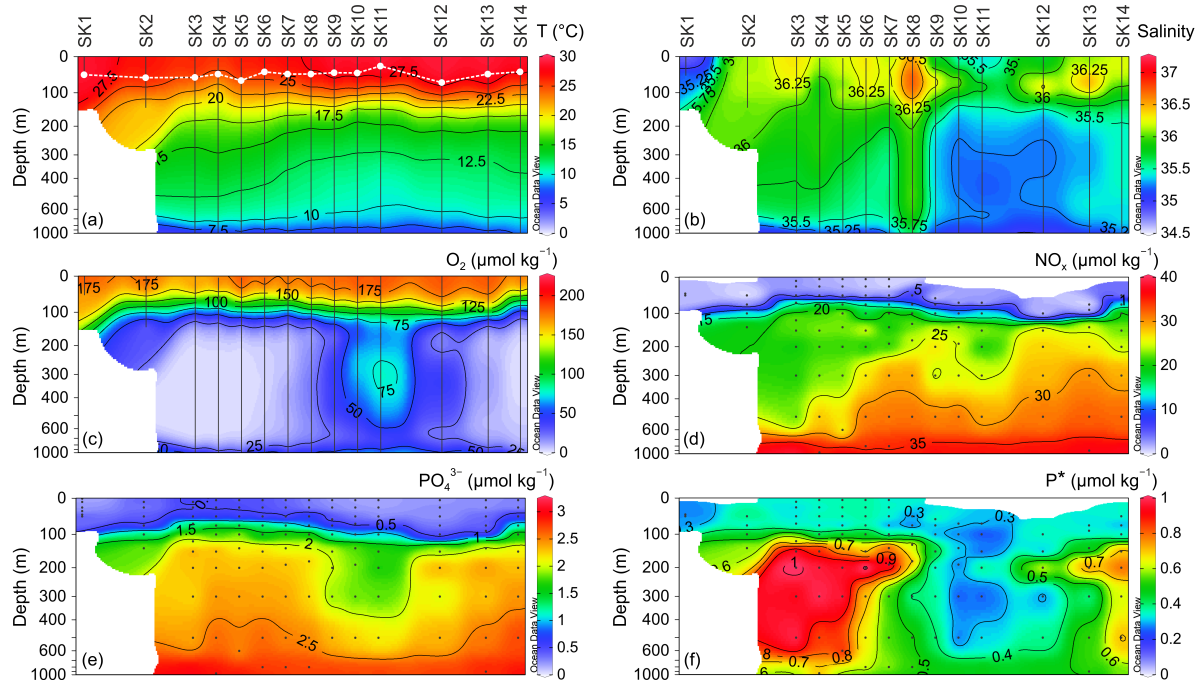


Figure 5.2: Vertical profiles of (a) temperature ( $T$ ), (b) salinity, (c)  $O_2$ , (d)  $NO_x$ , (e)  $PO_4^{3-}$  and (f)  $P^*$  at each station. White solid circles in (a) mark the mixed layer depth. Note the top of the y-axes is extended.

### 5.3.3 $N_2$ fixation rates

The minimum quantifiable rate for  $N_2$  fixation rates ranged from 0.001 and 2.83  $nmol\ N\ L^{-1}\ d^{-1}$ .  $N_2$  fixation rates were above minimum quantifiable rate in 29 and 31 of the 50 euphotic zone samples for light and dark conditions, respectively, and 13 of the 43 aphotic zone samples. Light  $N_2$  fixation rates at the surface ranged from  $0.04 \pm 0.03$  to  $17.4 \pm 1.5\ nmol\ N\ L^{-1}\ d^{-1}$  ( $1.9 \pm 0.3\ nmol\ N\ L^{-1}\ d^{-1}$ ,  $n = 14$ ) (Figure 5.3), with the highest rate at the coastal station SK1 where *Trichodesmium* bloom was witnessed (Figure 5.4) and the lowest rate at the southern station SK10. Excluding station SK1, these rates ranged up to  $4.7 \pm 2.8\ nmol\ N\ L^{-1}\ d^{-1}$  at station SK2. The average light  $N_2$  fixation rates at the surface of convective stations ( $1.0 \pm 0.6\ nmol\ N\ L^{-1}\ d^{-1}$ ,  $n = 5$ ) were significantly higher than at the non-convective stations ( $0.2 \pm 0.04\ nmol\ N\ L^{-1}\ d^{-1}$ ,  $n = 6$ ) (Table 5.3). Light  $N_2$  fixation rates at the surface overlying suboxic waters ranged from  $0.04 \pm 0.03$  to  $4.7 \pm 2.8\ nmol\ N\ L^{-1}\ d^{-1}$  ( $0.7 \pm 0.4\ nmol\ N\ L^{-1}\ d^{-1}$ ,  $n = 8$ ) while  $0.04 \pm 0.03$  to  $0.09 \pm 0.001\ nmol\ N\ L^{-1}\ d^{-1}$  ( $0.1 \pm 0.01\ nmol\ N\ L^{-1}\ d^{-1}$ ,  $n = 3$ ) for dysoxic waters.



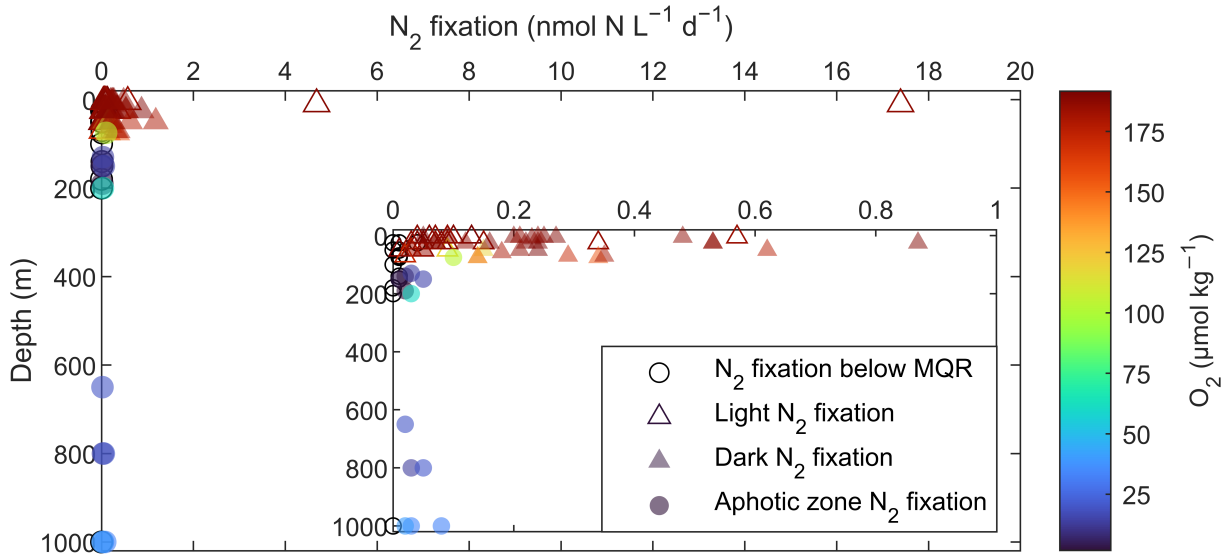


Figure 5.3: Vertical profiles of average light, dark and aphotic zone  $N_2$  fixation rates. The inset zooms the large variable region of  $N_2$  fixation rates. Open black circles represent the rates below minimum quantifiable rates (MQR).

Within the euphotic zone, light  $N_2$  fixation rates ranged from  $0.01 \pm 0.01$  to  $17.4 \pm 1.5$   $\text{nmol N L}^{-1} \text{d}^{-1}$  ( $0.85 \pm 0.11$   $\text{nmol N L}^{-1} \text{d}^{-1}$ ,  $n = 29$ ) and dark  $N_2$  fixation rates ranged from  $0.03 \pm 0.03$  to  $1.18 \pm 0.05$   $\text{nmol N L}^{-1} \text{d}^{-1}$  ( $0.3 \pm 0.02$   $\text{nmol N L}^{-1} \text{d}^{-1}$ ,  $n = 31$ ) (Figure 5.3). Aphotic zone  $N_2$  fixation rates ranged from 0.01 to 0.10  $\text{nmol N L}^{-1} \text{d}^{-1}$  ( $0.04 \pm 0.005$   $\text{nmol N L}^{-1} \text{d}^{-1}$ ,  $n = 13$ ) (Figure 5.3). The average  $N_2$  fixation rates in the suboxic waters ( $0.03 \pm 0.004$   $\text{nmol N L}^{-1} \text{d}^{-1}$ ,  $n = 8$ ) were not significantly different than the rates in the dysoxic waters ( $0.04 \pm 0.004$   $\text{nmol N L}^{-1} \text{d}^{-1}$ ,  $n = 4$ ).



Figure 5.4: *Trichodesmium* bloom observed near coastal station SK1.

The depth-integrated light and dark N<sub>2</sub> fixation rates ranged up to  $137.2 \pm 16.5$  and  $37.2 \pm 2.4$   $\mu\text{mol N m}^{-2} \text{ d}^{-1}$ , respectively, with highest values at station SK1 and SK7, respectively, (Table 5.2). The depth-integrated aphotic zone N<sub>2</sub> fixation rates ranged up to  $31.4 \pm 6.3$   $\mu\text{mol N m}^{-2} \text{ d}^{-1}$ , with the highest value at station SK9 (Table 5.2). The average depth-integrated light N<sub>2</sub> fixation rates at the convective stations were significantly higher than at the non-convective stations (Table 5.3). On the contrary, the average depth-integrated dark and aphotic zone N<sub>2</sub> fixation rates at the convective stations were significantly lower than at the non-convective stations (Table 5.3). Whole water column N<sub>2</sub> fixation rates ranged from 3.0 to  $137.2$   $\mu\text{mol N m}^{-2} \text{ d}^{-1}$  (average:  $24.5$   $\mu\text{mol N m}^{-2} \text{ d}^{-1}$ ). The contribution of aphotic zone N<sub>2</sub> fixation rates accounted for up to 95% of whole water column rates, with the highest contribution at the southernmost station SK11 (Table 5.2). N<sub>2</sub> fixation rates in the euphotic and aphotic zone were not correlated with any environmental parameter, apart from salinity with which light N<sub>2</sub> fixation rates were negatively correlated ( $r = -0.41$ ,  $p < 0.05$ ).

Table 5.2: Depth-integrated light, dark and aphotic zone N<sub>2</sub> fixation rates and contribution of aphotic zone to column N<sub>2</sub> fixation rates at each station. BD stands for below detection. Note that ‘contribution of aphotic zone to column N<sub>2</sub> fixation’ due to below detection/unavailable rates in the aphotic zone are indicated as hyphen.

Station	Light N <sub>2</sub> fixation ( $\mu\text{mol N m}^{-2} \text{ d}^{-1}$ )	Dark N <sub>2</sub> fixation ( $\mu\text{mol N m}^{-2} \text{ d}^{-1}$ )	Aphotic zone N <sub>2</sub> fixation ( $\mu\text{mol N m}^{-2} \text{ d}^{-1}$ )	Contribution of aphotic zone to column N <sub>2</sub> fixation (%)
SK1	$137.2 \pm 16.5$	BD	–	–
SK2	$38.5 \pm 30.0$	$1.7 \pm 0.9$	$1.3 \pm 0.5$	3.1
SK3	BD	$1.7 \pm 0.5$	BD	–
SK4	$4.0 \pm 0.2$	$7.6 \pm 1.8$	BD	–
SK5	$3.5 \pm 0.5$	$8.2 \pm 7.3$	BD	–
SK6	$3.0 \pm 0.7$	$9.7 \pm 6.5$	$0.6 \pm 0.1$	12.9
SK7	$1.3 \pm 0.4$	$37.2 \pm 2.4$	$18.2 \pm 7.6$	90.2
SK8	$1.1 \pm 0.7$	$33.8 \pm 4.9$	$15.1 \pm 10.3$	88.7
SK9	$0.7 \pm 0.3$	$12.5 \pm 4.9$	$31.4 \pm 6.3$	92.5
SK10	$0.6 \pm 0.5$	$8.9 \pm 6.7$	$12.0 \pm 5.3$	89.7
SK11	$1.0 \pm 0.7$	$5.1 \pm 2.5$	$20.1 \pm 6.0$	95.3
SK12	$5.5 \pm 0.7$	$18.2 \pm 10.1$	$4.3 \pm 2.7$	44.1
SK13	$3.0 \pm 0.6$	BD	BD	–
SK14	$7.4 \pm 3.9$	BD	BD	–

## 5.4 Discussion

### 5.4.1 Highest N<sub>2</sub> fixation concurs with *Trichodesmium* bloom

At a *Trichodesmium* bloom station SK1, where temperature was around 29 °C and NO<sub>x</sub> concentration was undetectable — a conducive warm and N<sub>r</sub> deficient environment for *Trichodesmium* ([Capone et al., 1997](#)) — the light N<sub>2</sub> fixation rate at the surface was an order of magnitude higher than other stations. The occurrence of highest rate at the coastal station appears to be because of higher supply of its limiting nutrients (PO<sub>4</sub><sup>3-</sup> and Fe) through terrestrial and riverine inputs. Though the surface PO<sub>4</sub><sup>3-</sup> concentration at station SK1 was lowest than that observed at other stations, but this is attributable to its consumption during diazotrophs production ([Cloern, 2021](#)). The observation of higher N<sub>2</sub> fixation rates near the coast supports previous arrays of evidences that ocean margins contribute a larger amount of new N ([Selden et al., 2019](#)). The highest light N<sub>2</sub> fixation rate that occurred at the surface of the coastal station is one to three orders of magnitude lower than the highest rates previously reported during the spring inter-monsoon at the eastern coast of the Arabian Sea ([Ahmed et al., 2017](#); [Gandhi et al., 2011](#); [Kumar et al., 2017](#)). Previous studies ascribed high N<sub>2</sub> fixation rates to NO<sub>x</sub> deficient waters, we found undetectable NO<sub>x</sub> and comparable PO<sub>4</sub><sup>3-</sup> concentration at station SK1. This high difference between the rates could probably be because we did not collect water directly from the bloom and also the sampling depth corresponded to 10 m whereas in their studies, previous studies sampled at 0 m, where *Trichodesmium* dominate due to its positive buoyancy ([Shiozaki et al., 2010](#)); thus, patchiness of diazotroph abundance seems to be a reason. Several studies have visibly reported the seasonal occurrence of *Trichodesmium* in the eastern and central Arabian Sea during calmer, warmer, and oligotrophic spring and autumn inter-monsoon ([Ahmed et al., 2017](#); [Basu et al., 2011](#); [Capone et al., 1998](#); [Desa et al., 2005](#); [Devassy et al., 1978](#); [Gandhi et al., 2011](#); [Parab et al., 2006](#); [Parab and Matondkar, 2012](#)). However, *Trichodesmium* bloom observed during the winter monsoon hints towards its perennial occurrence in the Arabian Sea.



### 5.4.2 N<sub>2</sub> fixation in N<sub>r</sub>-rich and N<sub>r</sub>-deficient waters

We voyaged through contrasting physicochemical conditions in the Arabian Sea. These conditions ranged from surface waters near the equator devoid of nutrients (NO<sub>x</sub>: below detection, PO<sub>4</sub><sup>3-</sup>: 0.4–0.5 µmol L<sup>-1</sup>) to the northern Arabian Sea rich in nutrients (NO<sub>x</sub>: 0.6–2.6 µmol L<sup>-1</sup>, PO<sub>4</sub><sup>3-</sup>: 0.2–0.3 µmol L<sup>-1</sup>) owing to influence of winter monsoon driven convective mixing. The convective mixing shows its influence on seawater temperature and nutrients concentrations between stations SK2 and SK7, where convective mixing prevails (*Madhupratap et al.*, 1996). In surface waters, temperature reached as low as 26 °C at station SK4 and NO<sub>x</sub> concentration reached as high as 2.6 µmol L<sup>-1</sup> at station SK3. On the contrary, the non-convective stations with relatively warmer waters but undetectable NO<sub>x</sub> concentration seem like ideal niches for diazotrophs. Yet, significantly higher average light N<sub>2</sub> fixation rates occurred in surface waters of the convective stations than that in the non-convective stations. The suboxic waters at the convective stations in the Arabian Sea, contain one of the three major denitrification sites of the global ocean (*Morrison et al.*, 1999), which is indicative through reduced NO<sub>x</sub> concentrations and an elevated P\* in the suboxic waters. Additionally, the suboxic waters of the Arabian Sea are reported for enriched concentration of Fe (*Moffett et al.*, 2007). *Shiozaki et al.* (2014) also observed higher dissolved Fe concentration in the surface waters of the norther than in the southern Arabian Sea during the winter monsoon. Thus, at the convective stations which dominate in the northern Arabian Sea, though we observed no correlation of rates with NO<sub>x</sub> or PO<sub>4</sub><sup>3-</sup> concentrations, elevated P\* and Fe supplied from deeper to surface waters appear to be a reason for higher light N<sub>2</sub> fixation rates. The winter convection could further enhance light N<sub>2</sub> fixation rates by the end of its phase i.e., during the month of February when convective mixing is stronger than that in December (the month when sampling was

Table 5.3: Average of light, dark and aphotic zone N<sub>2</sub> fixation rates at convective and non-convective stations. Number of data points are indicated in brackets.

	Convective stations	Non-convective stations
Surface N <sub>2</sub> fixation (nmol N L <sup>-1</sup> d <sup>-1</sup> )	1.0 ± 0.6 (5)	0.2 ± 0.04 (6)
Depth-integrated light N <sub>2</sub> fixation (µmol N m <sup>-2</sup> d <sup>-1</sup> )	10.1 ± 6.0 (5)	2.8 ± 0.6 (7)
Depth-integrated dark N <sub>2</sub> fixation (µmol N m <sup>-2</sup> d <sup>-1</sup> )	11.0 ± 1.7 (6)	15.7 ± 2.8 (5)
Depth-integrated aphotic zone N <sub>2</sub> fixation (µmol N m <sup>-2</sup> d <sup>-1</sup> )	6.7 ± 2.5 (3)	16.6 ± 2.9 (5)

performed). N is reported to be suppressive for N<sub>2</sub> fixation (*Chen et al.*, 2008; *Falkowski*, 1983; *Knapp*, 2012; *Zhang et al.*, 2015), conversely, we observed substantial light N<sub>2</sub> fixation rates at the surface despite high ambient concentrations of NO<sub>x</sub>, indicating that excess PO<sub>4</sub><sup>3-</sup> and Fe availability over NO<sub>x</sub> plays primary role in stimulating diazotrophy in the northern Arabian Sea. Further, the non-convective stations with undetectable NO<sub>x</sub> but detectable PO<sub>4</sub><sup>3-</sup> concentration — seemingly diazotrophy conducive — were Fe limited (*Shiozaki et al.*, 2014), owing to lower aeolian dust deposition in comparison to the northern Arabian Sea (*Jickells et al.*, 2005); and thus, Fe plays a governing role for diazotrophy in the southern Arabian Sea.

Light N<sub>2</sub> fixation rates at the surface overlying suboxic waters of the Arabian Sea ranged from  $0.04 \pm 0.03$  to  $4.7 \pm 2.8$  nmol N L<sup>-1</sup> d<sup>-1</sup> ( $0.7 \pm 0.4$  nmol N L<sup>-1</sup> d<sup>-1</sup>, n = 8), and are in good agreement with the Eastern Tropical South Pacific which showed a large variability in rates and ranged from 0.01 to 2.3 nmol N L<sup>-1</sup> d<sup>-1</sup> with an exclusion of highest rate (24.8 nmol N L<sup>-1</sup> d<sup>-1</sup>) (*Bonnet et al.*, 2013; *Chang et al.*, 2019; *Dekaezemacker et al.*, 2013; *Fernandez et al.*, 2011; *Löscher et al.*, 2014, 2016; *Selden et al.*, 2021), and the Eastern Tropical North Pacific which reached a maximum rate of 3.3 nmol N L<sup>-1</sup> d<sup>-1</sup> (*Jayakumar et al.*, 2017).

### 5.4.3 Active non-cyanobacterial diazotrophy in the Arabian Sea

To investigate non-cyanobacterial diazotrophic activity in the euphotic zone, we performed incubations under dark conditions. In the eastern Arabian Sea, *Kumar et al.* (2017) found major contribution (up to 52%) of NCDs towards total N<sub>2</sub> fixation, whereas in the present study the rates were below minimum quantifiable rates at the eastern Arabian Sea station SK1. However at the convective and non-convective stations, we found that depth-integrated dark N<sub>2</sub> fixation rates were several folds higher compared to light N<sub>2</sub> fixation rates, which is attributable to the dominance of NCDs that corroborates with the previously reported evidences of higher NCDs than the cyanobacterial diazotrophs in the Arabian Sea (*Bird and Wyman*, 2013; *Jayakumar et al.*, 2012; *Shiozaki et al.*, 2014). Further, significantly higher dark N<sub>2</sub> fixation rates at convective compared to the non-convective stations suggest that unlike cyanobacterial diazotrophs, NCDs prevailing in the

euphotic zone appear to be more sensitive to  $\text{NO}_x$  concentrations. This study corroborates that NCDs are the dominating contributors for the source of new N within the euphotic zone of the Arabian Sea.

The aphotic zone  $\text{N}_2$  fixation rates were low ( $< 0.1 \text{ nmol N L}^{-1} \text{ d}^{-1}$ ), but persistent throughout the water column. In the other two major suboxic OMZs of the global ocean,  $\text{N}_2$  fixation rates were on average  $0.8 \pm 0.5 \text{ nmol N L}^{-1} \text{ d}^{-1}$  in the Eastern Tropical North Pacific ([Jayakumar et al., 2017](#)), while the rates were less than  $0.5 \pm 1.4 \text{ nmol N L}^{-1} \text{ d}^{-1}$  for all the studies conducted so far in the Eastern Tropical South Pacific, excluding one study with an average rate of  $1.3 \pm 1.2 \text{ nmol N L}^{-1} \text{ d}^{-1}$  ([Selden et al., 2021](#)). Conclusively in the suboxic OMZ waters of the Arabian Sea,  $\text{N}_2$  fixation rates ( $0.03 \pm 0.01 \text{ nmol N L}^{-1} \text{ d}^{-1}$ ) are modest but an order of magnitude lower compared to the rates within the OMZs of the Pacific. Surprisingly, ([Chang et al., 2019](#)) observed below detection rates in the presence of high *nifH* (a marker gene for  $\text{N}_2$  fixation) concentrations in the  $\text{O}_2$ -deficient waters of the Eastern Tropical South Pacific. The rates variability within the major OMZs of the global ocean can be due to ecological diversity of diazotrophs ([Zehr and Capone, 2020](#)), their patchiness ([Selden et al., 2019](#)) and flexibility towards  $\text{O}_2$ .

Table 5.4:  $\text{N}_r$  input in the euphotic zone, aphotic zone and water column of the Arabian Sea, estimated using  $\text{N}_2$  fixation rates from the respective zones.

	Range ( $\text{Tg N y}^{-1}$ )	Average ( $\text{Tg N y}^{-1}$ )
Euphotic zone	0.02—4.35	0.50
Aphotic zone	0.02—0.99	0.41
Water column	0.09—4.35	0.78

#### 5.4.4 Is $\text{N}_2$ fixation insufficient to compensate $\text{N}_r$ -loss through denitrification?

Globally, there is a net imbalance between  $\text{N}_r$ -gain and -loss in the ocean, with an inclination of weighing scale towards  $\text{N}_r$ -loss through denitrification ([Codispoti, 2007](#); [Benavides et al., 2018a](#)). While [Codispoti \(2007\)](#) tried to call for observations to put these imbalanced estimates on firmer ground, the true potential of marine  $\text{N}_2$  fixation as a prominent source of N remained inconclusive. Among the global ocean, the Arabian Sea, containing one of the three perennial and largest volumes of suboxic waters, has been reported for

about 20 to 40% of the global oceanic N<sub>r</sub>-loss through water column denitrification ([Bange et al., 2000, 2005](#)). It loses  $\sim 60$  Tg N y<sup>-1</sup> through water column denitrification ([Bange et al., 2005](#); [Codispoti, 2007](#)). We estimated diazotrophic N input for the Arabian Sea (area:  $\sim 6.2 \times 10^6$  km<sup>2</sup>) by extrapolating water column N<sub>2</sub> fixation rates ranging from 3.0 to 137.2  $\mu\text{mol N m}^{-2} \text{ d}^{-1}$  (average: 24.5  $\mu\text{mol N m}^{-2} \text{ d}^{-1}$ ). The annual N<sub>r</sub>-gain for the Arabian Sea ranged between 0.09 to 4.35 Tg N y<sup>-1</sup> (average: 0.78 Tg N y<sup>-1</sup>) (Table 5.4), and on an average diazotrophy yields lower N<sub>r</sub>-gain than the N<sub>r</sub>-loss through denitrification in the Arabian Sea. Our estimates of N<sub>r</sub>-gain through diazotrophy are far higher than the previous reports for the Arabian Sea ([Bange et al., 2000](#); [Capone et al., 1998](#); [Gandhi et al., 2011](#)), where only *Trichodesmium* bloom associated rates were considered or only N<sub>2</sub> fixation rates within the euphotic zone were considered owing to unavailability of data from the aphotic zone. Therefore, the present study's large spatial resolution of N<sub>2</sub> fixation rates and their significance in the aphotic zone clue towards a steady state of N<sub>r</sub> in the Arabian Sea. This study provides quantitative evidence for a close spatial coupling between N<sub>2</sub> fixation and N<sub>r</sub>-loss (arising from denitrification) in the Arabian Sea as proposed by [Deutsch et al. \(2007\)](#) and [Brandes et al. \(1998\)](#), and as observed in the OMZ off Peru ([Löscher et al., 2014](#)). Yet, we do not affirm N<sub>r</sub>-loss as a control on N<sub>2</sub> fixation in the Arabian Sea, since we observed similar rates in the suboxic and dysoxic waters, indicating independency of prevailing NCDs on O<sub>2</sub> and NO<sub>x</sub>. Nonetheless, this study asserts that the extent of imbalance in the estimated global marine N budget can be shortened by evaluating the newly recognised niches of diazotrophs.

## 5.5 Conclusions

In this study, we showcase the most extensive data set to date of N<sub>2</sub> fixation above and within the oxygen minimum zone of the Arabian Sea, encompassing the contrasting physico-chemical conditions of the northern and the southern Arabian Sea. Higher rates in the euphotic zone than in the aphotic zone were observed, but the rates in the aphotic zone were persistent throughout the water column. The occurrence of N<sub>2</sub> fixation in the suboxic waters warrants the close spatial coupling between N<sub>2</sub> fixation and N<sub>r</sub>-loss process of denitrification. Similar rates within the suboxic and dysoxic waters discourage

---

the historical beliefs for diazotrophic niches. This study asserts the need to quantify diazotrophy in  $\text{NO}_x$ -rich and oxygenated dark and cold waters.



## Chapter 6

# Contribution of dark C fixation towards C sink in the ocean aphotic zone

### 6.1 Introduction

The marine C budget forms a key part of the global C budget which is required to support climate change mitigation policies. While various carbon dioxide (CO<sub>2</sub>) removal mechanisms are proposed to remove ~1000 billion tons of atmospheric CO<sub>2</sub> by 2100 by increasing ocean C uptake, the prerequisite estimate of C sources and sinks is imprecise ([Burd \*et al.\*, 2010](#)). One such area of investigation for C budget is the aphotic zone of the ocean. The OMZs within the aphotic zone are a potential site of CO<sub>2</sub> assimilation. The OMZs possess abundant and diversified chemoautotrophs (such as anammox and nitrifying organisms) which are light-independent microorganisms that use inorganic nutrients to cater the energy need.

It has been reported that heterotrophic C demand in the aphotic zone does not reconcile with the supply of organic matter produced in the euphotic zone ([del Giorgio and Duarte, 2002](#)), indicating a gap between the demand and supply of C. This discrepancy may stem from the unaccounted autochthonously produced organic C via chemoautotrophic inorganic C assimilation in the aphotic zone (hereafter, dark C fixation). Evidently, in the northeast Atlantic, the organic C demand of mesopelagic prokaryotes is replenished by dark C fixation, contributing up to 72% to their daily demand ([Baltar](#)

*et al.*, 2010). Previous studies have indicated that dark C fixation affects the C cycle by providing additional organic substrates (*Close et al.*, 2014; *Herndl et al.*, 2005; *Podlaska et al.*, 2012), which could contribute to intensification of OMZs. Yet, the role of dark C fixation towards CO<sub>2</sub> sequestration remains inconclusive, indicating the need to investigate and demystify this overlooked C sink.

The OMZs could be favourable for chemoautotrophs since less energy is required to reduce inorganic C to organic C in anaerobic environment compared to aerobic environment (*Hügler and Sievert*, 2011; *McCollom and Amend*, 2005). Additionally, the sinking C to OMZs is insufficient to support prokaryotic C demand and thus, alternative C sources are required in the OMZs (*Ragavan and Kumar*, 2021). Therefore, it appears that chemoautotrophy in the OMZs can form an integral component of the C cycle to a greater extent and dark C fixation can contribute towards intensification of OMZs.

The dark C fixation has been explored in the suboxic ( $O_2 \leq 0.5 \text{ mL L}^{-1}$ ) oceanic basins like the Baltic Sea, the Black Sea and the Cariaco Basin and in coastal regions like the Eastern Tropical North and South Pacific (*Günter et al.*, 2008; *Jørgensen et al.*, 1991; *Podlaska et al.*, 2012; *Taylor et al.*, 2001; *Vargas et al.*, 2021). In contrast, the open ocean OMZs within the aphotic zone largely remained unassessed. The Arabian Sea possesses one of the most intense and largest OMZs of the global ocean. It is well known for the high abundance and activity of anammox and nitrifying organisms (*Jayakumar et al.*, 2009; *Lüke et al.*, 2016; *Villanueva et al.*, 2014). Recent isotope based studies have proposed that dark C fixation contributes to sinking C fluxes in the OMZ of the Arabian Sea ( $\sim 17\%$ ) (*Keil et al.*, 2016; *Lengger et al.*, 2019). Here, we examine the Arabian Sea for its dark C fixation potential, relative importance to C fixation in the water column and the effect of OMZ's O<sub>2</sub> concentrations on C fixation. For this purpose, we conducted C fixation measurements in the euphotic and aphotic zone of the northern (having suboxic OMZ waters,  $O_2 \leq 0.5 \text{ mL L}^{-1}$ ) and southern (having hypoxic OMZ waters,  $0.5 < O_2 \leq 1.5 \text{ mL L}^{-1}$ ) Arabian Sea.



## 6.2 Materials and Methods

Seawater samples were collected in the Arabian Sea at 14 stations (SK1–SK14) from surface to up to 1000 m depth during the winter monsoon (16 Dec 2019 – 6 Jan 2020) on-board ORV *Sagar Kanya* (SK–364) (Figure 6.1). Samples were collected using Niskin bottles mounted on a Sea-Bird CTD rosette sampler.

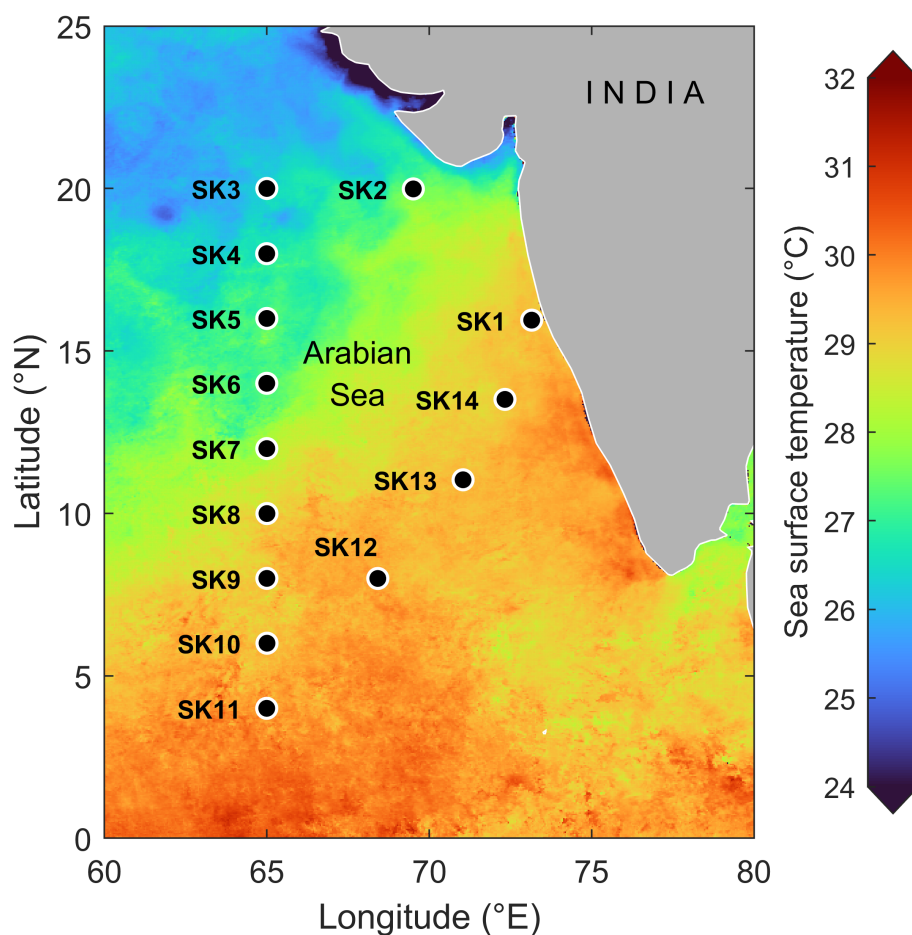


Figure 6.1: Sampling stations (SK1–SK14) superimposed on sea surface temperature (4 km resolution data obtained from Aqua/MODIS for Dec 2019) in the Arabian Sea during the research cruise expedition ORV *Sagar Kanya* (SK–364)

The measurement of nutrients, DIC, and mass and  $\delta^{13}\text{C}$  of POC are discussed in Chapter 2. Samples for C fixation experiments were taken from 3–4 depths of the euphotic zone and 3–4 depths of the aphotic zone and were incubated in a similar manner as discussed in Chapter 5.

## 6.3 Results

### 6.3.1 Environmental conditions

Sea surface temperature ranged from 26 to 29.4 °C and was minimum at station SK4 in the northern Arabian Sea, whereas maximum at the southernmost station SK11 (Figure 6.2a). Sea surface salinity ranged from 34.7 to 36.6 with the least and the highest value at stations

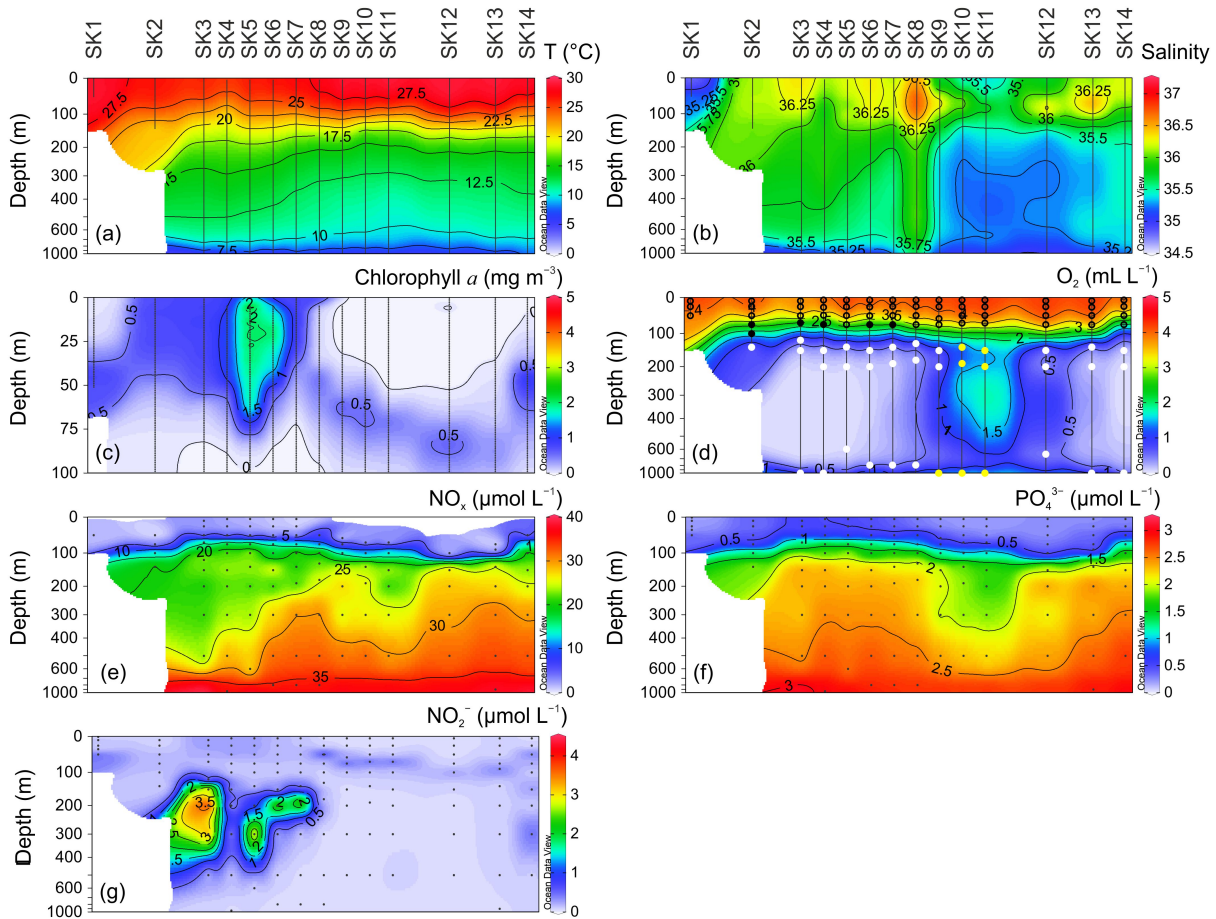


Figure 6.2: Vertical profiles of (a) temperature (T), (b) salinity, (c) chlorophyll *a* (Chl *a*), (d) O<sub>2</sub>, (e) NO<sub>x</sub>, (f) PO<sub>4</sub><sup>3-</sup> and (g) NO<sub>2</sub><sup>-</sup> at each station. Black open, solid black, white and yellow circles in the O<sub>2</sub> profile mark the seawater sampling depths for incubation experiments corresponding to the euphotic zone, aphotic zone's oxycline, suboxic and hypoxic waters, respectively. Note the difference in depth for the Chl *a* profile and that the top of the y-axes is extended for all the profiles except for Chl *a* profile.

SK1 and SK8, respectively (Figure 6.2b). Deep chlorophyll *a* maximum concentration was at station SK5 (Figure 6.2c). Deep chlorophyll *a* maximum depth increased towards the southern Arabian Sea.

$\text{NO}_x$  and  $\text{PO}_4^{3-}$  concentrations increased with depth (Figure 6.2e, f). The surface water concentrations of  $\text{NO}_x$  were above detection only in the northern Arabian Sea (SK3–SK7) (Figure 6.2e). The  $\text{PO}_4^{3-}$  concentrations were higher in the northern relative to the southern Arabian Sea (Figure 6.2f). Along with this, the nutrient stoichiometric ratio of N:P ranged from 0.8 to 14.1 ( $9.8 \pm 3.8$ ,  $n = 106$ ) which is lower than the Redfield ratio of 16 (Redfield, 1958, 1934). The  $\text{NO}_2^-$  concentration showed maxima in the suboxic OMZ waters of the northern Arabian Sea with the highest value at station SK3 (Figure 6.2g).

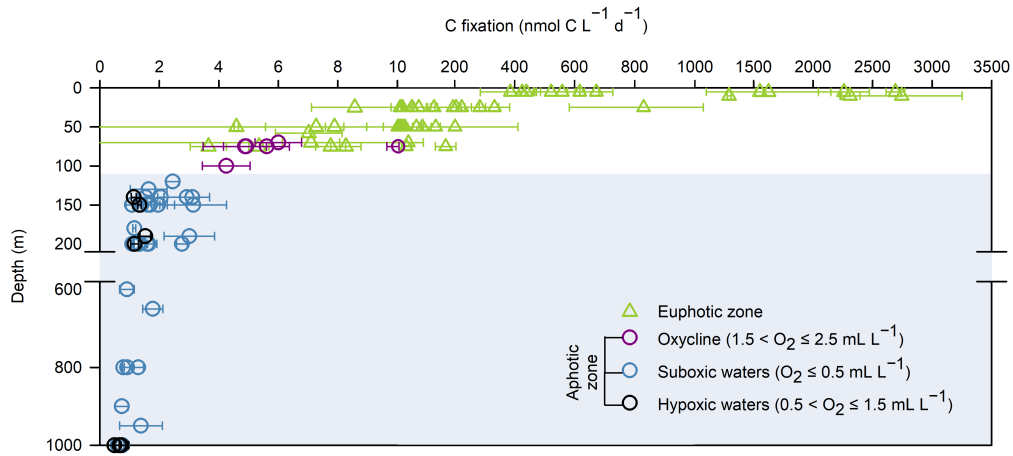


Figure 6.3: Vertical profile of C fixation rates in the euphotic and aphotic zone. Shaded background indicates the OMZ within the aphotic zone. Note the break in the y-axis between 200 and 600 m.

### 6.3.2 C fixation rates

C fixation rates in the euphotic zone (hereafter, light C fixation rates) sharply decreased with depth from  $2745.0 \pm 507.3$  to  $3.6 \pm 0.6$   $\text{nmol C L}^{-1} \text{ d}^{-1}$  (Figure 6.3). Light C fixation rates at the surface ranged from  $385.7 \pm 100.1$  to  $2745.0 \pm 507.3$   $\text{nmol C L}^{-1} \text{ d}^{-1}$  ( $1292.4 \pm 56.5$   $\text{nmol C L}^{-1} \text{ d}^{-1}$ ,  $n = 14$ ) with the lowest and the highest value at station SK13 and SK3, respectively (Figure 6.4a). Dark C fixation rates from the aphotic zone were categorised into three sections: (a) oxycline ( $1.5 < \text{O}_2 \leq 2.5$   $\text{mL L}^{-1}$ ) dark

C fixation rates, (b) hypoxic region dark C fixation rates and (c) suboxic region dark C fixation rates (Figure 6.3). Dark C fixation rates ranged from  $0.5 \pm 0.2$  to  $6.0 \pm 0.8$   $\text{nmol C L}^{-1} \text{ d}^{-1}$  except at 75 m depth of SK2 station where  $12.4 \pm 2.8$   $\text{nmol C L}^{-1} \text{ d}^{-1}$  rate was

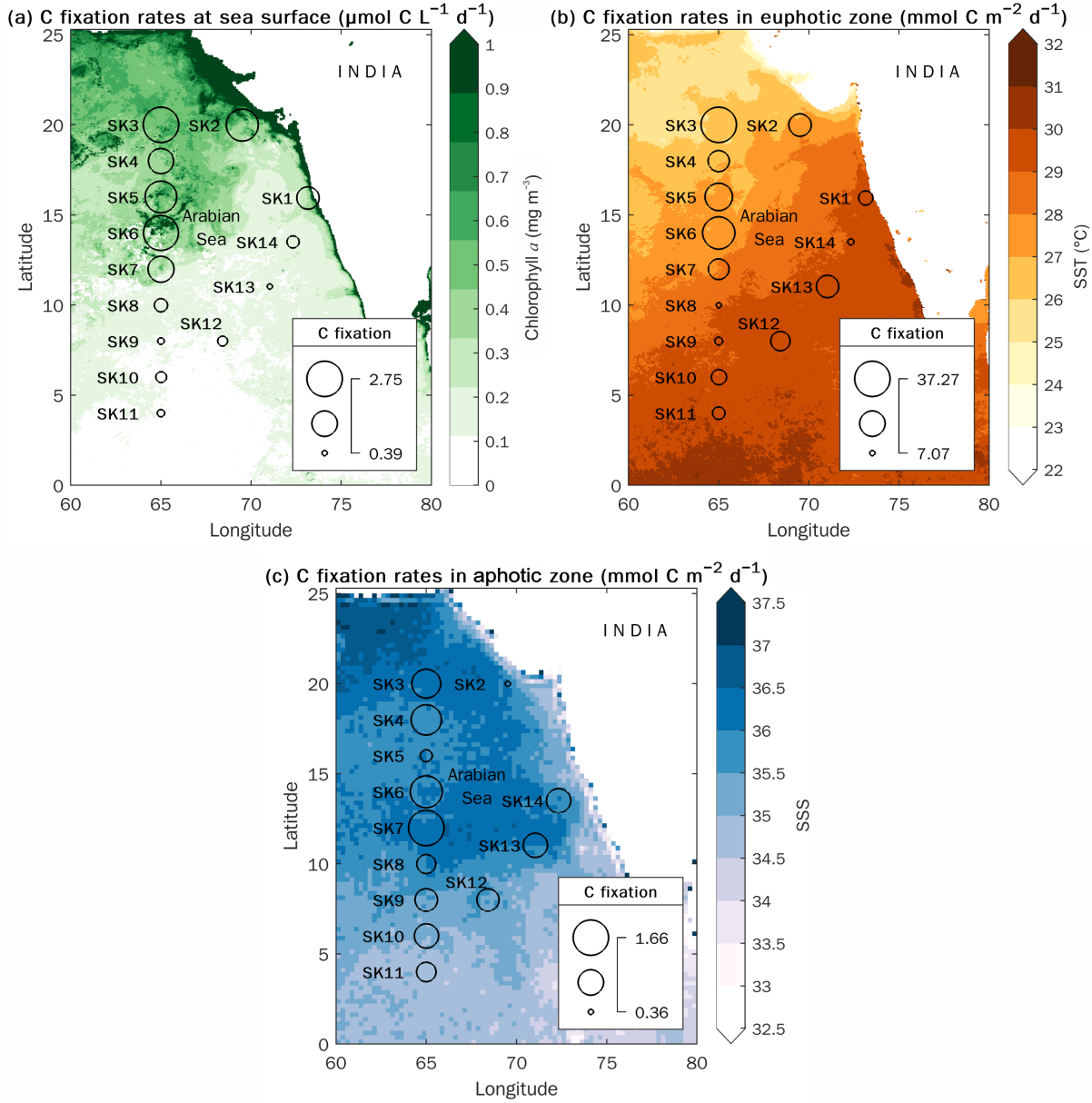


Figure 6.4: C fixation rates (a) at sea surface ( $\mu\text{mol C L}^{-1} \text{ d}^{-1}$ ), (b) in the euphotic zone ( $\text{mmol C m}^{-2} \text{ d}^{-1}$ ) and (c) in the aphotic zone ( $\text{mmol C m}^{-2} \text{ d}^{-1}$ ) at sampling stations (SK1–SK14) in the Arabian Sea. Background contours: (a) Chl *a*: sea surface chlorophyll *a* concentration (4 km resolution data obtained from Aqua/MODIS for Dec 2019), (b) SST: sea surface temperature (4 km resolution data obtained from Aqua/MODIS for Dec 2019) and (c) SSS: sea surface salinity (40 km resolution data obtained from RSS-SMAP-NASA for Dec 2019). Note that sampling in the aphotic zone was not done at SK1.

observed (Figure 6.3). The highest dark C fixation rates were observed in the oxycline region and ranged from  $4.2 \pm 0.8$  to  $12.4 \pm 2.8$   $\text{nmol C L}^{-1} \text{ d}^{-1}$  ( $6.3 \pm 0.6$   $\text{nmol C L}^{-1} \text{ d}^{-1}$ ,  $n = 6$ ). The average dark C fixation rates in the suboxic OMZ waters ( $1.63 \pm 0.08$   $\text{nmol C L}^{-1} \text{ d}^{-1}$ ,  $n = 30$ ) were significantly different than in the hypoxic OMZ waters ( $1.00 \pm 0.06$   $\text{nmol C L}^{-1} \text{ d}^{-1}$ ,  $n = 7$ ). The depth-integrated light C fixation rates ranged from  $7.1 \pm 0.78$  to  $37.3 \pm 8.8$   $\text{mmol C m}^{-2} \text{ d}^{-1}$  with the highest rate at northern station SK3 (Figure 6.4b). The depth-integrated dark C fixation rates ranged from  $0.4 \pm 0.06$  to  $1.7 \pm 0.4$   $\text{mmol C m}^{-2} \text{ d}^{-1}$  (Figure 6.4c).

Light C fixation rates were negatively correlated with  $\text{NO}_2^-$  and  $\text{PO}_4^{3-}$  concentrations, and positively with  $\text{O}_2$  concentrations (Figure 6.5). Dark C fixation was negatively correlated with  $\text{NO}_x$  and  $\text{PO}_4^{3-}$  concentrations, and positively with  $\text{NO}_2^-$  concentrations. Light C fixation rates and dark C fixation both were positively correlated with POC.

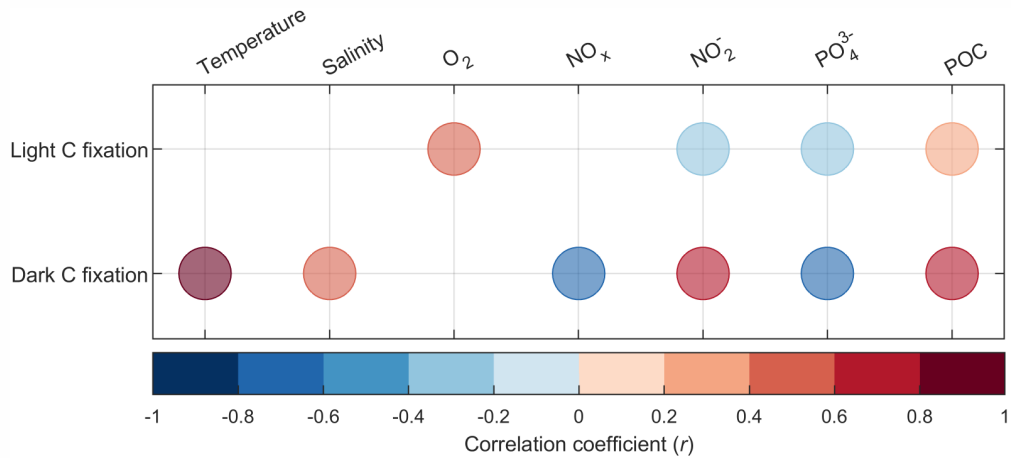


Figure 6.5: Spearman's correlation matrix with correlation coefficient ( $r$ ). Indicated correlations are significant at  $p < 0.05$ . Note that only the parameters which significantly correlated with light and/or dark C fixation are indicated.

## 6.4 Discussion

### 6.4.1 Light C fixation in the Arabian Sea

Our expedition, performed during winter, transited through a biogeochemical gradient: from the colder and highly productive northern Arabian Sea to the warmer and less productive southern Arabian Sea (Figure 6.4a, b). During winter, the Arabian Sea water densifies due to excess evaporation over precipitation and net heat loss due to the prevalence of cool and dry north-easterly winds (*Madhupratap et al.*, 1996). This causes convection (particularly north of 10 °N) and leads to the replenishment of surface water with nutrient-rich subsurface water through convective mixing. Evidently in this study as well, the nutricline shoaled towards the northern Arabian Sea (Figure 6.2e, f), and an explicit difference in surface chlorophyll *a* and light C fixation rates was observed between the northern and southern Arabian Sea, where both chlorophyll *a* and light C fixation rates tailed off with distance from north to south (Figure 6.4a). The depth-integrated light C fixation rates ranged from  $7.1 \pm 0.78$  to  $37.3 \pm 8.8$  mmol C m<sup>-2</sup> d<sup>-1</sup>, higher in the northern Arabian Sea in conjugation with nutrient availability (Figure 6.2e, f). Therefore, lower nutrient availability in the euphotic zone might presumably cause lower productivity in the southern Arabian Sea. During December (the month when sampling was performed), the winter convection begins and become stronger by the end of February and therefore, the nutrient upward flux could be relatively high in latter. This might result in higher light C fixation rates in the later phase of convective mixing than that of its initial phase. Light C fixation rates were negatively correlated with NO<sub>2</sub><sup>-</sup> and PO<sub>4</sub><sup>3-</sup> concentrations (Figure 6.5), indicating nutrients consumption during proliferation. However, light C fixation rates in this study are considerably lower than that reported by *Madhupratap et al.* (1996) in the central Arabian Sea during the winter monsoon of 1995 (Feb); ca. 27.9 to 67.2 mmol C m<sup>-2</sup> d<sup>-1</sup> and *Barber et al.* (2001) from the coast of Oman to the central Arabian Sea during the winter monsoon of 1995 (Dec); ca. 76 to 121 mmol C m<sup>-2</sup> d<sup>-1</sup>. These observations indicate a decrease in light C fixation rates in the Arabian Sea within the last two decades. Moreover, *Roxy et al.* (2016) also reported a prolonged decrease in chlorophyll *a* of up to 30% in the Arabian Sea during 1998–2013, which they



attributed to the suppressed nutrient exchange due to enhanced ocean stratification due to rapid warming of the Indian Ocean. A large decrease in the global marine light C fixation rates was also observed during 1997–2006 due to enhanced ocean warming and stratification (*Behrenfeld et al., 2006*). Perhaps, increased stratification and a consequential decrease in convective mixing might be a reason for decreased light C fixation rates during the winter monsoon within the last two decades in the Arabian Sea.

### 6.4.2 Dark C fixation in the Arabian Sea

Dark C fixation rates ranged from  $0.5 \pm 0.2$  to  $12.4 \pm 2.8$  nmol C L<sup>-1</sup> d<sup>-1</sup> and gradually decreased with depth (Figure 6.3). Similarly, a decrease in dark C fixation rates from 6.2 to 0.1 nmol C L<sup>-1</sup> d<sup>-1</sup> was observed at the depth of 100–4700 m in the tropical Atlantic Ocean (*Bergauer et al., 2013*). Contrary to these observations, *Zhou et al. (2017)* reported an increase in dark C fixation in the South China Sea at the depth of 200–1500 m from 20 to 80 nmol C L<sup>-1</sup> d<sup>-1</sup> (i.e., 0.01 to 0.04 µg C L<sup>-1</sup> h<sup>-1</sup>), and they attributed it to relatively high nutrients and temperature in the South China Sea. Dark C fixation rates in the suboxic basins of the Baltic Sea, the Black Sea and the Cariaco Basin broadly ranged from 0.02 to 2.5 µmol C L<sup>-1</sup> d<sup>-1</sup> (*Günter et al., 2008; Jørgensen et al., 1991; Taylor et al., 2001*), which are substantially higher than our rates. In all these studies, the highest dark C fixation rates were associated with the sulfidic and anoxic waters, where chemoautotrophy is primarily fuelled by the sulphur species. In the coastal regions of the Eastern Tropical North Pacific, where dark C fixation rates ranged up to 6.4 µmol C L<sup>-1</sup> d<sup>-1</sup> (*Podlaska et al., 2012*), the chemoautotrophy was ascribed to the nitrification and anammox processes. In our study, we observed the highest dark C fixation rates in the upper oxycline, which we attributed to ammonium oxidisers, as they are the dominant chemoautotrophs in the global ocean (*Middelburg, 2011*). These chemoautotrophs support up to 50% of the total dark C fixation in the upper oxycline of the Eastern Tropical South Pacific (*Molina and Farías, 2009*).

### 6.4.3 Dark C fixation intensifies OMZs

In the present study, the depth-integrated dark C fixation ranged up to  $1.7 \text{ mmol C m}^{-2} \text{ d}^{-1}$ , which represents a substantial amount of autochthonously produced new organic matter. Thus, dark C fixation to some extent can fuel the C demand of heterotrophs in the aphotic zone, which is reportedly not satisfied with the supply of organic matter from the euphotic zone (*del Giorgio and Duarte, 2002*). Additionally, dark C fixation can act as an alternative C source required in the intense OMZ of the Arabian Sea. Furthermore, substantial rates of dark C fixation in the OMZ provide hint for some dark C fixation contribution to sinking C fluxes in the OMZ of the Arabian Sea, as suspected by *Keil et al. (2016)* and *Lengger et al. (2019)*. Noticeably, dark C fixation rates might increase in future because OMZs are currently expanding owing to global warming induced rise in ocean temperature and increase in upper ocean stratification (*Breitburg et al., 2018*; *Keeling et al., 2010*).

### 6.4.4 Chemoautotrophs responsible for dark C fixation

Dark C fixation was negatively correlated with  $\text{NO}_x$  and  $\text{PO}_4^{3-}$  concentrations (Figure 6.5), which suggests consumption of nutrients by chemoautotrophs while fixing C for forming their biomass (*Cloern, 2021*). Notably, dark C fixation was positively correlated with  $\text{NO}_2^-$  concentration. The  $\text{NO}_2^-$  maxima in the suboxic OMZ waters of the northern Arabian Sea owing to partial denitrification ( $\text{NO}_3^-$  reduction) provides a reaction substrate for anammox bacteria. The presence of anammox bacteria has been reported in the OMZ of the northern Arabian Sea (*Pitcher et al., 2011*; *Villanueva et al., 2014*). Additionally, the members of SUP05 (chemoautotrophs) were reportedly higher at the core of OMZ accompanied by high  $\text{NO}_2^-$  concentration (*Fernandes et al., 2020*). Therefore, the coupling among  $\text{NO}_2^-$  concentration and chemoautotrophs indicates that prevalence of anammox or SUP05 bacteria in the suboxic OMZ waters resulted in higher dark C fixation in the suboxic OMZ waters than in the hypoxic OMZ waters. Dark C fixation was positively correlated with POC, which indicates that dark C fixation plays a crucial role towards the sustenance of food web by providing new organic matter in the aphotic zone of the



Arabian Sea.

In the aphotic zone, various chemoautotrophs assimilate DIC and oxidise the reduced compounds as electron donors (e.g.,  $\text{NH}_4^+$ ,  $\text{NO}_2^-$ ,  $\text{S}^{2-}$ ) to yield energy. The  $\text{NH}_4^+$  and  $\text{NO}_2^-$  are released as product/intermediate of remineralisation and denitrification, respectively, and accumulate in the OMZs, which potentially makes OMZs a preferential niche for chemoautotrophs. The suboxic OMZs waters host a diverse and rich assemblage of chemoautotrophs, such as anammox bacteria (anaerobically oxidises  $\text{NH}_4^+$  with  $\text{NO}_2^-$  to  $\text{N}_2$ ), autotrophic denitrifiers (anaerobically reduces  $\text{NO}_3^-$  to  $\text{N}_2$ ), ammonium oxidisers, nitrite oxidisers, methanogens, anaerobic methane oxidisers and sulphur oxidisers (*Chronopoulou et al.*, 2017; *Kuypers et al.*, 2003; *Naqvi et al.*, 2010; *Saito et al.*, 2020; *Thamdrup et al.*, 2019; *van Vliet et al.*, 2021).  $\text{NO}_2^-$  accumulates in the suboxic OMZ waters of the central northeast Arabian Sea primarily via  $\text{NO}_3^-$  reduction and to a certain extent via ammonium oxidation, which is indicative of active chemoautotrophy by ammonium oxidisers (*Lam et al.*, 2011). In contrast to the suboxic waters, the hypoxic/oxygenated waters in the aphotic zone are a habitat for ammonium oxidisers, nitrite oxidisers and aerobic methane oxidisers (*Middelburg*, 2011; *Pachiadaki et al.*, 2017; *Valentine et al.*, 2001). The suboxic OMZ waters of the Arabian Sea have been reported for the occurrence of anammox bacteria (*Fernandes et al.*, 2020; *Lücke et al.*, 2016; *Pitcher et al.*, 2011; *Villanueva et al.*, 2014; *Ward et al.*, 2009) and methanogenesis (*Owens et al.*, 1991). The prevalence of anammox bacteria at the zones of  $\text{NO}_3^-$  decrease and  $\text{NO}_2^-$  accumulation (*Lam and Kuypers*, 2011), and the detection of their signature lipid biomarker (*Jaeschke et al.*, 2007) and gene sequences (*Lam et al.*, 2011; *Woebken et al.*, 2008) in the suboxic OMZ waters of the Arabian Sea are consistent with our observation of significantly higher average dark C fixation rates in the suboxic OMZ waters than in the hypoxic OMZ waters. Notably, the contribution of C fixation by anammox bacteria (estimated based on  $\text{N}_2$  production rates by anammox bacteria in the central northern Arabian Sea from *Bulow et al.* (2010) and using a conversion factor of 0.066 mol C / mol  $\text{NH}_4^+$  for anammox reported by *Strous et al.* (1998)) to the total dark C fixation in the suboxic OMZ waters (owing to the prevalence of anammox bacteria in the suboxic waters (*Lam and Kuypers*, 2011)) of the Arabian Sea ranged between 1 and 47%. Dark C fixation occurred in the entire aphotic zone and at all the stations, suggesting ammonium oxidisers might be a reason for this. Reportedly, ammonium oxidisers are among the most

abundant organisms below the euphotic zone ([Karner et al., 2001](#); [Wuchter et al., 2006](#)), and they further increase dark C fixation under the increased supply of  $\text{NH}_4^+$  ([Podlaska et al., 2012](#)). Notably, *Thaumarchaeota* — an ammonium oxidiser that is ubiquitously present in the global ocean, was significantly higher in the OMZ (250–750 m) than in the waters below the OMZ layer of the tropical Atlantic Ocean ([Bergauer et al., 2013](#)). Therefore, the preferential existence of ammonium oxidisers in the OMZs could also explain the dark C fixation in the OMZ of the Arabian Sea. However, the microbiome in the aphotic zone of the Arabian Sea is poorly quantified and thus, lacks consensus on the presence, affinity for reagent substrate and C fixing ability of nitrite oxidisers, ammonium oxidisers, methane oxidisers and methanogens along with various other chemoautotrophs. The pivotal organisms responsible for C fixation in the OMZ of the Arabian Sea remain inconclusive. Therefore, further investigations are imperative to assess the microbiome, specific rates of chemoautotrophs and their possible seasonal variations for a complete understanding of dark C fixation in the Arabian Sea.

Table 6.1: Dark C fixation associated with the global dark ocean.

Global dark C fixation ( $\text{Pg C y}^{-1}$ )	Reference
0.11 <sup>a</sup>	<a href="#">Middelburg (2011)</a>
0.39 <sup>a</sup>	<a href="#">Wuchter et al. (2006)</a>
0.33–1.2 <sup>a</sup>	<a href="#">Meador et al. (2020)</a>
0.79 <sup>b</sup>	<a href="#">Herndl et al. (2005)</a>
0.8–1.1 <sup>c</sup>	<a href="#">Reinthal et al. (2010)</a>
2.4–7.4 <sup>c</sup>	This study

<sup>a</sup>Nitrification of ammonium in the global dark ocean.

<sup>b</sup>C fixation by archaea in the global dark ocean.

<sup>c</sup>Extrapolation of measured dark C fixation rates.

### 6.4.5 Role of dark C fixation in the global ocean

The extrapolation of suboxic region dark C fixation rates (0.60 to 3.14  $\text{nmol C L}^{-1} \text{ d}^{-1}$ ) to the global ocean suboxic waters (volume:  $38.6 \times 10^{18} \text{ L}$ , [Fu et al. \(2018\)](#)) range from 0.10 to 0.53  $\text{Pg C y}^{-1}$ , while the hypoxic region dark C fixation rates (0.49 to 1.53  $\text{nmol C L}^{-1} \text{ d}^{-1}$ ) to the global ocean hypoxic waters (volume:  $62.9 \times 10^{18} \text{ L}$ , [Fu et al. \(2018\)](#)) range from 0.13 to 0.42  $\text{Pg C y}^{-1}$ . Interestingly, the oxycline region dark C fixation

rates ( $4.2$  to  $12.4 \text{ nmol C L}^{-1} \text{ d}^{-1}$ ) to the global ocean oxycline waters (volume:  $118 \times 10^{18} \text{ L}$ , through personal communication with Dr. Weiwei Fu) range from  $2.17$  to  $6.41 \text{ Pg C y}^{-1}$ . The total dark C fixation in these three regions is  $2.4$  to  $7.36 \text{ Pg C y}^{-1}$ ; ca.  $4.8$  to  $14.7\%$  of global ocean primary production (*Field et al., 1998*). Notably, the reported contributions of dark C fixation in the global ocean towards C sink are widely different (Table 6.1). Previous studies reported dark C fixation between  $0.11$  and  $1.2 \text{ Pg C y}^{-1}$  associated with nitrification of the ammonium released through remineralisation of organic matter in the global dark ocean (*Meador et al., 2020*; *Middelburg, 2011*; *Wuchter et al., 2006*). *Herndl et al. (2005)* reported  $0.79 \text{ Pg C y}^{-1}$  (i.e.,  $6.55 \times 10^{13} \text{ mol C y}^{-1}$ ) dark C fixation performed by archaea in the global dark ocean, while *Reinthal et al. (2010)* extrapolated the measured dark C fixation rates to the global dark ocean between  $0.8$  and  $1.1 \text{ Pg C y}^{-1}$ .

#### 6.4.6 Dark C fixation — a sink or a source of greenhouse gases?

The amount of  $\text{CO}_2$  fixed via chemoautotrophic C fixation below the euphotic zone is currently overlooked and thus, impedes accurate global C budget estimates. Furthermore, some of the processes involved in dark C fixation are also associated with the release of other potent greenhouse gases —  $\text{N}_2\text{O}$  and  $\text{CH}_4$ , where  $\text{N}_2\text{O}$  and  $\text{CH}_4$  have  $\sim 300$  and  $20$  times, respectively, greater global warming potential per molecule than  $\text{CO}_2$  on a 100-year horizon (*Ramaswamy et al., 2001*). Anammox bacteria and nitrifiers simultaneously liberate  $\text{N}_2\text{O}$  as a metabolic intermediate and methanogens liberate  $\text{CH}_4$  as a product while assimilating the respired  $\text{CO}_2$ . Some of the released  $\text{CH}_4$  is simultaneously assimilated by methane oxidisers, further complicating the C cycle. Therefore, additional studies are required to elucidate the net effect of chemoautotrophy on the C cycle and its role towards C sink. Conclusively, dark C fixation in the ocean could significantly modulate climate change by acting as one of the major sinks for anthropogenic  $\text{CO}_2$ , and therefore, should be recognised in the marine C budget estimates.

## 6.5 Conclusions

Dark C fixation in the aphotic zone suggests chemoautotrophy is widespread and substantially provides new organic matter to the food web in the dark realm of the Arabian Sea. Significantly higher average dark C fixation rates in the suboxic OMZ waters than in the hypoxic OMZ waters are likely related to nutrients availability and to the preferential dominance of nitrite oxidisers and anammox bacteria in the suboxic OMZ waters. However, the microbiome in the Arabian Sea is poorly quantified, resulting in uncertainty in identification of organisms responsible for dark C fixation. The estimates of dark C fixation in the global ocean contribute significantly towards CO<sub>2</sub> drawdown and thus, should not be overlooked in the global C budget estimates.

# Chapter 7

## Summary and scope for future works

### 7.1 Summary

This thesis work attempted to understand the spatial and temporal variability of  $N_2$  and C fixation and their potential environmental controls in the northern Indian Ocean. The major findings of the thesis are as follows:

#### 7.1.1 $N_2$ and C fixation in the Bay of Bengal during the summer monsoon

- i.  $N_2$  fixation rates were low ( $< 6.7 \text{ nmol N L}^{-1} \text{ d}^{-1}$ ) in the oligotrophic Bay of Bengal contrary to the traditional assumption of oligotrophy favouring the diazotrophy.
- ii. The N:P ratios in the dissolved pool of the euphotic zone was less than the Redfield Ratio of 16, that suggested C fixation in the Bay of Bengal was  $N_r$  limited. Yet, the contribution of  $N_2$  fixation to C fixation was negligible ( $< 1\%$ ).
- iii. The upper bound of observed  $N_2$  fixation rates was higher than that reported in other oceanic regimes, such as the Eastern Tropical South Pacific, the Tropical Northwest Atlantic, and the Equatorial and Southern Indian Ocean.
- iv. The anticipated reason for low  $N_2$  fixation rates in the Bay of Bengal could be cloud cover and turbidity due to copious riverine discharge during the summer monsoon.

### 7.1.2 N<sub>2</sub> and C fixation in the Bay of Bengal during the spring inter-monsoon

- i. N<sub>2</sub> fixation rates in the euphotic zone were low ( $< 0.38 \text{ nmol N L}^{-1} \text{ d}^{-1}$ ) and contributed maximum up to 2% to C fixation.
- ii. Despite having a favourable niche in the oligotrophic Bay of Bengal with below detection NO<sub>3</sub><sup>-</sup> and N:P ratios lower than the Redfield Ratio, the suspected reason for low N<sub>2</sub> fixation rates and cyanobacterial diazotrophic abundance could be unexpected instability of the water column owing to the least fresh water induced stratification during the spring inter-monsoon.
- iii. Volumetric N<sub>2</sub> fixation rates estimated in the euphotic and aphotic zone were equally low. The aphotic zone integrated N<sub>2</sub> fixation rates contributed up to 100% of water column N<sub>2</sub> fixation activity, that indicated N<sub>2</sub> fixation in the aphotic zone is a significant component of the nitrogen cycle.
- iv. Interestingly, significantly higher N<sub>2</sub> fixation rates occurred below the OMZ ( $> 600 \text{ m}$  depth) where  $0.5 < \text{O}_2 \leq 1.6 \text{ mL L}^{-1}$ , rather than within the OMZ where  $\text{O}_2 \leq 0.5 \text{ mL L}^{-1}$ , which suggested that low concentrations of O<sub>2</sub> and NO<sub>x</sub> are not a firm niche requirement for diazotrophs.

### 7.1.3 N<sub>2</sub> fixation in the Arabian Sea during the winter monsoon

- i. N<sub>2</sub> fixation rates in the Arabian Sea were higher in the convection dominated regions than in the convection unaffected regions during the winter monsoon owing to lower N:P ratios and higher iron availability in the convection dominated regions.
- ii. The aphotic zone N<sub>2</sub> fixation rates were low ( $< 0.1 \text{ nmol N L}^{-1} \text{ d}^{-1}$ ), but accounted for up to 95% of the whole water column rates.
- iii. N<sub>2</sub> fixation rates in the OMZs of the Arabian Sea were modest and comparable with another OMZs of the Eastern Tropical North and South Pacific.

- iv. Diazotrophy in the aphotic zone appeared less sensitive to  $O_2$  and  $NO_x$  concentrations owing to similar  $N_2$  fixation rates in the suboxic and hypoxic OMZ waters, adding evidence to recent studies that long believed assumptions often made about  $N_2$  fixation should be reconsidered.

#### **7.1.4 Contribution of dark C fixation towards C sink in the ocean aphotic zone**

- i. C fixation rates in the euphotic zone ranged from 3.6 to 2745.0  $nmol\ C\ L^{-1}\ d^{-1}$ , while C fixation rates in the aphotic zone ranged from 0.5 to 12.4  $nmol\ C\ L^{-1}\ d^{-1}$ .
- ii. The highest dark C fixation rates were observed in the upper oxycline, which were attributed to ammonium oxidisers owing to their dominance in the global ocean.
- iii. The average C fixation rates in the suboxic OMZ waters of the Arabian Sea were significantly higher than in the hypoxic waters of the OMZ, which was likely related to nutrients availability and to the preferential dominance of nitrite oxidisers and anammox bacteria in the suboxic waters.
- iv. The contribution of C fixation by anammox bacteria to the total dark C fixation in the suboxic OMZ waters of the Arabian Sea ranged between 1 and 47%.
- v. The extrapolation of measured aphotic zone C fixation to the global ocean contributed up to 15% of primary production of the global ocean.

## **7.2 Scope for future works**

This thesis work presented significant findings but more work needs to be done on this research topic for improving our understanding of the  $N_2$  and C fixation. We suggest to carry the following work in future studies:

- i. Geochemical analyses indicate that marine  $N_2$  fixation may be underestimated. The large distribution of active diazotrophy found in this thesis from sunlit to aphotic

waters, suggests that  $N_2$  fixation in waters, which have traditionally been overlooked for  $N_2$  fixation, could increase the current estimates of  $N_r$  input. Despite substantial research progress including this thesis, the potential environmental controls of  $N_2$  fixation are not comprehensively understood. In turn, this leads to uncertainty in model-based projections of the oceanic N cycle. It is therefore essential to identify the distribution, abundance and activity of diazotrophs in order to understand their influence on the N cycle.

- ii. The different monsoon seasons constrain the  $N_2$  and C fixation rates differently owing to different physico-chemical conditions. Further exploring the rates during different monsoon seasons may help to conclude the factors governing the  $N_2$  and C fixation in the northern Indian Ocean.
- iii. The diazotrophy in the Bay of Bengal remains enigmatic despite suitable stratified, warm, and oligotrophic (but relatively high iron and phosphate) settings in this basin, thus raising the need to reconsider the traditional believed niches for diazotrophs.
- iv. The results of this thesis indicated that non-cyanobacterial diazotrophy was widespread and active in the aphotic zone of the water column. Further, non-cyanobacterial diazotrophy was relatively more active than cyanobacterial diazotrophy. Thus, their role in the future ocean research should be considered.
- v. While various  $CO_2$  removal mechanisms are proposed to remove  $\sim 1000$  billion tons of atmospheric  $CO_2$  by 2100 by increasing ocean C uptake, the marine C budget needs to be re-evaluated by taking into account chemoautotrophic C fixation activity.
- vi. This thesis indicated that C fixation by anammox bacteria could contribute up to 47% of the total dark C fixation in the suboxic waters of the Arabian Sea. Similarly, the role of other chemoautotrophs in dark C fixation could be investigated along with the effect of OMZs on chemoautotrophs and dark C fixation.



# References

- MATLAB version 9.11.0.1847648 (R2021b) Update 2*, The Mathworks, Inc., Natick, Massachusetts, 2021. [Cited on page 33.]
- Ahmed, A., M. Gauns, S. Kurian, P. Bardhan, A. Pratihary, H. Naik, D. M. Shenoy, and S. W. A. Naqvi, Nitrogen fixation rates in the eastern Arabian Sea, *Estuarine, Coastal and Shelf Science*, 191, 74–83, 2017. [Cited on pages 10, 12, 64, and 72.]
- Altabet, M., and J. Mccarthy, Temporal and spatial variations in the natural abundance of  $^{15}\text{N}$  in PON from a warm-core ring, *Deep Sea Research Part A. Oceanographic Research Papers*, 32, 755–772, 1985. [Cited on page 42.]
- Altabet, M. A., Constraints on oceanic N balance/imbalance from sedimentary  $^{15}\text{N}$  records, *Biogeosciences*, 4, 75–86, 2007. [Cited on page 7.]
- Baer, S. E., S. Rauschenberg, C. A. Garcia, N. S. Garcia, A. C. Martiny, B. S. Twining, and M. W. Lomas, Carbon and nitrogen productivity during spring in the oligotrophic Indian Ocean along the GO-SHIP IO9N transect, *Deep Sea Research Part II: Topical Studies in Oceanography*, 161, 81 – 91, 2019. [Cited on pages 57 and 60.]
- Baltar, F., J. Arístegui, E. Sintes, J. M. Gasol, T. Reinthaler, and G. J. Herndl, Significance of non-sinking particulate organic carbon and dark  $\text{CO}_2$  fixation to heterotrophic carbon demand in the mesopelagic northeast Atlantic, *Geophysical Research Letters*, 37, 2010, \_eprint: <https://agupubs.onlinelibrary.wiley.com/doi/pdf/10.1029/2010GL043105>. [Cited on page 79.]
- Bange, H. W., T. Rixen, A. M. Johansen, R. L. Siefert, R. Ramesh, V. Ittekkot, M. R. Hoffmann, and M. O. Andreae, A revised nitrogen budget for the Arabian Sea, *Global Biogeochemical Cycles*, 14, 1283–1297, 2000, \_eprint: <https://agupubs.onlinelibrary.wiley.com/doi/pdf/10.1029/1999GB001228>. [Cited on page 76.]

- Bange, H. W., S. W. A. Naqvi, and L. A. Codispoti, The nitrogen cycle in the Arabian Sea, *Progress in Oceanography*, 65, 145–158, 2005. [Cited on page 76.]
- Barber, R. T., J. Marra, R. C. Bidigare, L. A. Codispoti, D. Halpern, Z. Johnson, M. Latasa, R. Goericke, and S. L. Smith, Primary productivity and its regulation in the Arabian Sea during 1995, *Deep Sea Research Part II: Topical Studies in Oceanography*, 48, 1127–1172, 2001. [Cited on pages 11, 12, and 86.]
- Basu, S., S. G. P. Matondkar, and I. Furtado, Enumeration of bacteria from a *Trichodesmium* spp. bloom of the Eastern Arabian Sea: elucidation of their possible role in biogeochemistry, *Journal of Applied Phycology*, 23, 309–319, 2011. [Cited on page 72.]
- Behrenfeld, M. J., et al., Climate-driven trends in contemporary ocean productivity, *Nature*, 444, 752–755, 2006. [Cited on page 87.]
- Benavides, M., Five decades of N<sub>2</sub> fixation research in the North Atlantic Ocean, *Frontiers in Marine Science*, 2, 40, 2015. [Cited on page 44.]
- Benavides, M., P. Moisander, H. Berthelot, T. Dittmar, O. Grosso, and S. Bonnet, Mesopelagic N<sub>2</sub> Fixation Related to Organic Matter Composition in the Solomon and Bismarck Seas (Southwest Pacific), *PLoS ONE*, *In Press*, 2015. [Cited on pages 8 and 58.]
- Benavides, M., I. Berman-Frank, S. Bonnet, and L. Riemann, Deep Into Oceanic N<sub>2</sub> Fixation, *Frontiers in Marine Science*, 5, 2018a. [Cited on pages 7 and 75.]
- Benavides, M., et al., Aphotic N<sub>2</sub> fixation along an oligotrophic to ultraoligotrophic transect in the western tropical South Pacific Ocean, *Biogeosciences*, 15, 3107–3119, 2018b. [Cited on page 6.]
- Bergauer, K., E. Sintes, J. van Bleijswijk, H. Witte, and G. J. Herndl, Abundance and distribution of archaeal acetyl-CoA/propionyl-CoA carboxylase genes indicative for putatively chemoautotrophic Archaea in the tropical Atlantic’s interior, *FEMS Microbiology Ecology*, 84, 461–473, 2013, eprint: <https://academic.oup.com/femsec/article-pdf/84/3/461/19534421/84-3-461.pdf>. [Cited on pages 87 and 90.]

- Bergman, B., G. Sandh, S. Lin, J. Larsson, and E. J. Carpenter, *Trichodesmium*—a widespread marine cyanobacterium with unusual nitrogen fixation properties, *FEMS Microbiol Rev*, 37, 286–302, 2013, edition: 2012/09/20 Publisher: Blackwell Publishing Ltd. [Cited on page 5.]
- Berman-Frank, I., P. Lundgren, Y.-B. Chen, H. Küpper, Z. Kolber, B. Bergman, and P. Falkowski, Segregation of Nitrogen Fixation and Oxygenic Photosynthesis in the Marine Cyanobacterium *Trichodesmium*, *Science*, 294, 1534–1537, 2001, \_eprint: <https://www.science.org/doi/pdf/10.1126/science.1064082>. [Cited on page 5.]
- Berman-Frank, I., A. Quigg, Z. V. Finkel, A. J. Irwin, and L. Haramaty, Nitrogen-fixation strategies and Fe requirements in cyanobacteria, *Limnology and Oceanography*, 52, 2260–2269, 2007, \_eprint: <https://aslopubs.onlinelibrary.wiley.com/doi/pdf/10.4319/lo.2007.52.5.2260>. [Cited on page 5.]
- Betancourt, D. A., T. M. Loveless, J. W. Brown, and P. E. Bishop, Characterization of Diazotrophs Containing Mo-Independent Nitrogenases, Isolated from Diverse Natural Environments, *Applied and Environmental Microbiology*, 74, 3471–3480, 2008, \_eprint: <https://journals.asm.org/doi/pdf/10.1128/AEM.02694-07>. [Cited on page 4.]
- Bhaskar, J., R. Nagappa, M. Gauns, and V. Fernandes, Preponderance of a few diatom species among the highly diverse microphytoplankton assemblages in the Bay of Bengal, *Marine Biology*, 152, 63–75, 2007. [Cited on page 43.]
- Bigg, G., Regional oceanography: An introduction, *International Journal of Climatology - INT J CLIMATOL*, 15, 587–587, 1995. [Cited on page 41.]
- Bird, C., and M. Wyman, Transcriptionally active heterotrophic diazotrophs are widespread in the upper water column of the Arabian Sea, *FEMS Microbiology Ecology*, 84, 189–200, 2013, \_eprint: <https://onlinelibrary.wiley.com/doi/pdf/10.1111/1574-6941.12049>. [Cited on pages 12, 13, 59, 64, 65, and 74.]
- Bird, C., J. M. Martinez, A. G. O'Donnell, and M. Wyman, Spatial Distribution and Transcriptional Activity of an Uncultured Clade of Planktonic Diazotrophic -Proteobacteria in the Arabian Sea, *Applied and Environmental Microbiology*, 71, 2079–2085, 2005,

- \_eprint: <https://journals.asm.org/doi/pdf/10.1128/AEM.71.4.2079-2085.2005>. [Cited on pages 12 and 64.]
- Blais, M., J.- Tremblay, A. D. Jungblut, J. Gagnon, J. Martin, M. Thaler, and C. Lovejoy, Nitrogen fixation and identification of potential diazotrophs in the Canadian Arctic, *Global Biogeochemical Cycles*, 26, 2012, \_eprint: <https://agupubs.onlinelibrary.wiley.com/doi/pdf/10.1029/2011GB004096>. [Cited on pages 59 and 63.]
- Bombar, D., R. Paerl, and L. Riemann, Marine Non-Cyanobacterial Diazotrophs: Moving beyond Molecular Detection, *Trends in Microbiology*, 24, 2016. [Cited on pages 6, 58, and 59.]
- Bonnet, S., J. Dekaezemacker, K. Turk-Kubo, T. Moutin, M. Hamersley, O. Grosso, J. Zehr, and D. Capone, Aphotic N<sub>2</sub> Fixation in the Eastern Tropical South Pacific Ocean, *PloS one*, 8, e81,265, 2013. [Cited on pages 6, 8, 47, 58, 65, and 74.]
- Bonnet, S., M. Caffin, H. Berthelot, O. Grosso, M. Benavides, S. Helias-Nunige, C. Guieu, M. Stenegren, and R. Foster, In depth characterization of diazotroph activity across the Western Tropical South Pacific hot spot of N<sub>2</sub> fixation, *Biogeosciences Discussions*, pp. 1–30, 2018. [Cited on page 59.]
- Boyd, P., et al., High Level Review of a Wide Range of Proposed Marine Geoengineering Techniques, *Research Report*, ARRAY(0x55702ae7f8c8), 2019, iSSN: 1020-4873 Series: GESAMP Reports & Studies Series. [Cited on page 2.]
- Boyd, P. W., and S. C. Doney, Modelling regional responses by marine pelagic ecosystems to global climate change, *Geophysical Research Letters*, 29, 53–1–53–4, 2002, \_eprint: <https://agupubs.onlinelibrary.wiley.com/doi/pdf/10.1029/2001GL014130>. [Cited on page 45.]
- Brandes, J. A., A. H. Devol, T. Yoshinari, D. A. Jayakumar, and S. W. A. Naqvi, Isotopic composition of nitrate in the central Arabian Sea and eastern tropical North Pacific: A tracer for mixing and nitrogen cycles, *Limnology and Oceanography*, 43, 1680–1689, 1998, \_eprint:

- <https://aslopubs.onlinelibrary.wiley.com/doi/pdf/10.4319/lo.1998.43.7.1680>. [Cited on pages 12, 64, and 76.]
- Breitburg, D., et al., Declining oxygen in the global ocean and coastal waters, *Science*, 359, eaam7240, 2018, \_eprint: <https://www.science.org/doi/pdf/10.1126/science.aam7240>. [Cited on page 88.]
- Bristow, L. A., et al., N<sub>2</sub> production rates limited by nitrite availability in the Bay of Bengal oxygen minimum zone, *Nature Geoscience*, 10, 24–29, 2017. [Cited on pages 47 and 57.]
- Broda, E., and G. A. Peschek, Nitrogen fixation as evidence for the reducing nature of the early biosphere, *Biosystems*, 16, 1–8, 1983. [Cited on page 4.]
- Bulow, S. E., J. J. Rich, H. S. Naik, A. K. Pratihary, and B. B. Ward, Denitrification exceeds anammox as a nitrogen loss pathway in the Arabian Sea oxygen minimum zone, *Deep Sea Research Part I: Oceanographic Research Papers*, 57, 384–393, 2010. [Cited on page 89.]
- Burd, A. B., et al., Assessing the apparent imbalance between geochemical and biochemical indicators of meso- and bathypelagic biological activity: What the @\$\$ is wrong with present calculations of carbon budgets?, *Deep Sea Research Part II: Topical Studies in Oceanography*, 57, 1557–1571, 2010. [Cited on pages 2 and 79.]
- Burgess, B. K., and D. J. Lowe, Mechanism of Molybdenum Nitrogenase, *Chemical Reviews*, 96, 2983–3012, 1996, \_eprint: <https://doi.org/10.1021/cr950055x>. [Cited on pages 13 and 64.]
- Cai, X., and K. Gao, Levels of Daily Light Doses Under Changed Day-Night Cycles Regulate Temporal Segregation of Photosynthesis and N<sub>2</sub> Fixation in the Cyanobacterium *Trichodesmium erythraeum* IMS101, *PLOS ONE*, 10, e0135401, 2015. [Cited on page 43.]
- Capone, D., J. O’Neil, J. Zehr, and E. Carpenter, Basis for Diel Variation in Nitrogenase Activity in the Marine Planktonic Cyanobacterium *Trichodesmium thiebautii*, *Applied and environmental microbiology*, 56, 3532–6, 1990. [Cited on page 43.]

- Capone, D., D. Bronk, M. Mulholland, and E. Carpenter, *Nitrogen in the Marine Environment*, 2008. [Cited on pages 40 and 42.]
- Capone, D. G., J. P. Zehr, H. W. Paerl, B. Bergman, and E. J. Carpenter, *Trichodesmium*, a Globally Significant Marine Cyanobacterium, *Science*, 276, 1221–1229, 1997. [Cited on pages 12, 60, 64, and 72.]
- Capone, D. G., A. Subramaniam, J. P. Montoya, M. Voss, C. Humborg, A. M. Johansen, R. L. Siefert, and E. J. Carpenter, An extensive bloom of the N<sub>2</sub>-fixing cyanobacterium *Trichodesmium erythraeum* in the central Arabian Sea, *Marine Ecology Progress Series*, 172, 281–292, 1998. [Cited on pages 10, 12, 61, 64, 72, and 76.]
- Carpenter, E. J., A. Subramaniam, and D. G. Capone, Biomass and primary productivity of the cyanobacterium *Trichodesmium* spp. in the tropical N Atlantic ocean, *Deep Sea Research Part I: Oceanographic Research Papers*, 51, 173–203, 2004. [Cited on pages 12 and 64.]
- Chang, B. X., A. Jayakumar, B. Widner, P. Bernhardt, C. W. Mordy, M. R. Mulholland, and B. B. Ward, Low rates of dinitrogen fixation in the eastern tropical South Pacific, *Limnology and Oceanography*, 64, 1913–1923, 2019, eprint: <https://aslopubs.onlinelibrary.wiley.com/doi/pdf/10.1002/lno.11159>. [Cited on pages 8, 47, 65, 74, and 75.]
- Chao, L. L., Statistics, Methods and Analysis, *McGraw-Hill Book Company*, p. 237, 1974. [Cited on page 33.]
- Chavez, F., M. Messié, and J. Pennington, Marine Primary Production in Relation to Climate Variability and Change, *Annual review of marine science*, 3, 227–60, 2011. [Cited on page 44.]
- Chen, T.-Y., Y.-l. L. Chen, D.-S. Sheu, H.-Y. Chen, Y.-H. Lin, and T. Shiozaki, Community and abundance of heterotrophic diazotrophs in the northern South China Sea: Revealing the potential importance of a new alphaproteobacterium in N<sub>2</sub> fixation, *Deep Sea Research Part I: Oceanographic Research Papers*, 143, 104–114, 2019. [Cited on page 58.]

- Chen, Y.-L., H.-Y. Chen, S.-h. Tuo, and K. Ohki, Seasonal dynamics of new production from *Trichodesmium* N<sub>2</sub> fixation and nitrate uptake in the upstream Kuroshio and South China Sea basin, *Limnology and Oceanography*, 53, 1705–1721, 2008. [Cited on pages 44 and 74.]
- Chen, Y.-l. L., H.-Y. Chen, Y.-H. Lin, T.-C. Yong, Y. Taniuchi, and S.-h. Tuo, The relative contributions of unicellular and filamentous diazotrophs to N<sub>2</sub> fixation in the South China Sea and the upstream Kuroshio, *Deep Sea Research Part I: Oceanographic Research Papers*, 85, 56–71, 2014. [Cited on page 56.]
- Cheng, Q., Perspectives in Biological Nitrogen Fixation Research, *Journal of Integrative Plant Biology*, 50, 786–798, 2008, eprint: <https://onlinelibrary.wiley.com/doi/pdf/10.1111/j.1744-7909.2008.00700.x>. [Cited on page 3.]
- Cheung, S., X. Xia, C. Guo, and H. Liu, Diazotroph community structure in the deep oxygen minimum zone of the Costa Rica Dome, *Journal of Plankton Research*, 38, fbw003, 2016. [Cited on page 59.]
- Chinni, V., S. K. Singh, R. Bhushan, R. Rengarajan, and V. V. S. S. Sarma, Spatial variability in dissolved iron concentrations in the marginal and open waters of the Indian Ocean, *Marine Chemistry*, 208, 11 – 28, 2019. [Cited on pages 11, 42, and 56.]
- Choudhury, A. K., and R. Pal, Phytoplankton and nutrient dynamics of shallow coastal stations at Bay of Bengal, Eastern Indian coast, *Aquatic Ecology*, 44, 55–71, 2010. [Cited on page 35.]
- Chronopoulou, P.-M., F. Shelley, W. J. Pritchard, S. T. Maanoja, and M. Trimmer, Origin and fate of methane in the Eastern Tropical North Pacific oxygen minimum zone, *The ISME Journal*, 11, 1386–1399, 2017. [Cited on page 89.]
- Church, M., C. Mahaffey, R. Letelier, R. Lukas, J. Zehr, and D. Karl, Physical forcing of nitrogen fixation diazotroph community structure in the North Pacific subtropical gyre, *Global Biogeochem. Cycles*, 23, 2009. [Cited on page 45.]
- Clancy, V., I. Pihillagawa Gedara, P. Grinberg, J. Meija, Z. Mester, E. Pagliano, S. Willie,

- and L. Yang, MOOS-3: Seawater certified reference material for nutrients, 2014, publisher: National Research Council of Canada. [Cited on page 19.]
- Cloern, J., Use Care When Interpreting Correlations: The Ammonium Example in the San Francisco Estuary, *San Francisco Estuary and Watershed Science*, 19, 2021. [Cited on pages 59, 72, and 88.]
- Close, H. G., S. G. Wakeham, and A. Pearson, Lipid and  $^{13}\text{C}$  signatures of submicron and suspended particulate organic matter in the Eastern Tropical North Pacific: Implications for the contribution of Bacteria, *Deep Sea Research Part I: Oceanographic Research Papers*, 85, 15–34, 2014. [Cited on page 80.]
- Codispoti, L. A., An oceanic fixed nitrogen sink exceeding 400 Tg N a<sup>1</sup> vs the concept of homeostasis in the fixed-nitrogen inventory, *Biogeosciences*, 4, 233–253, 2007. [Cited on pages 75 and 76.]
- de Boyer Montégut, C., G. Madec, A. Fischer, A. Lazar, and D. Iudicone, Mixed layer depth over the global ocean: An examination of profile data and a profile-based climatology, *Journal of Geophysical Research*, 109, 2004. [Cited on pages 36, 49, and 66.]
- Dekaezemacker, J., S. Bonnet, O. Grosso, T. Moutin, M. Bressac, and D. Capone, Evidence of active dinitrogen fixation in surface waters of the Eastern Tropical South Pacific during El Nino and La Nina events and evaluation of its potential nutrient controls, *Global Biogeochemical Cycles*, 27, 2013. [Cited on page 74.]
- del Giorgio, P. A., and C. M. Duarte, Respiration in the open ocean, *Nature*, 420, 379–384, 2002. [Cited on pages 79 and 88.]
- Desa, E., S. T., S. Matondkar, J. Goes, A. Mascarenhas, S. Parab, N. Shaikh, and C. Fernandes, Detection of *Trichodesmium* bloom patches along the eastern Arabian Sea by IRS-P4/OCM ocean color sensor and by in-situ measurements, *Indian Journal of Marine Sciences*, 34, 2005. [Cited on page 72.]
- DeSousa, S., M. Dileepkumar, S. Sardessai, S. Vvss, and P. Shirodkar, Seasonal variability in oxygen and nutrients in the central and eastern Arabian Sea, *Current Science*, 71, 847–851, 1996. [Cited on page 11.]



- Deutsch, C., N. Gruber, R. M. Key, J. L. Sarmiento, and A. Ganachaud, Denitrification and N<sub>2</sub> fixation in the Pacific Ocean, *Global Biogeochemical Cycles*, 15, 483–506, 2001, \_eprint: <https://agupubs.onlinelibrary.wiley.com/doi/pdf/10.1029/2000GB001291>. [Cited on page 8.]
- Deutsch, C., J. Sarmiento, D. Sigman, N. Gruber, and J. Dunne, Spatial coupling of nitrogen inputs and losses in the ocean. *Nature*, *Nature*, 445, 163–167, 2007. [Cited on pages 8, 12, 13, 64, 66, and 76.]
- Devassy, V., P. Bhattathiri, and S. Qasim, *Trichodesmium* Phenomenon, *Indian Journal of Marine Sciences*, 7, 168–186, 1978. [Cited on page 72.]
- Devol, A. H., and H. E. Hartnett, Role of the oxygen-deficient zone in transfer of organic carbon to the deep ocean, *Limnology and Oceanography*, 46, 1684–1690, 2001, \_eprint: <https://aslopubs.onlinelibrary.wiley.com/doi/pdf/10.4319/lo.2001.46.7.1684>. [Cited on page 9.]
- DeVries, T., Atmospheric CO<sub>2</sub> and Sea Surface Temperature Variability Cannot Explain Recent Decadal Variability of the Ocean CO<sub>2</sub> Sink, *Geophysical Research Letters*, 49, e2021GL096018, 2022, \_eprint: <https://agupubs.onlinelibrary.wiley.com/doi/pdf/10.1029/2021GL096018>. [Cited on page 9.]
- DeVries, T., F. Primeau, and C. Deutsch, The sequestration efficiency of the biological pump, *Geophysical Research Letters*, 39, 2012, \_eprint: <https://agupubs.onlinelibrary.wiley.com/doi/pdf/10.1029/2012GL051963>. [Cited on page 9.]
- Dlugokencky, E., and P. Tans, Trends in atmospheric carbon dioxide, National Oceanic & Atmospheric Administration, Earth System Research Laboratory (NOAA/ESRL), 2018. [Cited on page 1.]
- Duce, R., et al., Impacts of Atmospheric Anthropogenic Nitrogen on the Open Ocean, *Science (New York, N.Y.)*, 320, 893–7, 2008. [Cited on page 35.]
- Dugdale, R. C., and F. P. Wilkerson, The use of <sup>15</sup>N to measure nitrogen uptake in eutrophic oceans; experimental consider-

- ations, *Limnology and Oceanography*, *31*, 673–689, 1986, \_eprint: <https://aspubs.onlinelibrary.wiley.com/doi/pdf/10.4319/lo.1986.31.4.0673>. [Cited on page 29.]
- Dutta, M. K., S. Kumar, R. Mukherjee, P. Sanyal, and S. K. Mukhopadhyay, The post-monsoon carbon biogeochemistry of the Hooghly–Sundarbans estuarine system under different levels of anthropogenic impacts, *Biogeosciences*, *16*, 289–307, 2019. [Cited on page 35.]
- Eady, R. R., StructureFunction Relationships of Alternative Nitrogenases, *Chemical Reviews*, *96*, 3013–3030, 1996, \_eprint: <https://doi.org/10.1021/cr950057h>. [Cited on page 4.]
- Eady, R. R., and J. R. Postgate, Nitrogenase, *Nature*, *249*, 805–810, 1974. [Cited on page 4.]
- Falkowski, P., Light-shade adaptation and vertical mixing of marine phytoplankton: A comparative field study, *Journal of Marine Research*, *41*, 215–237, 1983. [Cited on pages 5, 59, and 74.]
- Falkowski, P., Evolution of the nitrogen cycle and its influence on the biological sequestration of CO<sub>2</sub> in the ocean, *Nature*, *387*, 272–275, 1997. [Cited on page 63.]
- Falkowski, P., R. Barber, and V. Smetacek, Biogeochemical Controls and Feedbacks on Ocean Primary Production, *Science (New York, N.Y.)*, *281*, 200–7, 1998. [Cited on pages 2 and 5.]
- Farnelid, H., M. Bentzon-Tilia, A. Andersson, S. Bertilsson, G. Jost, M. Labrenz, K. Jürgens, and L. Riemann, Active nitrogen-fixing heterotrophic bacteria at and below the chemocline of the central Baltic Sea, *The ISME journal*, *7*, 2013. [Cited on pages 58 and 59.]
- Fay, P., Oxygen relations of nitrogen fixation in Cyanobacteria, *Microbiol Rev*, *56*, 1992. [Cited on page 4.]
- Fernandes, G. L., B. D. Shenoy, and S. R. Damare, Diversity of Bacterial Community in the Oxygen Minimum Zones of Arabian Sea and Bay of Bengal as Deduced by Illumina Sequencing., *Front Microbiol*, *10*, 3153, 2020. [Cited on pages 88 and 89.]

- Fernandez, C., L. Farias, and O. Ulloa, Nitrogen Fixation in Denitrified Marine Waters, *PloS one*, 6, e20,539, 2011. [Cited on pages 6, 8, 47, 58, 59, 65, and 74.]
- Field, C., M. Behrenfeld, J. Randerson, and P. Falkowski, Primary Production of the Biosphere: Integrating Terrestrial and Oceanic Components, *sci*, 281, 237–240, 1998. [Cited on pages 1, 9, and 91.]
- Fitzsimmons, J. N., R. Zhang, and E. A. Boyle, Dissolved iron in the tropical North Atlantic Ocean, *Marine Chemistry*, 154, 87–99, 2013. [Cited on page 56.]
- Flombaum, P., et al., Present and future global distributions of the marine Cyanobacteria *Prochlorococcus* and *Synechococcus*, *Proceedings of the National Academy of Sciences of the United States of America*, 110, 2013. [Cited on page 60.]
- Fredriksson, C., G. Malin, P. Siddiqui, and B. Bergman, Aerobic nitrogen fixation is confined to a subset of cells in the non-heterocystous cyanobacterium *Symploca* PCC 8002, *New Phytologist*, 140, 531 – 538, 1998, publisher: Cambridge University Press. [Cited on pages 6 and 43.]
- Fu, F.-X., M. R. Mulholland, N. S. Garcia, A. Beck, P. W. Bernhardt, M. E. Warner, S. A. Sañudo-Wilhelmy, and D. A. Hutchins, Interactions between changing pCO<sub>2</sub>, N<sub>2</sub> fixation, and Fe limitation in the marine unicellular cyanobacterium *Crocospaera*, *Limnology and Oceanography*, 53, 2472–2484, 2008, \_eprint: <https://aslopubs.onlinelibrary.wiley.com/doi/pdf/10.4319/lo.2008.53.6.2472>. [Cited on page 45.]
- Fu, W., F. Primeau, J. Keith Moore, K. Lindsay, and J. T. Randerson, Reversal of Increasing Tropical Ocean Hypoxia Trends With Sustained Climate Warming, *Global Biogeochemical Cycles*, 32, 551–564, 2018, \_eprint: <https://agupubs.onlinelibrary.wiley.com/doi/pdf/10.1002/2017GB005788>. [Cited on page 90.]
- Gadgil, S., The Indian Monsoon and Its Variability, *Annual Review of Earth and Planetary Sciences*, 31, 429–467, 2003, \_eprint: <https://doi.org/10.1146/annurev.earth.31.100901.141251>. [Cited on page 35.]

- Gallon, J., N<sub>2</sub> fixation in phototrophs: Adaptation to a specialized way of life, *Plant and Soil*, 230, 39–48, 2001. [Cited on pages 6 and 43.]
- Gallon, J. R., Reconciling the incompatible: N<sub>2</sub> fixation and O<sub>2</sub>, *New Phytologist*, 122, 571–609, 1992, \_eprint: <https://nph.onlinelibrary.wiley.com/doi/pdf/10.1111/j.1469-8137.1992.tb00087.x>. [Cited on pages 5 and 6.]
- Gandhi, N., A. Singh, S. Prakash, R. Ramesh, M. Raman, M. S. Sheshshayee, and S. Shetye, First direct measurements of N<sub>2</sub> fixation during a *Trichodesmium* bloom in the eastern Arabian Sea, *Global Biogeochemical Cycles*, 25, 2011, \_eprint: <https://agupubs.onlinelibrary.wiley.com/doi/pdf/10.1029/2010GB003970>. [Cited on pages 10, 12, 42, 45, 48, 57, 61, 64, 72, and 76.]
- Geider, R. J., H. L. MacIntyre, and T. M. Kana, A dynamic regulatory model of phytoplanktonic acclimation to light, nutrients, and temperature, *Limnology and Oceanography*, 43, 679–694, 1998, \_eprint: <https://aslopubs.onlinelibrary.wiley.com/doi/pdf/10.4319/lo.1998.43.4.0679>. [Cited on page 59.]
- Gimenez, A., M. Baklouti, T. Wagener, and T. Moutin, Diazotrophy as the main driver of the oligotrophy gradient in the western tropical South Pacific Ocean: results from a one-dimensional biogeochemical–physical coupled model, *Biogeosciences*, 15, 6573–6589, 2018. [Cited on page 56.]
- Goering, J. J., R. C. Dugdale, and D. W. Menzel, Estimates of in situ rates of nitrogen uptake by *Trichodesmium* sp. in the tropical Atlantic Ocean, *Limnology and Oceanography*, 11, 614–620, 1966, \_eprint: <https://aslopubs.onlinelibrary.wiley.com/doi/pdf/10.4319/lo.1966.11.4.0614>. [Cited on page 44.]
- Goes, J. I., et al., Influence of the Amazon River discharge on the biogeography of phytoplankton communities in the western tropical north Atlantic, *Progress in Oceanography*, 120, 29–40, 2014. [Cited on page 60.]
- Gomes, H., J. Goes, and T. Saino, Influence of physical processes and freshwater discharge

- on the seasonality of phytoplankton regime in the Bay of Bengal, *Continental Shelf Research*, 20, 313–330, 2000. [Cited on page 43.]
- Gopalkrishna, V., and J. Sastry, Surface circulation over the shelf off the coast of India during the southwest monsoon, *Indian J Mar Sci*, 14, 62–65, 1985. [Cited on page 42.]
- Gradoville, M., D. Bombar, B. Crump, R. Letelier, J. Zehr, and A. White, Diversity and activity of nitrogen-fixing communities across ocean basins, *Limnology and Oceanography*, 2017. [Cited on pages 50, 59, and 67.]
- Grand, M., C. Measures, M. Hatta, W. Hiscock, W. Landing, P. Morton, C. Buck, P. Barrett, and J. Resing, Dissolved Fe and Al in the upper 1000 m of the eastern Indian Ocean: A high-resolution transect along 95°E from the Antarctic margin to the Bay of Bengal, *Global Biogeochemical Cycles*, 29, 2015. [Cited on pages 11 and 42.]
- Grobbelaar, N., T. C. Huang, H. Y. Lin, and T. J. Chow, Dinitrogen-fixing endogenous rhythm in *Synechococcus* RF-1, *FEMS Microbiology Letters*, 37, 173 – 177, 1986. [Cited on page 43.]
- Großkopf, T., et al., Doubling of marine dinitrogen-fixation rates based on direct measurements, *Nature*, 488, 361–364, 2012. [Cited on page 8.]
- Gruber, N., and J. L. Sarmiento, Global patterns of marine nitrogen fixation and denitrification, *Global Biogeochemical Cycles*, 11, 235 – 266, 1997. [Cited on page 8.]
- Günter, J., M. V. Zubkov, E. Yakushev, M. Labrenz, and K. Jürgens, High abundance and dark CO<sub>2</sub> fixation of chemolithoautotrophic prokaryotes in anoxic waters of the Baltic Sea, *Limnology and Oceanography*, 53, 14–22, 2008, eprint: <https://aslopubs.onlinelibrary.wiley.com/doi/pdf/10.4319/lo.2008.53.1.0014>. [Cited on pages 10, 80, and 87.]
- Hamersley, M. R., K. A. Turk, A. Leinweber, N. Gruber, J. P. Zehr, T. Gunderson, and D. G. Capone, Nitrogen fixation within the water column associated with two hypoxic basins in the Southern California Bight, *Aquatic Microbial Ecology*, 63, 193 – 205, 2011, place: Oldendorf/Luhe Publisher: Inter-Research. [Cited on page 58.]

- Harding, K., K. A. Turk-Kubo, R. E. Sipler, M. M. Mills, D. A. Bronk, and J. P. Zehr, Symbiotic unicellular cyanobacteria fix nitrogen in the Arctic Ocean, *Proceedings of the National Academy of Sciences*, *115*, 13,371–13,375, 2018, \_eprint: <https://www.pnas.org/doi/pdf/10.1073/pnas.1813658115>. [Cited on pages 59 and 63.]
- Harikumar, R., T. M. B. Nair, G. S. Bhat, S. Nayak, V. S. Reddem, and S. S. C. Shenoi, Ship-Mounted Real-Time Surface Observational System on board Indian Vessels for Validation and Refinement of Model Forcing Fields\*, *Journal of Atmospheric and Oceanic Technology*, *30*, 626–637, 2013. [Cited on page 36.]
- Hegde, S., A. Anil, J. Patil, S. Mitbavkar, V. Krishnamurthy, and V. Gopalakrishna, Influence of environmental settings on the prevalence of *Trichodesmium* spp. in the Bay of Bengal, *Marine Ecology Progress Series*, *356*, 2008. [Cited on page 60.]
- Herndl, G. J., T. Reinthaler, E. Teira, H. v. Aken, C. Veth, A. Pernthaler, and J. Pernthaler, Contribution of *Archaea* to Total Prokaryotic Production in the Deep Atlantic Ocean, *Applied and Environmental Microbiology*, *71*, 2303–2309, 2005, \_eprint: <https://journals.asm.org/doi/pdf/10.1128/AEM.71.5.2303-2309.2005>. [Cited on pages 80, 90, and 91.]
- Hewson, I., P. Moisander, K. Achilles, C. Carlson, B. Jenkins, E. Mondragon, A. Morrison, and J. Zehr, Characteristics of diazotrophs in surface to abyssopelagic waters of the Sargasso Sea, *Aquatic Microbial Ecology - AQUAT MICROB ECOL*, *46*, 15–30, 2007. [Cited on page 58.]
- Holl, C. M., and J. P. Montoya, Interactions between nitrate uptake and nitrogen fixation in continuous cultures of the marine diazotroph *Trichodesmium* (cyanobacteria), *Journal of Phycology*, *41*, 1178–1183, 2005, \_eprint: <https://onlinelibrary.wiley.com/doi/pdf/10.1111/j.1529-8817.2005.00146.x>. [Cited on page 63.]
- Huang, T.-C., and T.-J. Chow, New type of N<sub>2</sub>-fixing unicellular cyanobacterium (blue-green alga), *FEMS Microbiology Letters*, *36*, 109–110, 1986, \_eprint: <https://academic.oup.com/femsle/article-pdf/36/1/109/19392511/36-1-109.pdf>. [Cited on page 60.]

- Hutchins, D. A., F.-X. Fu, Y. Zhang, M. E. Warner, Y. Feng, K. Portune, P. W. Bernhardt, and M. R. Mulholland, CO<sub>2</sub> control of *Trichodesmium* N<sub>2</sub> fixation, photosynthesis, growth rates, and elemental ratios: Implications for past, present, and future ocean biogeochemistry, *Limnology and Oceanography*, 52, 1293–1304, 2007, \_eprint: <https://aslopubs.onlinelibrary.wiley.com/doi/pdf/10.4319/lo.2007.52.4.1293>. [Cited on page 45.]
- Hügler, M., and S. Sievert, Beyond the Calvin cycle: autotrophic carbon fixation in the ocean., *Annual review of marine science*, 3, 261–89, 2011. [Cited on pages 7 and 80.]
- Inomura, K., J. Bragg, L. Riemann, and M. Follows, A quantitative model of nitrogen fixation in the presence of ammonium, *PLOS ONE*, 13, e0208282, 2018. [Cited on page 59.]
- Jaeschke, A., E. C. Hopmans, S. G. Wakeham, S. Schouten, and J. S. Sinninghe Damsté, The presence of ladderane lipids in the oxygen minimum zone of the Arabian Sea indicates nitrogen loss through anammox, *Limnology and Oceanography*, 52, 780–786, 2007, \_eprint: <https://aslopubs.onlinelibrary.wiley.com/doi/pdf/10.4319/lo.2007.52.2.0780>. [Cited on page 89.]
- Jayakumar, A., and B. B. Ward, Diversity and distribution of nitrogen fixation genes in the oxygen minimum zones of the world oceans, *Biogeosciences*, 17, 5953–5966, 2020. [Cited on page 47.]
- Jayakumar, A., S. W. A. Naqvi, and B. B. Ward, Distribution and Relative Quantification of Key Genes Involved in Fixed Nitrogen Loss from the Arabian Sea Oxygen Minimum Zone, in *Indian Ocean Biogeochemical Processes and Ecological Variability*, pp. 187–203, American Geophysical Union (AGU), 2009, \_eprint: <https://agupubs.onlinelibrary.wiley.com/doi/pdf/10.1029/2008GM000730>. [Cited on pages 13 and 80.]
- Jayakumar, A., M. Al-Rshaidat, B. Ward, and M. Mulholland, Diversity, distribution, and expression of diazotroph *nifH* genes in oxygen-deficient waters of the Arabian Sea, *FEMS microbiology ecology*, 82, 2012. [Cited on pages 12, 13, 58, 59, 61, 64, 65, and 74.]

- Jayakumar, A., B. X. Chang, B. Widner, P. Bernhardt, M. R. Mulholland, and B. B. Ward, Biological nitrogen fixation in the oxygen-minimum region of the eastern tropical North Pacific ocean, *The ISME Journal*, *11*, 2356–2367, 2017. [Cited on pages 8, 47, 58, 64, 74, and 75.]
- Jickells, T. D., et al., Global Iron Connections Between Desert Dust, Ocean Biogeochemistry, and Climate, *Science*, *308*, 67–71, 2005, \_eprint: <https://www.science.org/doi/pdf/10.1126/science.1105959>. [Cited on page 74.]
- Joerger, R. D., P. E. Bishop, and H. J. Evans, Bacterial Alternative Nitrogen Fixation Systems, *CRC Critical Reviews in Microbiology*, *16*, 1–14, 1988, publisher: Taylor & Francis \_eprint: <https://doi.org/10.3109/10408418809104465>. [Cited on page 4.]
- Johnson, K., S. Riser, and M. Ravichandran, Oxygen Variability Controls Denitrification in the Bay of Bengal Oxygen Minimum Zone, *Geophysical Research Letters*, *46*, 2019. [Cited on page 47.]
- Joos, F., and R. Spahni, Rates of change in natural and anthropogenic radiative forcing over the past 20,000 years, *Proceedings of the National Academy of Sciences*, *105*, 1425–1430, 2008, \_eprint: <https://www.pnas.org/doi/pdf/10.1073/pnas.0707386105>. [Cited on page 1.]
- Jørgensen, B. B., H. Fossing, C. O. Wirsen, and H. W. Jannasch, Sulfide oxidation in the anoxic Black Sea chemocline, *Deep Sea Research Part A. Oceanographic Research Papers*, *38*, S1083–S1103, 1991. [Cited on pages 80 and 87.]
- Karl, D., R. Letelier, L. Tupas, D. JE, J. Christian, and H. DV, The Role of Nitrogen Fixation in Biogeochemical Cycling in the Subtropical North Pacific Ocean, *Nature*, *388*, 533–8, 1997. [Cited on page 2.]
- Karl, D., R. Bidigare, M. Church, J. Dore, R. Letelier, C. Mahaffey, and J. Zehr, The Nitrogen Cycle in the North Pacific Trades Biome: An Evolving Paradigm, in *Nitrogen in the Marine Environment*, pp. 705–769, 2008. [Cited on pages 6 and 43.]
- Karl, D., et al., Dinitrogen fixation in the world’s oceans, *Biogeochemistry*, *57*, 47–98, 2002. [Cited on pages 6, 12, 56, 63, and 64.]



- Karner, M. B., E. F. DeLong, and D. M. Karl, Archaeal dominance in the mesopelagic zone of the Pacific Ocean, *Nature*, 409, 507–510, 2001. [Cited on page 90.]
- Keeling, R. F., A. Körtzinger, and N. Gruber, Ocean Deoxygenation in a Warming World, *Annual Review of Marine Science*, 2, 199–229, 2010, \_eprint: <https://doi.org/10.1146/annurev.marine.010908.163855>. [Cited on page 88.]
- Keil, R. G., J. A. Neibauer, C. Biladeau, K. van der Elst, and A. H. Devol, A multiproxy approach to understanding the “enhanced” flux of organic matter through the oxygen-deficient waters of the Arabian Sea, *Biogeosciences*, 13, 2077–2092, 2016. [Cited on pages 80 and 88.]
- Knapp, A., The sensitivity of marine N<sub>2</sub> fixation to dissolved inorganic nitrogen, *Frontiers in Microbiology*, 3, 374, 2012. [Cited on pages 59 and 74.]
- Knapp, A., K. Casciotti, W. Berelson, and M. Prokopenko, Low rates of nitrogen fixation in Eastern Tropical South Pacific surface waters, *Proceedings of the National Academy of Sciences*, 113, 201515,641, 2016. [Cited on pages 44 and 47.]
- Krishna, M. S., M. H. K. Prasad, D. B. Rao, R. Viswanadham, V. V. S. S. Sarma, and N. P. C. Reddy, Export of dissolved inorganic nutrients to the northern Indian Ocean from the Indian monsoonal rivers during discharge period, *Geochimica et Cosmochimica Acta*, 172, 430 – 443, 2016. [Cited on page 41.]
- Kumar, K., R. A. Mella-Herrera, and J. W. Golden, Cyanobacterial heterocysts, *Cold Spring Harb Perspect Biol*, 2, a000,315–a000,315, 2010, edition: 2010/02/24 Publisher: Cold Spring Harbor Laboratory Press. [Cited on page 6.]
- Kumar, P. K., A. Singh, R. Ramesh, and T. Nallathambi, N<sub>2</sub> Fixation in the Eastern Arabian Sea: Probable Role of Heterotrophic Diazotrophs, *Frontiers in Marine Science*, 4, 80, 2017. [Cited on pages 10, 12, 57, 64, 72, and 74.]
- Kumar, S., R. Ramesh, S. Sardesai, and M. S. Sheshshayee, High new production in the Bay of Bengal: Possible causes and implications, *Geophysical Research Letters*, 31, 2004, \_eprint: <https://agupubs.onlinelibrary.wiley.com/doi/pdf/10.1029/2004GL021005>. [Cited on pages 11 and 41.]

- Kustka, A. B., S. A. Sañudo-Wilhelmy, E. J. Carpenter, D. Capone, J. Burns, and W. G. Sunda, Iron requirements for dinitrogen- and ammonium-supported growth in cultures of *Trichodesmium* (IMS 101): Comparison with nitrogen fixation rates and iron: carbon ratios of field populations, *Limnology and Oceanography*, 48, 1869–1884, 2003, \_eprint: <https://aslopubs.onlinelibrary.wiley.com/doi/pdf/10.4319/lo.2003.48.5.1869>. [Cited on page 5.]
- Kuypers, M. M. M., A. O. Sliekers, G. Lavik, M. Schmid, B. B. Jørgensen, J. G. Kuenen, J. S. Sinninghe Damsté, M. Strous, and M. S. M. Jetten, Anaerobic ammonium oxidation by anammox bacteria in the Black Sea, *Nature*, 422, 608–611, 2003. [Cited on page 89.]
- Lam, P., and M. M. Kuypers, Microbial Nitrogen Cycling Processes in Oxygen Minimum Zones, *Annual Review of Marine Science*, 3, 317–345, 2011, \_eprint: <https://doi.org/10.1146/annurev-marine-120709-142814>. [Cited on page 89.]
- Lam, P., M. M. Jensen, A. Kock, K. A. Lettmann, Y. Plancherel, G. Lavik, H. W. Bange, and M. M. M. Kuypers, Origin and fate of the secondary nitrite maximum in the Arabian Sea, *Biogeosciences*, 8, 1565–1577, 2011. [Cited on page 89.]
- Landolfi, A., W. Koeve, H. Dietze, P. Kähler, and A. Oschlies, A new perspective on environmental controls of marine nitrogen fixation, *Geophysical Research Letters*, 42, 4482–4489, 2015, \_eprint: <https://agupubs.onlinelibrary.wiley.com/doi/pdf/10.1002/2015GL063756>. [Cited on page 56.]
- Landolfi, A., P. Kähler, W. Koeve, and A. Oschlies, Global Marine N<sub>2</sub> Fixation Estimates: From Observations to Models, *Frontiers in Microbiology*, 9, 2018. [Cited on page 7.]
- Lengger, S. K., et al., Dark carbon fixation in the Arabian Sea oxygen minimum zone contributes to sedimentary organic carbon (SOM), *Global Biogeochemical Cycles*, 33, 1715–1732, 2019, \_eprint: <https://agupubs.onlinelibrary.wiley.com/doi/pdf/10.1029/2019GB006282>. [Cited on pages 80 and 88.]

- Levitan, O., G. ROSENBERG, I. SETLIK, E. SETLIKOVA, J. Grígel, J. Klepetar, O. Prasil, and I. Berman-Frank, Elevated CO<sub>2</sub> enhances nitrogen fixation and growth in the marine cyanobacterium *Trichodesmium*, *Global Change Biology*, *13*, 531 – 538, 2007. [Cited on page 45.]
- Loick-Wilde, N., S. C. Weber, B. J. Conroy, D. G. Capone, V. J. Coles, P. M. Medeiros, D. K. Steinberg, and J. P. Montoya, Nitrogen sources and net growth efficiency of zooplankton in three Amazon River plume food webs, *Limnology and Oceanography*, *61*, 460–481, 2016, \_eprint: <https://aslopubs.onlinelibrary.wiley.com/doi/pdf/10.1002/lno.10227>. [Cited on page 60.]
- Lorrain, A., N. Savoye, L. Chauvaud, Y.-M. Paulet, and N. Naulet, Decarbonation and preservation method for the analysis of organic C and N contents and stable isotope ratios of low-carbonate suspended particulate material, *Analytica Chimica Acta*, *491*, 125–133, 2003. [Cited on page 24.]
- Luo, Y.-W., I. Lima, D. Karl, C. Deutsch, and S. Doney, Data-based assessment of environmental controls on global marine nitrogen fixation, *Biogeosciences*, *11*, 691–708, 2014. [Cited on page 43.]
- Luo, Y.-W., et al., Database of diazotrophs in global ocean: Abundance, biomass and nitrogen fixation rates, *Earth System Science Data*, *4*, 47–73, 2012. [Cited on pages 6, 7, 8, and 10.]
- Löscher, C., A. Bourbonnais, J. Dekaezemacker, C. Charoenpong, M. Altabet, H. Bange, R. Czeschel, and C. Hoffmann, N<sub>2</sub> fixation in eddies of the eastern tropical South Pacific Ocean, *Biogeosciences*, *13*, 2889–2899, 2016. [Cited on page 74.]
- Löscher, C., W. Mohr, H. Bange, and D. Canfield, No nitrogen fixation in the Bay of Bengal?, *Biogeosciences*, *17*, 851–864, 2020. [Cited on pages 43, 44, 57, and 61.]
- Löscher, C., et al., Facets of diazotrophy in the oxygen minimum zone waters off Peru, *The ISME journal*, *8*, 2014. [Cited on pages 8, 47, 59, 65, 74, and 76.]
- Lüke, C., D. Speth, M. Kox, L. Villanueva, and M. S. M. Jetten, Metagenomic analysis

- of nitrogen and methane cycling in the Arabian Sea oxygen minimum zone, *PeerJ*, 4, e1924, 2016. [Cited on pages 13, 80, and 89.]
- Madhupratap, M., S. PrasannaKumar, P. Bhattathiri, M. Dileepkumar, S. Raghukumar, K. Nair, and R. Nagappa, Mechanism of the biological response to winter cooling in the northeastern Arabian Sea, *Nature*, 384, 1996. [Cited on pages 12, 63, 73, and 86.]
- Madhupratap, M., M. Gauns, N. Ramaiah, S. P. Kumar, P. M. Muraleedharan, S. N. d. Sousa, S. Sardesai, and U. Muraleedharan, Biogeochemistry of the Bay of Bengal: physical, chemical and primary productivity characteristics of the central and western Bay of Bengal during summer monsoon 2001, *Deep Sea Research Part II: Topical Studies in Oceanography*, 50, 881 – 896, 2003. [Cited on page 44.]
- Mazard, S. L., N. J. Fuller, K. M. Orcutt, O. Bridle, and D. J. Scanlan, PCR Analysis of the Distribution of Unicellular Cyanobacterial Diazotrophs in the Arabian Sea, *Applied and Environmental Microbiology*, 70, 7355–7364, 2004, \_eprint: <https://journals.asm.org/doi/pdf/10.1128/AEM.70.12.7355-7364.2004>. [Cited on pages 61 and 64.]
- McCollom, T. M., and J. P. Amend, A thermodynamic assessment of energy requirements for biomass synthesis by chemolithoautotrophic micro-organisms in oxic and anoxic environments, *Geobiology*, 3, 135–144, 2005, \_eprint: <https://onlinelibrary.wiley.com/doi/pdf/10.1111/j.1472-4669.2005.00045.x>. [Cited on pages 7 and 80.]
- McCreary, J. P., R. Murtugudde, J. Vialard, P. N. Vinayachandran, J. D. Wiggert, R. R. Hood, D. Shankar, and S. Shetye, Biophysical Processes in the Indian Ocean, in *Indian Ocean Biogeochemical Processes and Ecological Variability*, pp. 9–32, American Geophysical Union (AGU), 2009, \_eprint: <https://agupubs.onlinelibrary.wiley.com/doi/pdf/10.1029/2008GM000768>. [Cited on page 12.]
- Meador, T. B., N. Schoffelen, T. G. Ferdelman, O. Rebello, A. Khachikyan, and M. Könneke, Carbon recycling efficiency and phosphate turnover by marine nitrifying archaea, *Science Advances*, 6, eaba1799, 2020, \_eprint:

- <https://www.science.org/doi/pdf/10.1126/sciadv.aba1799>. [Cited on pages 10, 90, and 91.]
- Middelburg, J. J., Chemoautotrophy in the ocean, *Geophysical Research Letters*, 38, 2011, \_eprint: <https://agupubs.onlinelibrary.wiley.com/doi/pdf/10.1029/2011GL049725>. [Cited on pages 7, 10, 87, 89, 90, and 91.]
- Mignot, A., H. Claustre, J. Uitz, A. Poteau, F. D’Ortenzio, and X. Xing, Understanding the seasonal dynamics of phytoplankton biomass and the deep chlorophyll maximum in oligotrophic environments: A Bio-Argo float investigation, *Global Biogeochemical Cycles*, 28, 856–876, 2014, \_eprint: <https://agupubs.onlinelibrary.wiley.com/doi/pdf/10.1002/2013GB004781>. [Cited on page 59.]
- Miller, A. F., and W. H. Orme-Johnson, The dependence on iron availability of allocation of iron to nitrogenase components in *Klebsiella pneumoniae* and *Escherichia coli*, *Journal of Biological Chemistry*, 267, 9398–9408, 1992. [Cited on page 5.]
- Miller, R. W., and R. R. Eady, Molybdenum and vanadium nitrogenases of *Azotobacter chroococcum*. Low temperature favours N<sub>2</sub> reduction by vanadium nitrogenase, *Biochemical Journal*, 256, 429–432, 1988, \_eprint: <https://portlandpress.com/biochemj/article-pdf/256/2/429/595010/bj2560429.pdf>. [Cited on page 4.]
- Mills, M. M., C. Ridame, M. Davey, J. La Roche, and R. J. Geider, Iron and phosphorus co-limit nitrogen fixation in the eastern tropical North Atlantic, *Nature*, 429, 292–294, 2004. [Cited on pages 5 and 42.]
- Miyake, Y., and E. Wada, The abundance ratio of <sup>15</sup>N/<sup>14</sup>N in marine environments, *Rec Oceanogr Works Jpn*, 9, 37–53, 1967. [Cited on page 42.]
- Moffett, J. W., T. J. Goepfert, and S. W. A. Naqvi, Reduced iron associated with secondary nitrite maxima in the Arabian Sea, *Deep Sea Research Part I: Oceanographic Research Papers*, 54, 1341–1349, 2007. [Cited on page 73.]
- Molina, V., and L. Farías, Aerobic ammonium oxidation in the oxycline and oxygen minimum zone of the eastern tropical South Pacific off northern Chile (20°S), *Deep Sea*

- Research Part II: Topical Studies in Oceanography*, 56, 1032–1041, 2009. [Cited on page 87.]
- Montoya, J., M. Voss, P. Kähler, and D. G. Capone, A Simple, High-Precision, High-Sensitivity Tracer Assay for N<sub>2</sub> Fixation, *Applied and environmental microbiology*, 62, 986–993, 1996. [Cited on page 21.]
- Montoya, J. P., C. M. Holl, J. P. Zehr, A. Hansen, T. A. Villareal, and D. G. Capone, High rates of N<sub>2</sub> fixation by unicellular diazotrophs in the oligotrophic Pacific Ocean, *Nature*, 430, 1027–1031, 2004. [Cited on page 56.]
- Moore, C. M., et al., Processes and patterns of oceanic nutrient limitation, *Nature Geoscience*, 6, 701, 2013, publisher: Nature Publishing Group, a division of Macmillan Publishers Limited. All Rights Reserved. [Cited on page 2.]
- Morrison, J. M., et al., The oxygen minimum zone in the Arabian Sea during 1995, *Deep Sea Research Part II: Topical Studies in Oceanography*, 46, 1903–1931, 1999. [Cited on page 73.]
- Mulholland, M. R., and D. G. Capone, Dinitrogen Fixation in the Indian Ocean, in *Indian Ocean Biogeochemical Processes and Ecological Variability*, pp. 167–186, American Geophysical Union (AGU), 2009, \_eprint: <https://agupubs.onlinelibrary.wiley.com/doi/pdf/10.1029/2009GM000850>. [Cited on pages 12 and 64.]
- Naqvi, S. W. A., H. W. Bange, L. Farías, P. M. S. Monteiro, M. I. Scranton, and J. Zhang, Marine hypoxia/anoxia as a source of CH<sub>4</sub> and N<sub>2</sub>O, *Biogeosciences*, 7, 2159–2190, 2010. [Cited on page 89.]
- Owens, N. J. P., C. S. Law, R. F. C. Mantoura, P. H. Burkill, and C. A. Llewellyn, Methane flux to the atmosphere from the Arabian Sea, *Nature*, 354, 293–296, 1991. [Cited on page 89.]
- Pachiadaki, M. G., et al., Major role of nitrite-oxidizing bacteria in dark ocean carbon fixation, *Science*, 358, 1046–1051, 2017, \_eprint: <https://www.science.org/doi/pdf/10.1126/science.aan8260>. [Cited on pages 7 and 89.]

- Parab, S. G., and S. G. P. Matondkar, Primary productivity and nitrogen fixation by *Trichodesmium* spp. in the Arabian Sea, *Journal of Marine Systems*, 105-108, 82–95, 2012. [Cited on page 72.]
- Parab, S. G., S. G. P. Matondkar, H. d. R. Gomes, and J. I. Goes, Monsoon driven changes in phytoplankton populations in the eastern Arabian Sea as revealed by microscopy and HPLC pigment analysis, *Continental Shelf Research*, 26, 2538–2558, 2006. [Cited on page 72.]
- Patra, P. K., M. D. Kumar, N. Mahowald, and V. V. S. S. Sarma, Atmospheric deposition and surface stratification as controls of contrasting chlorophyll abundance in the North Indian Ocean, *Journal of Geophysical Research: Oceans*, 112, 2007, eprint: <https://agupubs.onlinelibrary.wiley.com/doi/pdf/10.1029/2006JC003885>. [Cited on page 41.]
- Pitcher, A., L. Villanueva, E. C. Hopmans, S. Schouten, G.-J. Reichart, and J. S. Sinninghe Damsté, Niche segregation of ammonia-oxidizing archaea and anammox bacteria in the Arabian Sea oxygen minimum zone, *The ISME Journal*, 5, 1896–1904, 2011. [Cited on pages 88 and 89.]
- Podlaska, A., S. G. Wakeham, K. A. Fanning, and G. T. Taylor, Microbial community structure and productivity in the oxygen minimum zone of the eastern tropical North Pacific, *Deep Sea Research Part I: Oceanographic Research Papers*, 66, 77–89, 2012. [Cited on pages 10, 80, 87, and 90.]
- Postgate, J., *Nitrogen fixation*, third ed., Cambridge University Press, Cambridge, 1998. [Cited on page 5.]
- Prasad, T. G., Annual and seasonal mean buoyancy fluxes for the tropical Indian Ocean, *Current Science*, 73, 667–674, 1997, publisher: Current Science Association. [Cited on pages 11 and 41.]
- Prasanna Kumar, S., M. Madhupratap, M. Dileepkumar, P. Muraleedharan, S. Souza, M. Gauns, and S. Vvss, High biological productivity in the central Arabian Sea during the summer monsoon driven by Ekman pumping and lateral advection, *Current science*, 81, 1633–1638, 2001. [Cited on pages 11 and 42.]

- Prasanna Kumar, S., P. M. Muraleedharan, T. G. Prasad, M. Gauns, N. Ramaiah, S. N. de Souza, S. Sardesai, and M. Madhupratap, Why is the Bay of Bengal less productive during summer monsoon compared to the Arabian Sea?, *Geophysical Research Letters*, 29, 88–1–88–4, 2002, \_eprint: <https://agupubs.onlinelibrary.wiley.com/doi/pdf/10.1029/2002GL016013>. [Cited on pages 11, 35, 41, and 42.]
- Prasanna Kumar, S., J. Narvekar, N. Murukesh, S. P. Kumar, R. Nagappa, S. Sardesai, M. Gauns, V. Fernandes, and J. Bhaskar, Is the biological productivity in the Bay of Bengal light limited?, *Current Science*, 98, 2010a. [Cited on page 43.]
- Prasanna Kumar, S., et al., Seasonal cycle of physical forcing and biological response in the Bay of Bengal, *Indian Journal of Marine Sciences*, 39, 2010b. [Cited on pages 35 and 56.]
- Prasanna Kumar, S. P., and T. G. Prasad, Winter cooling in the northern Arabian Sea, *Current Science*, 71, 834–841, 1996, publisher: Temporary Publisher. [Cited on page 12.]
- Raes, E. J., et al., N<sub>2</sub> Fixation and New Insights Into Nitrification From the Ice-Edge to the Equator in the South Pacific Ocean, *Frontiers in Marine Science*, 7, 2020. [Cited on page 63.]
- Ragavan, P., and S. Kumar, Potential role of priming effect in the open ocean oxygen minimum zones: an outlook, *Hydrobiologia*, 848, 2437–2448, 2021. [Cited on page 80.]
- Rahav, E., E. Bar Zeev, S. Ohayon, H. Elifantz, N. Belkin, B. Herut, M. Mulholland, and I. Berman-Frank, Dinitrogen fixation in aphotic oxygenated marine environments, *Frontiers in microbiology*, 4, 227, 2013. [Cited on pages 8 and 58.]
- Ramaswamy, V., et al. (Eds.), *Radiative forcing of climate change*, vol. 18, Cambridge University Press, Cambridge, United Kingdom, 2001. [Cited on page 91.]
- Raven, J. A., The iron and molybdenum use efficiencies of plant growth with different energy, carbon and nitrogen sources, *New Phytologist*, 109, 279–287, 1988, \_eprint: <https://nph.onlinelibrary.wiley.com/doi/pdf/10.1111/j.1469-8137.1988.tb04196.x>. [Cited on page 5.]



- Reddy, K., and A. Mitsui, Simultaneous Production of Hydrogen and Oxygen as Affected by Light Intensity in Unicellular Aerobic Nitrogen Fixing Blue Green Alga *Synechococcus* SP. Miami BGO43511, pp. 785–788, 1984. [Cited on page 60.]
- Redfield, A., On The Proportions of Organic Derivations in Sea Water and Their Relation to The Composition of Plankton, in *James Johnstone Memorial*, vol. 1934, pp. 177–192, 1934. [Cited on pages 8, 36, 51, 66, and 83.]
- Redfield, A., The biological control of chemical factors in the environment, *Science progress*, 11, 150–170, 1958. [Cited on page 83.]
- Reinthal, T., H. M. v. Aken, and G. J. Herndl, Major contribution of autotrophy to microbial carbon cycling in the deep North Atlantic’s interior, *Deep Sea Research Part II: Topical Studies in Oceanography*, 57, 1572–1580, 2010. [Cited on pages 10, 90, and 91.]
- Resplandy, L., M. Lévy, G. Madec, S. Pous, O. Aumont, and D. Kumar, Contribution of mesoscale processes to nutrient budgets in the Arabian Sea, *Journal of Geophysical Research: Oceans*, 116, 2011, \_eprint: <https://agupubs.onlinelibrary.wiley.com/doi/pdf/10.1029/2011JC007006>. [Cited on page 12.]
- Riemann, L., H. Farnelid, and G. Steward, Nitrogenase genes in non-cyanobacterial plankton: Prevalence, diversity and regulation in marine waters, *AQUATIC MICROBIAL ECOLOGY*, 61, 2010. [Cited on page 6.]
- Rippka, R., and J. Waterbury, The synthesis of nitrogenase by non-heterocystous cyanobacteria, *FEMS Microbiology Letters*, 2, 83–86, 1977, \_eprint: <https://academic.oup.com/femsle/article-pdf/2/2/83/19390117/2-2-83.pdf>. [Cited on page 60.]
- Rocha, C. L. D. L., and U. Passow, Factors influencing the sinking of POC and the efficiency of the biological carbon pump, *Deep Sea Research Part II: Topical Studies in Oceanography*, 54, 639–658, 2007. [Cited on page 9.]
- Roxy, M. K., A. Modi, R. Murtugudde, V. Valsala, S. Panickal, S. Prasanna Kumar, M. Ravichandran, M. Vichi, and M. Lévy, A reduction in ma-

- rine primary productivity driven by rapid warming over the tropical Indian Ocean, *Geophysical Research Letters*, 43, 826–833, 2016, \_eprint: <https://agupubs.onlinelibrary.wiley.com/doi/pdf/10.1002/2015GL066979>. [Cited on page 86.]
- Saito, M. A., et al., Abundant nitrite-oxidizing metalloenzymes in the mesopelagic zone of the tropical Pacific Ocean, *Nature Geoscience*, 13, 355–362, 2020. [Cited on page 89.]
- Sarma, V. V. S. S., D. N. Rao, G. R. Rajula, H. B. Dalabehera, and K. Yadav, Organic Nutrients Support High Primary Production in the Bay of Bengal, *Geophysical Research Letters*, 46, 6706–6715, 2019, \_eprint: <https://agupubs.onlinelibrary.wiley.com/doi/pdf/10.1029/2019GL082262>. [Cited on page 57.]
- Sato, T., T. Shiozaki, Y. Taniuchi, H. Kasai, and K. Takahashi, Nitrogen Fixation and Diazotroph Community in the Subarctic Sea of Japan and Sea of Okhotsk, *Journal of Geophysical Research: Oceans*, 126, e2020JC017071, 2021, \_eprint: <https://agupubs.onlinelibrary.wiley.com/doi/pdf/10.1029/2020JC017071>. [Cited on page 63.]
- Saxena, H., D. Sahoo, M. A. Khan, S. Kumar, A. K. Sudheer, and A. Singh, Dinitrogen fixation rates in the Bay of Bengal during summer monsoon, *Environmental Research Communications*, 2, 051,007, 2020, publisher: IOP Publishing. [Cited on pages 56 and 57.]
- Sañudo-Willhelmy, S., A. Kustka, C. Gobler, D. Hutchins, M. Yang, K. Lwiza, J. Burns, J. Raven, and E. Carpenter, Phosphorus limitation of nitrogen fixation by *Trichodesmium* in the central Atlantic Ocean, *Nature*, 411, 66–9, 2001. [Cited on pages 5 and 42.]
- Schindler, D. W., Broecker, W. S. 1974. Chemical oceanography. Harcourt, Brace, Jovanovich, Inc., New York. 214 p. \$7.95., *Limnology and Oceanography*, 20, 299–300, 1975, \_eprint: <https://aslopubs.onlinelibrary.wiley.com/doi/pdf/10.4319/lo.1975.20.2.0299>. [Cited on page 1.]

- Schoffman, H., H. Lis, Y. Shaked, and N. Keren, Iron-Nutrient Interactions within Phytoplankton, *Frontiers in plant science*, 7, 1223, 2016. [Cited on page 5.]
- Selden, C. R., M. R. Mulholland, P. W. Bernhardt, B. Widner, A. Macías-Tapia, Q. Ji, and A. Jayakumar, Dinitrogen Fixation Across Physico-Chemical Gradients of the Eastern Tropical North Pacific Oxygen Deficient Zone, *Global Biogeochemical Cycles*, 33, 1187–1202, 2019, \_eprint: <https://agupubs.onlinelibrary.wiley.com/doi/pdf/10.1029/2019GB006242>. [Cited on pages 8, 64, 72, and 75.]
- Selden, C. R., M. R. Mulholland, B. Widner, P. Bernhardt, and A. Jayakumar, Toward resolving disparate accounts of the extent and magnitude of nitrogen fixation in the Eastern Tropical South Pacific oxygen deficient zone, *Limnology and Oceanography*, 66, 1950–1960, 2021, \_eprint: <https://aslopubs.onlinelibrary.wiley.com/doi/pdf/10.1002/lno.11735>. [Cited on pages 74 and 75.]
- Shenoi, S. S. C., D. Shankar, and S. R. Shetye, Differences in heat budgets of the near-surface Arabian Sea and Bay of Bengal: Implications for the summer monsoon, *Journal of Geophysical Research: Oceans*, 107, 5–1–5–14, 2002, \_eprint: <https://agupubs.onlinelibrary.wiley.com/doi/pdf/10.1029/2000JC000679>. [Cited on page 41.]
- Shetye, S., M. Sudhakar, B. Jena, and R. Mohan, Occurrence of Nitrogen Fixing Cyanobacterium *Trichodesmium* under Elevated pCO<sub>2</sub> Conditions in the Western Bay of Bengal, *International Journal of Oceanography*, 2013, 2013. [Cited on pages 45 and 60.]
- Shetye, S. R., S. S. C. Shenoi, A. D. Gouveia, G. S. Michael, D. Sundar, and G. Nampoothiri, Wind-driven coastal upwelling along the western boundary of the Bay of Bengal during the southwest monsoon, *Continental Shelf Research*, 11, 1397 – 1408, 1991. [Cited on pages 35 and 41.]
- Shiozaki, T., K. Furuya, T. Kodama, S. Kitajima, S. Takeda, T. Takemura, and J. Kanda, New estimation of N<sub>2</sub> fixation in the western and central Pacific Ocean and its marginal seas, *Global Biogeochemical Cycles*, 24, GB1015, 2010, \_eprint:

- <https://agupubs.onlinelibrary.wiley.com/doi/pdf/10.1029/2009GB003620>. [Cited on pages 56 and 72.]
- Shiozaki, T., M. Ijichi, T. Kodama, S. Takeda, and K. Furuya, Heterotrophic bacteria as major nitrogen fixers in the euphotic zone of the Indian Ocean, *Global Biogeochemical Cycles*, 28, 2014. [Cited on pages 12, 44, 64, 73, and 74.]
- Shiozaki, T., A. Fujiwara, M. Ijichi, N. Harada, S. Nishino, S. Nishi, T. Nagata, and K. Hamasaki, Diazotroph community structure and the role of nitrogen fixation in the nitrogen cycle in the Chukchi Sea (western Arctic Ocean), *Limnology and Oceanography*, 63, 2191–2205, 2018, \_eprint: <https://aslopubs.onlinelibrary.wiley.com/doi/pdf/10.1002/lno.10933>. [Cited on page 63.]
- Shiozaki, T., A. Fujiwara, K. Inomura, Y. Hirose, F. Hashihama, and N. Harada, Biological nitrogen fixation detected under Antarctic sea ice, *Nature Geoscience*, 13, 729–732, 2020. [Cited on pages 59 and 63.]
- Siegenthaler, U., and J. L. Sarmiento, Atmospheric carbon dioxide and the ocean, *Nature*, 365, 119–125, 1993. [Cited on page 9.]
- Singh, A., and R. Ramesh, Contribution of Riverine Dissolved Inorganic Nitrogen Flux to New Production in the Coastal Northern Indian Ocean: An Assessment, *International journal of oceanography*, 2011, 2011. [Cited on pages 11, 35, and 41.]
- Singh, A., N. Gandhi, and R. Ramesh, Contribution of atmospheric nitrogen deposition to new production in the nitrogen limited photic zone of the northern Indian Ocean, *Journal of Geophysical Research: Oceans*, 117, 2012, \_eprint: <https://agupubs.onlinelibrary.wiley.com/doi/pdf/10.1029/2011JC007737>. [Cited on page 41.]
- Singh, A., L. T. Bach, T. Fischer, H. Hauss, R. Kiko, A. J. Paul, P. Stange, P. Vandromme, and U. Riebesell, Niche construction by non-diazotrophs for N<sub>2</sub> fixers in the eastern tropical North Atlantic Ocean, *Geophysical Research Letters*, 44, 6904–6913, 2017, \_eprint: <https://agupubs.onlinelibrary.wiley.com/doi/pdf/10.1002/2017GL074218>. [Cited on page 42.]

- Singh, A., N. Gandhi, and R. Ramesh, Surplus supply of bioavailable nitrogen through N<sub>2</sub> fixation to primary producers in the eastern Arabian Sea during autumn, *Continental Shelf Research*, 181, 2019. [Cited on pages 5, 44, 45, and 63.]
- Sipler, R. E., D. Gong, S. E. Baer, M. P. Sanderson, Q. N. Roberts, M. R. Mulholland, and D. A. Bronk, Preliminary estimates of the contribution of Arctic nitrogen fixation to the global nitrogen budget, *Limnology and Oceanography Letters*, 2, 159–166, 2017, \_eprint: <https://aslopubs.onlinelibrary.wiley.com/doi/pdf/10.1002/lo.10046>. [Cited on page 63.]
- Slawyk, G., Y. Collos, and J.-C. Auclair, The use of the <sup>13</sup>C and <sup>15</sup>N isotopes for the simultaneous measurement of carbon and nitrogen turnover rates in marine phytoplankton, *Limnology and Oceanography*, 22, 925–932, 1977, \_eprint: <https://aslopubs.onlinelibrary.wiley.com/doi/pdf/10.4319/lo.1977.22.5.0925>. [Cited on page 21.]
- Smith, S. V., Phosphorus versus nitrogen limitation in the marine environment, *Limnology and Oceanography*, 29, 1149–1160, 1984, \_eprint: <https://aslopubs.onlinelibrary.wiley.com/doi/pdf/10.4319/lo.1984.29.6.1149>. [Cited on page 1.]
- Sohm, J., and E. Webb, Emerging patterns of marine nitrogen fixation, *Nature reviews. Microbiology*, 9, 499–508, 2011. [Cited on page 63.]
- Spiller, H., and K. T. Shanmugam, Physiological conditions for nitrogen fixation in a unicellular marine cyanobacterium, *Synechococcus* sp. strain SF1., *Journal of Bacteriology*, 169, 5379–5384, 1987, publisher: American Society for Microbiology Journals \_eprint: <https://jb.asm.org/content/169/12/5379.full.pdf>. [Cited on page 60.]
- Srinivas, B., and M. M. Sarin, Atmospheric deposition of N, P and Fe to the Northern Indian Ocean: Implications to C- and N-fixation, *Science of The Total Environment*, 456-457, 104–114, 2013. [Cited on pages 11, 12, and 42.]
- Stal, L. J., Is the distribution of nitrogen-fixing cyanobacteria in the oceans related to temperature?, *Environmental Microbiology*, 11, 1632–1645, 2009,

- \_eprint: <https://sfamjournals.onlinelibrary.wiley.com/doi/pdf/10.1111/j.1758-2229.2009.00016.x>. [Cited on page 63.]
- Sterner, R. W., and J. J. Elser, *The Biology of Elements from Molecules to the Biosphere*, Princeton University Press, 2002. [Cited on page 1.]
- Strous, M., J. J. Heijnen, J. G. Kuenen, and M. S. M. Jetten, The sequencing batch reactor as a powerful tool for the study of slowly growing anaerobic ammonium-oxidizing microorganisms, *Applied Microbiology and Biotechnology*, 50, 589–596, 1998. [Cited on page 89.]
- Subramanian, V., Sediment load of Indian rivers, *Current Science*, 64, 928–930, 1993, publisher: Temporary Publisher. [Cited on pages 11, 35, and 41.]
- Tang, W., et al., New insights into the distributions of nitrogen fixation and diazotrophs revealed by high-resolution sensing and sampling methods, *The ISME Journal*, 2020. [Cited on page 59.]
- Taylor, G. T., M. Iabichella, T.-Y. Ho, M. I. Scranton, R. C. Thunell, F. Muller-Karger, and R. Varela, Chemoautotrophy in the redox transition zone of the Cariaco Basin: A significant midwater source of organic carbon production, *Limnology and Oceanography*, 46, 148–163, 2001, \_eprint: <https://aslopubs.onlinelibrary.wiley.com/doi/pdf/10.4319/lo.2001.46.1.0148>. [Cited on pages 10, 80, and 87.]
- Thamdrup, B., H. G. R. Steinsdóttir, A. D. Bertagnolli, C. C. Padilla, N. V. Patin, E. Garcia-Robledo, L. A. Bristow, and F. J. Stewart, Anaerobic methane oxidation is an important sink for methane in the ocean's largest oxygen minimum zone, *Limnology and Oceanography*, 64, 2569–2585, 2019, \_eprint: <https://aslopubs.onlinelibrary.wiley.com/doi/pdf/10.1002/lno.11235>. [Cited on page 89.]
- Turner, J. T., Zooplankton fecal pellets, marine snow, phytodetritus and the ocean's biological pump, *Progress in Oceanography*, 130, 205–248, 2015. [Cited on page 9.]
- Tyrrell, T., The relative influence of nitrogen and phosphorus in oceanic primary productivity, *Nature*, 400, 529–531, 1999. [Cited on page 2.]

- Valentine, D. L., D. C. Blanton, W. S. Reeburgh, and M. Kastner, Water column methane oxidation adjacent to an area of active hydrate dissociation, Eel river Basin, *Geochimica et Cosmochimica Acta*, 65, 2633–2640, 2001. [Cited on pages 7 and 89.]
- van Vliet, D. M., F. B. von Meijnenfeldt, B. E. Dutilh, L. Villanueva, J. S. Sinninghe Damsté, A. J. Stams, and I. Sánchez-Andrea, The bacterial sulfur cycle in expanding dysoxic and euxinic marine waters, *Environmental Microbiology*, 23, 2834–2857, 2021, eprint: <https://sfamjournals.onlinelibrary.wiley.com/doi/pdf/10.1111/1462-2920.15265>. [Cited on page 89.]
- Vargas, C. A., et al., A source of isotopically light organic carbon in a low-pH anoxic marine zone, *Nature Communications*, 12, 1604, 2021. [Cited on pages 10 and 80.]
- Vernadsky, V. I., *The biosphere*, Springer Science & Business Media, 1998. [Cited on page 5.]
- Villanueva, L., D. R. Speth, T. van Alen, A. Hoischen, and M. S. M. Jetten, Shotgun metagenomic data reveals significant abundance but low diversity of “*Candidatus Scalindua*” marine anammox bacteria in the Arabian Sea oxygen minimum zone, *Frontiers in Microbiology*, 5, 31, 2014. [Cited on pages 13, 80, 88, and 89.]
- Ward, B. B., A. H. Devol, J. J. Rich, B. X. Chang, S. E. Bulow, H. Naik, A. Pratihary, and A. Jayakumar, Denitrification as the dominant nitrogen loss process in the Arabian Sea, *Nature*, 461, 78–81, 2009. [Cited on page 89.]
- Weiss, R. F., The solubility of nitrogen, oxygen and argon in water and seawater, *Deep Sea Research and Oceanographic Abstracts*, 17, 721 – 735, 1970. [Cited on page 31.]
- White, A. E., J. Granger, and K. Turk-Kubo, Questioning High Nitrogen Fixation Rate Measurements in the Southern Ocean, *Nature Geoscience*, 15, 29–30, 2022. [Cited on page 63.]
- Whitman, W., D. Coleman, and W. Wiebe, Prokaryotes: The unseen majority, *Proceedings of the National Academy of Sciences*, 95, 6578–6583, 1998. [Cited on page 1.]

- Woebken, D., P. Lam, M. M. M. Kuypers, S. W. A. Naqvi, B. Kartal, M. Strous, M. S. M. Jetten, B. M. Fuchs, and R. Amann, A microdiversity study of anammox bacteria reveals a novel *Candidatus Scalindua* phylotype in marine oxygen minimum zones, *Environmental Microbiology*, 10, 3106–3119, 2008, \_eprint: <https://sfamjournals.onlinelibrary.wiley.com/doi/pdf/10.1111/j.1462-2920.2008.01640.x>. [Cited on page 89.]
- Wu, C., J. Kan, H. Liu, L. Pujari, C. Guo, X. Wang, and J. Sun, Heterotrophic Bacteria Dominate the Diazotrophic Community in the Eastern Indian Ocean (EIO) during Pre-Southwest Monsoon, *Microbial Ecology*, 78, 2019. [Cited on page 43.]
- Wuchter, C., et al., Archaeal nitrification in the ocean, *Proceedings of the National Academy of Sciences*, 103, 12,317–12,322, 2006, publisher: National Academy of Sciences \_eprint: <https://www.pnas.org/content/103/33/12317.full.pdf>. [Cited on pages 10, 90, and 91.]
- Zehr, J., Nitrogen fixation by marine cyanobacteria, *Trends in microbiology*, 19, 162–73, 2011. [Cited on pages 5 and 6.]
- Zehr, J., M. Mellon, and S. Zani, New Nitrogen-Fixing Microorganisms Detected in Oligotrophic Oceans by Amplification of Nitrogenase (*nifH*) Genes, *Applied and Environmental Microbiology*, 64, 5067–5067, 1998. [Cited on page 6.]
- Zehr, J. P., and D. G. Capone, Changing perspectives in marine nitrogen fixation, *Science*, 368, 2020, publisher: American Association for the Advancement of Science \_eprint: <https://science.sciencemag.org/content/368/6492/eaay9514.full.pdf>. [Cited on pages xi, 3, 4, 6, and 75.]
- Zehr, J. P., and D. G. Capone, Factors Controlling N<sub>2</sub> Fixation, in *Marine Nitrogen Fixation*, pp. 95–115, Springer International Publishing, Cham, 2021. [Cited on page 5.]
- Zehr, J. P., and R. M. Kudela, Nitrogen Cycle of the Open Ocean: From Genes to Ecosystems, *Annual Review of Marine Science*, 3, 197–225, 2011, \_eprint: <https://doi.org/10.1146/annurev-marine-120709-142819>. [Cited on page 56.]
- Zhang, R., et al., Physical-biological coupling of N<sub>2</sub> fixation in the northwestern South China Sea coastal upwelling during sum-



- mer, *Limnology and Oceanography*, 60, 1411–1425, 2015, \_eprint: <https://aslopubs.onlinelibrary.wiley.com/doi/pdf/10.1002/lno.10111>. [Cited on page 74.]
- Zhou, W., J. Liao, Y. Guo, X. Yuan, H. Huang, T. Yuan, and S. Liu, High dark carbon fixation in the tropical South China Sea, *Continental Shelf Research*, 146, 82–88, 2017. [Cited on page 87.]



# List of Publications

## Publications in Journals

1. \***Saxena, H.**, Sahoo, D., Khan, M.A., Kumar, S., Sudheer, A.K., Singh, A. (2020). Dinitrogen fixation rates in the Bay of Bengal during summer monsoon. *Environmental Research Communications*, 2, 051007. <https://doi.org/10.1088/2515-7620/ab89fa>
2. Sahoo, D., **Saxena, H.**, Tripathi, N., Khan, M.A., Rahman, A., Kumar, S., Sudheer, A.K., Singh, A. (2020). Non-Redfieldian C:N:P ratio in the inorganic and organic pools of the Bay of Bengal during the summer monsoon. *Marine Ecology Progress Series*, 653, 41–55. <https://doi.org/10.3354/meps13498>
3. Sahoo, D., **Saxena, H.**, Nazirahmed, S., Kumar, S., Sudheer, A.K., Bhushan, R., Sahay, A., Singh, A. (2021). Role of eddies and N<sub>2</sub> fixation in regulating C:N:P proportions in the Bay of Bengal. *Biogeochemistry*, 155, 413–429. <https://doi.org/10.1007/s10533-021-00833-4>
4. Khan, M.A., Rahman, A., Sahoo, D., **Saxena, H.**, Singh, A., Kumar, S. (2022). Nitrous oxide in the central Bay of Bengal during the summer monsoon. *Regional Studies in Marine Science*, 52, 102314. <https://doi.org/10.1016/j.rsma.2022.102314>
5. \***Saxena, H.**, Sahoo, D., Nazirahmed, S., Rai, D.K., Khan, M.A., Sharma, N., Kumar, S., Singh, A. (2022). Contribution of carbon fixation toward carbon sink in the ocean twilight zone. *Geophysical Research Letters*, 49, e2022GL099044. <https://doi.org/10.1029/2022GL099044>

---

\*Associated with thesis work.

6. \***Saxena, H.**, Sahoo, D., Nazirahmed, S., Chaudhari, D., Rahi, P., Kumar, S., Benavides, M., Krishna, A.V., Sudheer, A.K., Singh, A. (2022). The Bay of Bengal: An enigmatic diazotrophic niche. *Journal of Geophysical Research: Biogeosciences* (under review)
7. \***Saxena, H.**, Sahoo, D., Nazirahmed, S., Rai, D.K., Kumar, S., Singh, A. (2022). Nitrogen fixation across the contrasting physicochemical conditions in the Arabian Sea (under preparation)
8. Sahoo, D., **Saxena, H.**, Nazirahmed, S., Khan, M.A., Rai, D.K., Sharma, N., Kumar, S., Sudheer, A.K., Bhushan, R., Singh, A. (2022). Role of winter convective mixing in changing C:N:P ratios in the Arabian Sea (under preparation)

---

\*Associated with thesis work.

# Presentations at Conferences and Schools

1. **Saxena, H.**, Sahoo, D., Nazirahmed, S., Rai, D.K., Khan, M.A., Sharma, N., Kumar, S., Sudheer, A.K., Singh, A. “Key role of overlooked twilight zone towards climate buffering” at *EGU General Assembly 2021*, online, on 30 Apr 2021. [Oral]
2. **Saxena, H.**, Sahoo, D., Nazirahmed, S., Krishna, A.V., Sudheer, A.K., Kumar, S., Singh, A. “Diazotrophy in the euphotic and oxygen minimum zone of the Bay of Bengal during spring inter-monsoon” at *ASLO 2021 Aquatic Sciences Meeting*, online, on 23 Jun 2021. [Oral]
3. **Saxena, H.**, Sahoo, D., Khan, M.A., Kumar, S., Sudheer, A.K., Singh, A. “N<sub>2</sub> and C fixation in the euphotic zone of the Bay of Bengal” at *SOLAS Virtual Summer School 2022*, online, on 13 Jun 2022. [Oral]



# Publications attached with the thesis

1. Saxena, H., Sahoo, D., Khan, M.A., Kumar, S., Sudheer, A.K., Singh, A. (2020). Dinitrogen fixation rates in the Bay of Bengal during summer monsoon. *Environmental Research Communications*, 2, 051007. <https://doi.org/10.1088/2515-7620/ab89fa>
2. Saxena, H., Sahoo, D., Nazirahmed, S., Rai, D.K., Khan, M.A., Sharma, N., Kumar, S., Singh, A. (2022). Contribution of carbon fixation toward carbon sink in the ocean twilight zone. *Geophysical Research Letters*, 49, e2022GL099044. <https://doi.org/10.1029/2022GL099044>